UNIVERSIDADE FEDERAL DE PERNAMBUCO
CENTRO DE TECNOLOGIA E GEOCIÊNCIAS
DEPARTAMENTO DE ENGENHARIA CIVIL E AMBIENTAL
PROGRAMA DE PÓS-GRADUAÇÃO EM ENGENHARIA CIVIL
TECNOLOGIA AMBIENTAL E RECURSOS HÍDRICOS

OSMAR LUIZ MOREIRA PEREIRA FONSECA DE MENEZES

BIOTIC AND ABIOTIC STRATEGIES FOR INSENSITIVE MUNITIONS COMPOUNDS REMEDIATION

Recife
2020

OSMAR LUIZ MOREIRA PEREIRA FONSECA DE MENEZES

BIOTIC AND ABIOTIC STRATEGIES FOR INSENSITIVE MUNITIONS COMPOUNDS REMEDIATION

Tese apresentada ao Programa de Pós-Graduação em Engenharia Civil da Universidade Federal de Pernambuco, como requisito parcial para a obtenção do título de Doutor em Engenharia Civil.

Área de concentração: Tecnologia Ambiental e Recursos Hídricos.

Orientador: Profª. Drª. Sávia Gavazza.
Coorientador: Profº. Dr. Jim A. Field.

Recife
2020

Catalogação na fonte
Bibliotecária Margareth Malta, CRB-4 / 1198

M543b Menezes, Osmar Luiz Moreira Pereira Fonseca de.
Biotic and abiotic strategies for insensitive munitions compounds remediation / Osmar Luiz Moreira Pereira Fonseca de Menezes - 2020.
143 folhas, il., gráfs., tabs.

Orientadora: Profa. Dra. Sávia Gavazza dos Santos Pessôa.
Coorientador: Prof. Dr. Jim A. Field.

Tese (Doutorado) – Universidade Federal de Pernambuco. CTG. Programa de Pós-Graduação em Engenharia Civil, 2020.
Inclui Referências e Apêndices.
Texto em inglês.

1. Engenharia Civil. 2. 2,4-Dinitroanisol (DNAN). 3. 3-Nitro-1,2,4-triazol-5-ona (NTO). 4. Biorremediação. 5. Humificação. 6. Respiração microbiana. 7. Sulfeto de ferro. I. Pessôa, Sávia Gavazza dos Santos (Orientadora). II. Field, Jim A. (Coorientador). III. Título

UFPE

624 CDD (22. ed.) BCTG/2021-2

OSMAR LUIZ MOREIRA PEREIRA FONSECA DE MENEZES

BIOTIC AND ABIOTIC STRATEGIES FOR INSENSITIVE MUNITIONS COMPOUNDS REMEDIATION

Tese apresentada ao Programa de Pós-Graduação em Engenharia Civil da Universidade Federal de Pernambuco, como requisito parcial para a obtenção do grau de Doutor em Engenharia Civil.

Aprovada em: 18/12/2020

Orientadora: Prof.ª Dr.ª Sávia Gavazza dos Santos Pessoa – Universidade Federal de Pernambuco
Coorientador: Prof. Dr. Jim A. Field – The University of Aizona

BANCA EXAMINADORA

Participação por videoconferência
Prof. Dr. Jim A. Field (Coorientador)
The University of Arizona

Participação por videoconferência
Prof.ª Dr.ª Elizabeth A. Edwards (Examinadora externa)
University of Toronto

Participação por videoconferência
Prof. Dr. Jim C. Spain (Examinador externo)
Georgia Institute of Technology and University of West Florida

Participação por videoconferência
Prof. Dr. Sérgio Francisco de Aquino (Examinador externo)
Universidade Federal de Ouro Preto

Participação por videoconferência
Prof.ª Dr.ª Lucymara Fassarella Agnez Lima (Examinadora externa)
Universidade Federal do Rio Grande do Norte

To my parents, Socorro and Tadeu.

To Sivaldo.

To every Latin American child who has ever dreamed of being a scientist.

ACKNOWLEDGMENTS

I am deeply grateful to Dr. Savia Gavazza, Dr. Jim A. Field, and Dr. Reyes Sierra-Alvarez, for all the guidance with kindness and joy. I feel very fortunate to have found those professors in my academic journey. Warm thanks to Dr. Lourdinha Florêcio and Dr. Mario T. Kato for the invaluable intellectual support. Thanks to Dr. Elizabeth A. Edwards, Dr. Jim C. Spain, Dr. Lucymara F. Agnez-Lima, and Dr. Sérgio F. Aquino, committee members, for the contributions.

Many thanks to all my friends at the Laboratory of Environmental Sanitation (Universidade Federal de Pernambuco, Brazil), especially those who directly contributed to this work in a brilliant way: Matheus Paraiso, Natanna Ferraz, and Danubia Freitas. I also want to express my gratitude to all the Field-Sierra Research group (University of Arizona, USA). Special thanks to my friend Dr. Warren M. Kadoya, with whom I had the pleasure to work and learn so much. All my gratitude to Dr. Camila L. Madeira, my friend, mentor, and source of scientific inspiration, with whom I am very pleased to share the co-first authorship of the NTO respiration paper. Thanks to other amazing people who directly or indirectly contributed to this work: Ronaldo Fonseca, Dr. Ana Paula Paim, Youngjae Yu, Dr. Robert A. Root, Dr. Jon Chorover, Kalyani V. Jog, Doyoung Park, Dr. Janet K. Hatt, Dr. Konstantinos T. Konstantinidis, Dr. Elsa M. Reyes-Reyes, Dr. Eugene A. Mash, Dr. Leif Abrell, and Dr. Armando Durazo.

This doctoral work was supported by Brazilian and American intuitions/programs, which I want to acknowledge: FACEPE (Science and Technology Foundation of the State of Pernambuco, Brazil), CAPES (Coordination for the Improvement of Higher Education Personnel, Brazil), CNPq (National Council for Scientific and Technological Development, Brazil), NSF (National Science Foundation, USA), and SERDEP (Strategic Environmental Research and Development Program, USA). I also want to acknowledge the institutional support from the Universidade Federal de Pernambuco (especially Andrea Negromonte) and The University of Arizona.

Thanks to Sivaldo Correia, with whom I share all my life adventures, including this one. I would also like to thank my friends Geninha Lopes, Otacilio Neto, Flavia Adolfo, and all my family. I want to express my immense love and gratitude to my parents, Socorro and Tadeu, sources of unconditional support. Eu quero expressar meu imenso amor e gratidão aos meus pais, Socorro e Tadeu, fontes de apoio inconditional.

ABSTRACT

Insensitive munitions compounds (IMCs), such as 2,4-dinitroanisole (DNAN) and 2-nitro-1,2,3-triazol-5-one (NTO), are ingredients of new munitions formulations being deployed by the military due to their lower risk of unintended explosions. Environmental contamination by IMCs can occur via industrial wastewater discharge into water bodies and pieces of undetonated ordnance on the soil, which can be dissolved by precipitation and reach ground and surface waters. The remediation of these pollutants is imperative to environmental protection since they and their reduced daughter products are toxic and potentially mutagenic. This Ph.D. thesis presents novel biotic and abiotic strategies for IMCs remediation. (i) Firstly, we show that both DNAN and NTO can be anoxically reduced by FeS minerals commonly present in soils and aquatic sediments, such as mackinawite, to their corresponding amines. The reduction process is surface-mediated. (ii) After that, we present the unusual biological process of NTO respiration. A highly-enriched culture composed mainly of *Geobacter anodireducens* (89.3%) and *Thauera* sp. (5.5%) could grow reducing NTO to 3-amino-1,2,4-triazol-5-one (ATO) while oxidizing acetate to CO_2. The process was linked to ATP production, constituting evidence for NTO respiration. (iii) Then, we explored the biotic and abiotic reactions leading to the removal of 2,4-diaminoanisole (DAAN), the reduced daughter products of DNAN, in biological sludge exposed to different electron (e^-) acceptor conditions: without added e^- acceptor, without added e^- acceptor amended with pyruvate, with nitrate, with sulfate, and with oxygen. We observed that DAAN removal in sludge was faster under oxygen exposure, with the contribution of abiotic DAAN autoxidation. A culture with 85% of unclassified microorganisms (according to a 16S rRNA sequencing) could be enriched to remove DAAN under aerobic conditions, but not under anaerobic conditions. (iv) Finally, we unveiled the mechanisms leading to the disappearance of DAAN into the natural organic matter, a phenomenon observed by previous works. We tested DAAN reactions with quinone model compounds and developed a new method to stop these fast reactions, capturing fleeting intermediates for analysis. The reactions involving DAAN and quinones were Michael addition, imine formation, and azo bond formation. An oligomerization process was responsible for capturing DAAN into humic-like insoluble substances. Overall, our results can be applied to develop biotic and abiotic remediation strategies to clean up training ranges, treat wastewater contaminated with DNAN and NTO, and assess DNAN and NTO natural attenuation.

Keywords: 2,4-Dinitroanisole (DNAN). 3-Nitro-1,2,4-triazol-5-one (NTO). Bioremediation. Humification. Iron sulfide. Microbial respiration.

RESUMO

Compostos de munições insensíveis (IMCs), como 2,4-dinitroanisol (DNAN) e 2-nitro-1,2,3-triazol-5-ona (NTO), são ingredientes de novas formulações de munições atualmente empregadas pelos militares devido ao seu menor risco de explosões acidentais. A contaminação ambiental por IMCs pode ocorrer por meio de descarte de efluentes industriais em corpos d'água e pedaços não detonados de munições sobre solo, os quais podem ser dissolvidos pela precipitação e atingir águas subterrâneas e superficiais. A remediação desses poluentes é imperativa para a proteção ambiental, uma vez que eles e seus produtos reduzidos são tóxicos e potencialmente mutagênicos. Esta tese de doutorado apresenta novas estratégias bióticas e abióticas para remediação de IMCs. (i) Primeiramente, mostramos que tanto DNAN quanto NTO podem ser anoxicamente reduzidos por minerais de FeS comumente presentes em solos e sedimentos aquáticos, como a mackinawita, formando suas aminas correspondentes. A redução é mediada pela superfície mineral. (ii) Depois disso, apresentamos o inusitado processo biológico da respiração de NTO. Uma cultura altamente enriquecida composta principalmente por *Geobacter anodireducens* (89,3%) e *Thauera* sp. (5,5%) pôde crescer reduzindo NTO a 3-amino-1,2,4-triazol-5-ona (ATO) enquanto oxidava acetato a CO_2. O processo estava vinculado à produção de ATP, o que constitui uma evidência da respiração de NTO. (iii) Em seguida, exploramos as reações bióticas e abióticas que levam à remoção de 2,4-diaminoanisol (DAAN), produto reduzido do DNAN, em lodo biológico exposto a diferentes condições aceptores de elétrons (e^-): sem aceptor de e^- adicionado, sem aceptor de e^- adicionado com adição de piruvato, com nitrato, com sulfato e com oxigênio. Observamos que a remoção do DAAN no lodo foi mais rápida sob exposição ao oxigênio, com a contribuição da autoxidação abiótica de DAAN. Uma cultura com 86% de microrganismos não classificados (de acordo com um sequenciamento de 16S rRNA) pôde ser enriquecidos para remover DAAN em condições aeróbias, mas não em condições anaeróbias. (iv) Por fim, desvendamos os mecanismos que levam ao desaparecimento do DAAN na matéria orgânica natural, um fenômeno observado por trabalhos anteriores. Testamos reações entre DAAN e compostos modelos de quinona e desenvolvemos um novo método para interromper essas reações rápidas, capturando intermediários fugazes para análise. As reações envolvendo DAAN e quinonas foram adição de Michael, formação de imina e formação de ligação azo. Um processo de oligomerização foi responsável por capturar DAAN em substâncias insolúveis similares a substâncias húmicas. No geral, nossos resultados podem ser aplicados para o desenvolvimento de estratégias bióticas e

abióticas de remediação de campos de treinamento, para o tratamento de efluentes contaminados com DNAN e NTO e na avaliação da atenuação natural de DNAN e NTO.

Palavras-chave: 2,4-Dinitroanisol (DNAN). 3-Nitro-1,2,4-triazol-5-ona (NTO). Biorremediação. Humificação. Respiração microbiana. Sulfeto de ferro.

LIST OF FIGURES

LIST OF TABLES

LIST OF ABREVIATIONS

2,4-DNT	2,4-Dinitrotoluene
AP	Ammonium perchlorate
ATO	3-Amino-1,2,4-triazol-5-one
ATP	Adenosine triphosphate
BQ	1,4-Benzoquinone
CCCP	Carbonyl cyanide *m*-chlorophenyl hydrazine
DAD	Diode array detector
DAAN	2,4-Diaminoanisole
DNAN	2,4-Dinitroanisole
DNT	2,4- and 2,6-Dinitrotoluene
DOC	Dissolved organic carbon
e^-	Electron
FID	Flame ionization detector
GC	Gas chromatography
HMX	Octahydro-1,3,5,7-tetranitro-1,3,5,7-tetrazocine
HPLC	High performance liquid chromatography
HQ	1,4-Hydroquinone
IMC	Insensitive munitions compound
iMENA	4-Methoxy-3-nitroaniline
MENA	2-Methoxy-5-nitroaniline
MBQ	Methoxybenzoquinone
MHQ	Methoxyhydroquione
NG	Nitroglycerin
NOM	Natural organic matter
NQ	Nitroguanidine
NTO	3-Nitro-1,2,4-triazol-5-one
OD600	Optical density at 600 nm
RNA	Ribonucleic acid
RDX	1,3,5-Hexahydro-1,3,5-trinitro-1,3,5-triazine
SA	Surface area
SSR	Solids/solution ratio
TCD	Thermal conductivity detector

TNT	2,4,6-Trinitrotoluene
UHPLC-HRAM-MS/MS	Ultra-high performance liquid chromatography high-resolution accurate-mass spectrometry
XANES	X-ray absorption near-edge spectroscopy
XRD	X-ray diffraction
ZVI	Zero-valent iron

CONTENTS

1 INTRODUCTION

1.1 WHY SHOULD WE WORRY ABOUT INSENSITIVE MUNITIONS COMPOUNDS?

Nitroaromatic and nitro-heterocyclic compounds are organic molecules with a nitro group (-NO_2) attached to an aromatic or heterocyclic ring, respectively. Naturally occurring nitro-compounds are relatively scarce. They were reported in plants, fungi, microbes, and mammals; however in low concentrations, working as antibiotics, antitumors, or signaling molecules (PARRY *et al.*, 2011). Most nitro-compounds released in the biosphere are synthetic. They are used for the production of dyes, plastics, pesticides, pharmaceuticals, and explosives. They can also result from the incomplete combustion of fossil fuels (JU; PARALES, 2010; SPAIN, 1995). Due to their xenobiotic character, synthetic nitro-compounds and their daughter products, i.e., the products of their (bio)transformation, are toxic and mutagenic, representing a threat to the environment (PUROHIT; BASU, 2000; SUNAHARA *et al.*, 2009).

There are some reports of contamination by nitro-compounds in Brazil. During monitoring campaigns, pesticides were found in soils, surface water, and living organisms all over the country (GOMES; BARIZON, 2014). Recently, Kraus (2018) described a heavily contaminated site in the Industrial Complex of Camaçari, Bahia, Brazil. The comprehensive list of contaminants included chloronitrobenzenes, which were used for pesticides production. Additionally, the explosive nitroaromatic 2,4,6-trinitrotoluene (TNT) was observed to be the main component of wastewaters from Brazilian explosive manufacturing plants (BARRETO-RODRIGUES *et al.*, 2007; LUDWICHK *et al.*, 2015). These wastewaters are classified as “hazardous residues” by Brazilian environmental regulations and cannot be released into the environment (BRASIL, 2010).

Worldwide, the manufacture and use of explosives, such as TNT and 1,3,5-hexahydro-1,3,5-trinitro-1,3,5-triazine (RDX), lead to the contamination of military training ranges, former manufacturing plants, and storage facilities (SPAIN, 1995). Recently, these conventional explosives are being replaced by insensitive munitions compounds (IMCs). IMCs require higher detonation temperature and are less susceptible to mechanical shocks, thus exhibiting a lower risk of accidental detonation than conventional explosives (POWELL, IAN J., 2016). 2,4-Dinitroanisole (DNAN) and 3-nitro-1,2,4-triazol-5-one (NTO) are the most abundant compounds in insensitive munitions formulations (Figure 1) (TAYLOR *et al.*, 2015b).

Figure 1 – Percentages of different munition compounds in insensitive munitions formulations. Legend: DNAN (2,4-dinitroanisole), NTO (3-nitro-1,2,4-triazol-5-one), NQ (nitroguanidine), RDX (1,3,5-hexahydro-1,3,5-trinitro-1,3,5-triazine), and AP (ammonium perchlorate).

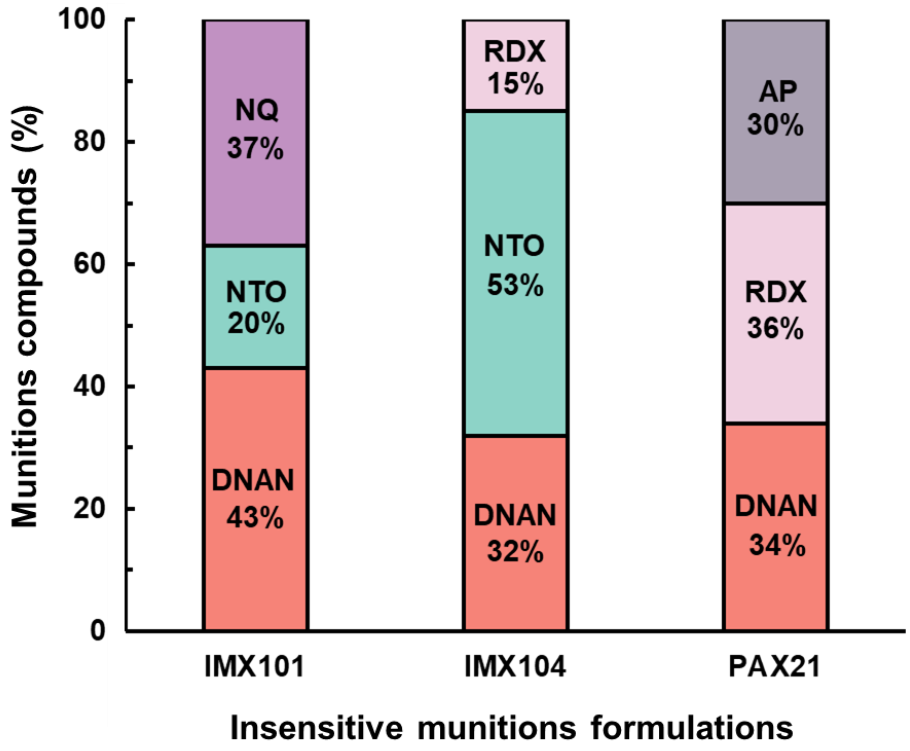

Source: adapted from Taylor et al. (2015).

Potential environmental contamination by IMCs can occur via industrial wastewater discharge into water bodies and large pieces of undetonated ordnance on the soil, which can be dissolved by precipitation and reach ground and surface waters (TAYLOR *et al.*, 2015a) (Figure 2). DNAN was observed to be severely toxic to methanogens, nitrifying bacteria, *Aliivibrio fischeri* (LIANG *et al.*, 2013), algae, ryegrass, earthworms (DODARD *et al.*, 2013), and zebrafish (OLIVARES *et al.*, 2016b). As an indication of its ecotoxicity, NTO causes testicular toxicity in male rats (CROUSE *et al.*, 2015; LENT *et al.*, 2020), neuromuscular anomalies in Japanese quail (JACKOVITZ *et al.*, 2018), disruption of swimming behavior in zebrafish embryos, and inhibition of methanogenic microorganisms (MADEIRA *et al.*, 2018). Additionally, NTO is a weak acid with high solubility (16,642 mg L^{-1}) that can cause the acidification of the soil and groundwater (TAYLOR *et al.*, 2015a). These reports evidence the need to develop remediation strategies to clean up IMCs contamination. The new strategies can have scientific applications to a vast range of nitroaromatic and nitro-heterocyclic compounds.

Figure 2 – Scheme of munitions compounds' release from ordnance in a military training range. Legend: NG (nitroglycerin), DNT (2,4- and 2,6-dinitrotoluene), NQ (nitroguanidine), TNT (2,4,6-trinitrotoluene), RDX (1,3,5-hexahydro-1,3,5-trinitro-1,3,5-triazine), HMX (octahydro-1,3,5,7-tetranitro-1,3,5,7-tetrazocine), DNAN (2,4-dinitroanisole), NTO (3-nitro-1,2,4-triazol-5-one), and AP (ammonium perchlorate).

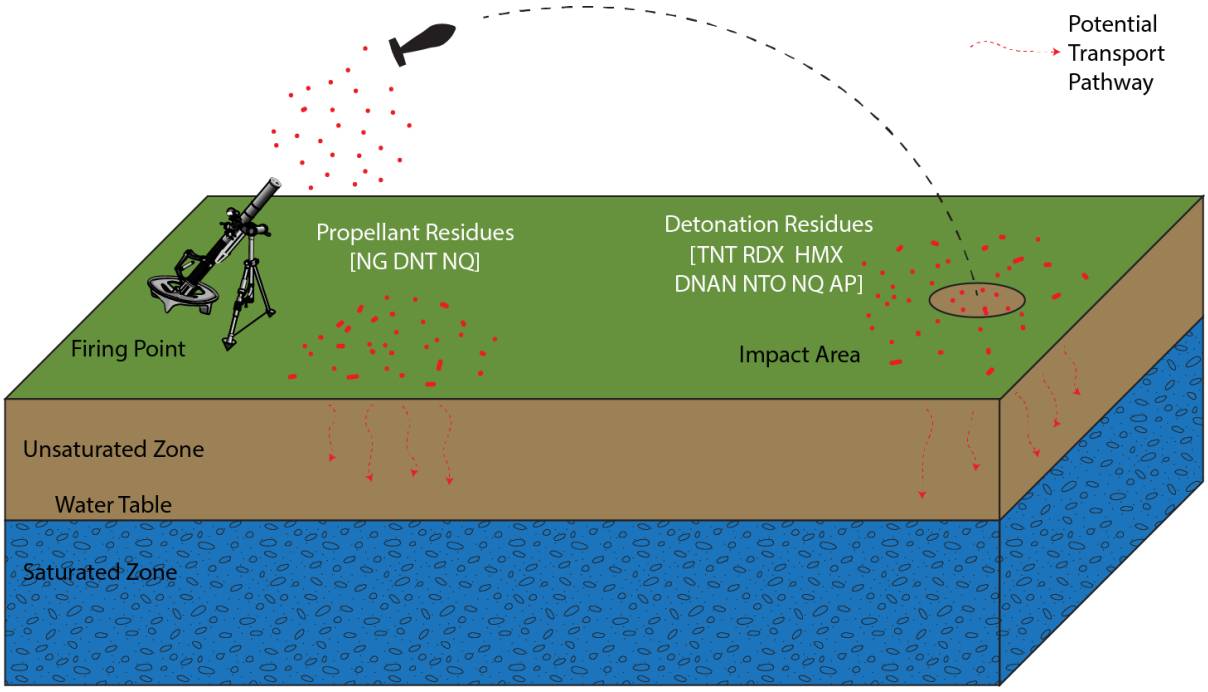

Source: SERDP-ESTCP (2020)

1.2 HOW ARE DNAN AND NTO TRANSFORMED IN THE ABSENCE OF O_2?

Aromatic or heterocyclic compounds substituted with electron-withdrawing groups, such as nitro groups, are known to be recalcitrant to oxidative pathways (FIELD *et al.*, 1995). On the other hand, the reduction of the nitro groups to amino groups is feasible and observed via both biotic and abiotic pathways (Figure 3). The reduction of DNAN's nitro group in the ortho position generates 2-methoxy-5-nitroaniline (MENA), whereas the reduction of the nitro group in the para position generates 4-methoxy-3-nitroaniline (iMENA). 2,4-Diaminoanisole (DAAN) is formed when both DNAN's nitro groups are reduced to amino groups (HAWARI *et al.*, 2015; OLIVARES *et al.*, 2016a). Additionally, the amine daughter product of NTO reduction is 3-amino-1,2,4-triazol-5-one (ATO) (KRZMARZICK *et al.*, 2015; LE CAMPION *et al.*, 1999a).

Abiotic reductive pathways can involve reactive minerals under anoxic conditions. Zero-valent iron (ZVI) was reported to reduce DNAN to its respective aromatic amines at regular temperature and near-neutral pH (HAWARI *et al.*, 2015; OU *et al.*, 2015). Another

study showed that both DNAN and NTO were reduced to their corresponding amines by sulfate green rust ($Fe^{2+}_4Fe^{3+}_2(OH)_{12}SO_4 \cdot 2H_2O$) (KHATIWADA *et al.*, 2018c). A third study demonstrated that Fe/Cu bimetallic systems could reduce DNAN to DAAN and NTO to urea under acidic conditions (KOUTSOSPYROS *et al.*, 2012). ATO was not detected but hypothesized as an intermediate (KITCHER *et al.*, 2017). FeS minerals, such as mackinawite, are very abundant in the lithosphere (MORSE *et al.*, 1987) and are frequently studied for the remediation of many organic and inorganic contaminants (GONG *et al.*, 2016), but were not tested yet for the reduction of IMCs.

Figure 3 – Reductive transformation of the insensitive munitions compounds DNAN and NTO.

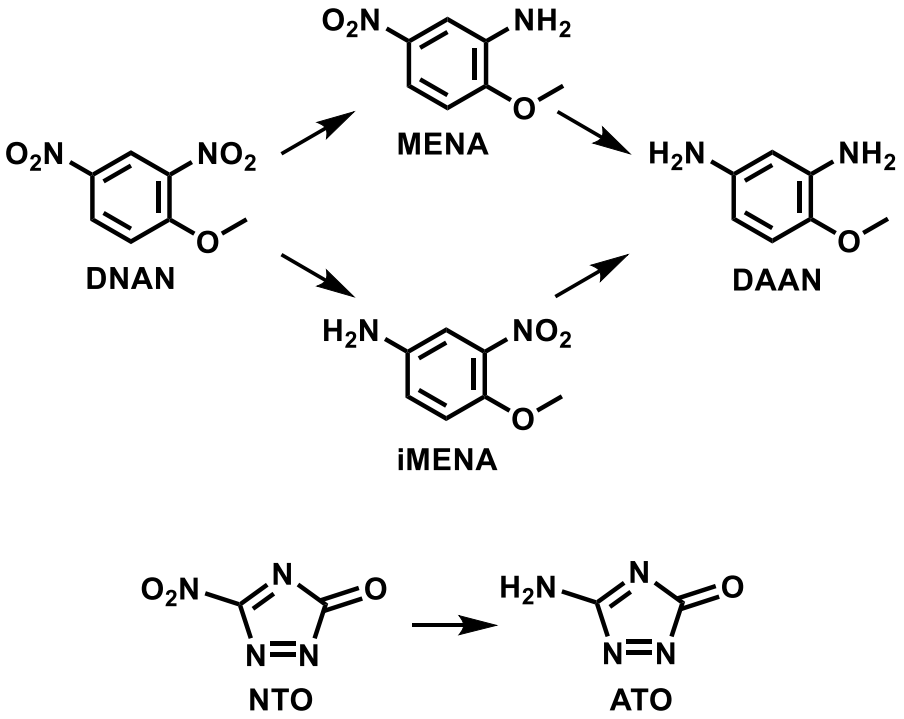

Although FIDA *et al.* (2014) observed the aerobic biodegradation of DNAN by *Nocardioides* sp., the aerobic biodegradation of nitro-compounds in soils is considered not reliable since the contamination can last long periods (AMARAL *et al.*, 2009). Alternatively, the reductive anaerobic biotransformation of DNAN and NTO in soils, sludges, and microbial pure cultures generates the same compounds described in Figure 3 (KRZMARZICK *et al.*, 2015; LE CAMPION *et al.*, 1999b; OLIVARES *et al.*, 2013), except that DNAN's biological reduction is regioselective and only generates quantifiable amounts of MENA as the intermediate (HAWARI *et al.*, 2015; OLIVARES *et al.*, 2016a). Many microorganisms can use nitro compounds as electron acceptors via co-metabolic processes using non-specific redox

enzymes (nitroreductases) with an excess of electron-donating substrates (SPAIN, 1995). Differently, the reduction of nitro-compounds via microbial respiration processes is specific and provides energy for cell growth, as demonstrated previously for TNT (ESTEVE-NUÑEZ *et al.*, 2000) and 2,4-dinitrotoluene (2,4-DNT) (HUANG *et al.*, 2015). To date, microorganisms were not reported to respire IMCs.

1.3 WHAT HAPPENS TO THE REDUCED DAUGHTER PRODUCTS?

ATO, the reduced product of NTO, was shown to be removed under aerobic conditions in soil columns (MADEIRA *et al.*, 2017), mineralized to CO_2, NH_4^+, and N_2 by an aerobic culture enriched from soil (MADEIRA *et al.*, 2019a), and mineralized to urea, CO_2, and N_2 via oxidation by manganese oxides (KHATIWADA *et al.*, 2018a).

The environmental fate of DAAN, the reduced product of DNAN, is more obscure. DAAN can undergo autoxidation in aerobic conditions, forming an azo dimer and a demethylated azo derivate (HAWARI *et al.*, 2015; PLATTEN *et al.*, 2010). Additionally, DAAN can participate in coupling reactions with nitroso intermediates of DNAN reduction, also forming azo compounds (KADOYA *et al.*, 2018). However, DAAN's removal in sludge under different electron acceptor conditions as a complementary technique to DNAN's anaerobic biotransformation was not assessed yet.

In soils, DAAN was observed to disappear after DNAN's reduction. Extraction techniques could not recover adsorbed DAAN, indicating covalent incorporation (HAWARI *et al.*, 2015). OLIVARES *et al.* (2017) observed that the DAAN disappearance was due to reactions with the soil's natural organic matter (NOM). Thorn *et al.* (1996b) and Weber *et al.* (1996) carefully described the incorporation of aniline, the simplest aromatic amine, into NOM due to covalent reactions with the quinone moieties of humic and fulvic acids. The mechanisms of the covalent reactions were Michael addition and imine formation (Figure 4) (KUTYREV, 1991; PARRIS, 1980). Due to NOM's high complexity, quinone compounds have been studied as reliable models for NOM (GULKOWSKA *et al.*, 2012). Table 1 summarizes studies about reactions between aromatic amines and quinones. These studies relied the use of specific catalysts, such as phenoloxidase enzymes or metal oxides, and were conducted under aerobic conditions. However, DAAN disappearance was observed without the use of specific catalysts and under anaerobic conditions. Thus, the literature still lacks studies about the nature of the reactions leading to DAAN incorporation in NOM without specific catalysts and in the absence of O_2.

Figure 4 – Scheme of Michael addition and imine formation reactions between aromatic amines and quinones moieties of natural organic matter (NOM).

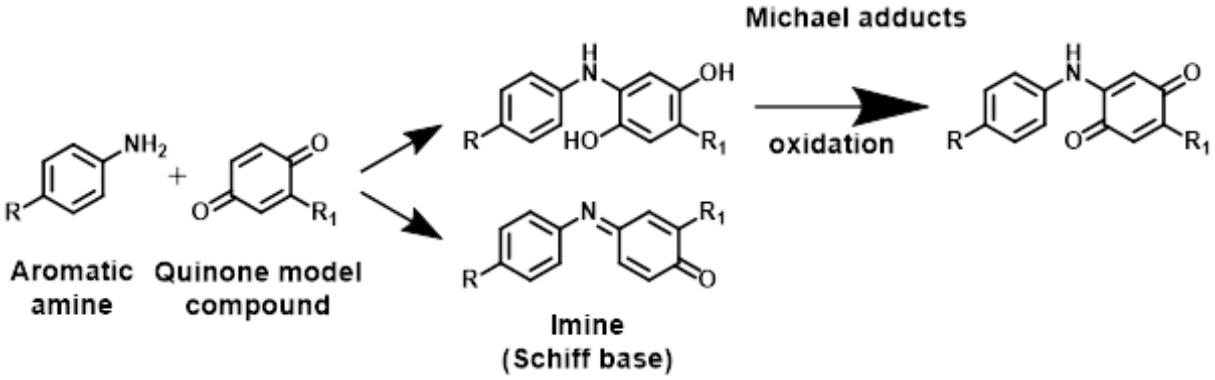

Table 1 – Review on the formation of Michael adducts and imines from the reactions between some aromatic amines and model quinone compounds (or phenolic precursors).

Aromatic amine	**Quinone or phenolic precursor**	**Michael adduct**	**Imine**	**Reference**
3,4-Dichloroaniline	4-Methylcatechol		Dimer	You *et al.* (1982)
3,4-Dichloroaniline	Methyl-1,4-benzoquinone	Dimer		Saxena and Bartha (1983)
Benzidine	2,6-Dimethyl-1,4-benzoquinone	Dimer	Dimer	Ononye *et al.* (1989)
4-Chloroaniline	Catechol	Trimer		Adrian *et al.* (1989)
Naphthalen-1-amine	2,6-Dimethyl-1,4-benzoquinone or 2,6-Di-t-butyl-1,4-benzoquinone		Dimers	Ononye and Graveel (1994)
4-Methylaniline	2,6-Dimethyl-1,4-benzoquinone	Dimer	Dimer	Ononye and Graveel (1994)
Sulfathiazole	4-Hydroxy-3-methoxybenzoic acid	Dimer	Dimer	Gulkowska *et al.* (2012)
Sulfathiazole	Cathecol, 4-methylcathecol, protocatechuic acid, or 2,4-dihydroxybenzoic acid	Dimers		Gulkowska *et al.* (2012)
Sulfathiazole	4-Hydroxy-3,5-dimethoxybenzoic acid		Dimer	GULKOWSKA *et al.* (2012)

2 RESEARCH OBJECTIVES

2.1 GENERAL OBJECTIVE

To develop new strategies for the reductive transformation of the insensitive munitions compounds DNAN and NTO and the removal of DAAN, DNAN's reduced daughter product.

2.2 SPECIFIC OBJECTIVES

a) To assess the ability of FeS minerals, such as mackinawite, in abiotically reducing DNAN and NTO;
b) to investigate the biotic process of NTO respiration by an anaerobic enrichment culture;
c) to evaluate DAAN removal in biological sludge under different electron acceptor conditions; and
d) to describe the nature of DAAN abiotic reactions with soil's natural organic matter in anoxic environments using quinones as model humic compounds.

3 DNAN AND NTO REDUCTION BY FES MINERAL SURFACES

Resulting publication: MENEZES, O.; YU, Y.; ROOT, R.; GAVAZZA; S. CHOROVER, J.; SIERRA-ALVAREZ, R.; FIELD, J. A. Abiotic reduction of insensitive munitions compounds 2,4-dinitroanisole (DNAN) and 2-nitro-1,2,3-triazol-5-one (NTO) by FeS mineral surfaces. In preparation.

Figure 5 – Graphical abstract for section 3.

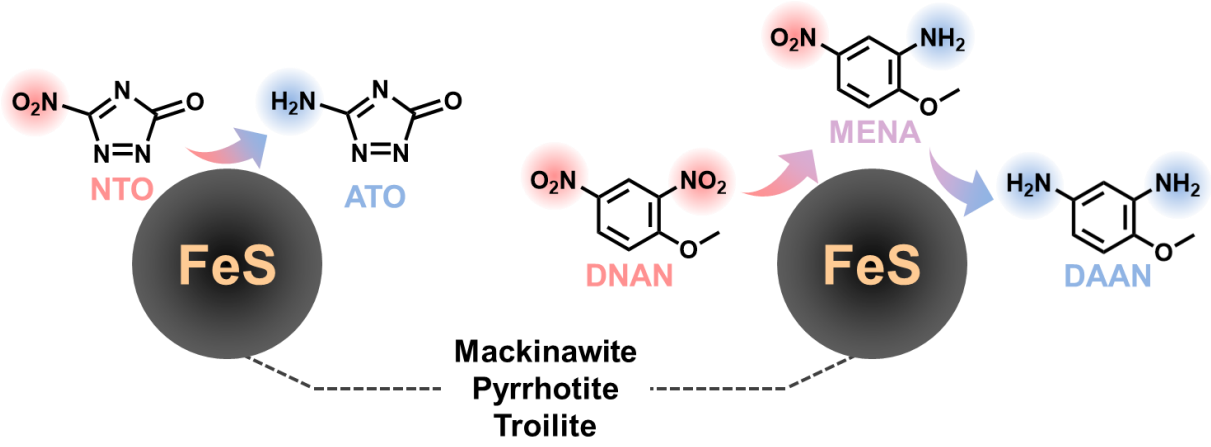

3.1 ABSTRACT

As the military applications of the insensitive munitions compounds (IMCs) 2,4-dinitroanisole (DNAN) and 2-nitro-1,2,3-triazol-5-one (NTO) increase, there is a growing need to understand the environmental fate of these contaminants and developing new remediation strategies. FeS minerals are very abundant in aquatic sediments, hydrothermal deposits, and as a coating layer of soil minerals. Herein, we show that FeS surfaces can abiotically transform DNAN and NTO to their corresponding amines under anoxic conditions and at environmentally occurring pH and temperature. We observed that mackinawite, a tetragonal FeS with a layered structure, reduced DNAN mainly to 2-methoxy-5-nitroaniline (MENA), which was partially reduced to 2-4-diaminoanisole (DAAN). The layers in the mackinawite structure were likely responsible for partial adsorption of MENA and DAAN. A commercial FeS (composed mainly of pyrrhotite and troilite) reduced DNAN all the way to DAAN. NTO was fully reduced to 3-amino-1,2,4-triazol-5-one (ATO) by both mackinawite and commercial FeS. We showed that the reactions were surface-mediated since they did not occur when only dissolved Fe^{2+} and S^{2-} were present. This is the first study to report the reduction of IMCs, including a nitro-heterocyclic compound (NTO), by FeS surfaces. Our results indicate that DNAN and NTO can

be rapidly transformed to their corresponding amines in soils and aquatic sediments rich in FeS minerals.

3.2 INTRODUCTION

The use of conventional explosives, such as 2,4,6-trinitrotoluene (TNT) and 1,3,5-trinitroperhydro-1,3,5-triazine (RDX), by military agencies has caused the contamination of soil and groundwater in many training ranges worldwide (BERNSTEIN; RONEN, 2012). Now, these conventional explosives are being replaced by insensitive munitions compounds (IMCs), such as 2,4-dinitroanisole (DNAN) and 2-nitro-1,2,3-triazol-5-one (NTO), which require higher ignition temperatures and are less vulnerable to mechanical shocks, being safer to handle (POWELL, 2016). However, IMCs still represent an environmental threat since pieces of undetonated ordnance can remain on the soil and be dissolved by precipitation, contaminating ground and surface waters (TAYLOR *et al.*, 2015a). DNAN, which has a moderately higher solubility than that of TNT (276 mg L^{-1} for DNAN, 128 mg L^{-1} for TNT) (BODDU *et al.*, 2008; PARK *et al.*, 2004), was observed to be toxic to several microorganisms (LIANG *et al.*, 2013), algae, ryegrass, earthworms (DODARD *et al.*, 2013), and zebrafish (OLIVARES *et al.*, 2016b). In its turn, NTO is highly soluble (16,642 mg L^{-1}) and, due to its low pKa (3.76), it can cause acidification of the groundwater and solubilize metals (TAYLOR *et al.*, 2015a). Additionally, NTO was found to be toxic to rats (LENT *et al.*, 2020), Japanese quails (JACKOVITZ *et al.*, 2018), and zebrafish embryos (MADEIRA *et al.*, 2018).

The nitro groups in the structures of NTO and DNAN provide electron-withdrawing characters to both compounds, making them resistant to oxidative degradation pathways, such as aerobic biodegradation in soils and sludges (OLIVARES *et al.*, 2013; OLIVARES *et al.*, 2016a), oxidation by reactive minerals, e.g., manganese oxides (KHATIWADA *et al.*, 2018a; KHATIWADA *et al.*, 2018b), and chemical oxidation by potassium permanganate (MADEIRA *et al.*, 2019b). Reductive pathways, on the other hand, can transform the nitro groups into amino groups, generating daughter compounds that can be chemically oxidized (MADEIRA *et al.*, 2019b), aerobically bioremoved (MADEIRA *et al.*, 2019a; MENEZES *et al.*, 2020), or incorporated into soil organic matter (only for DNAN reduced products) (KADOYA *et al.*, 2021). The reductive step can involve reactive minerals under anoxic conditions. For instance, zero-valent iron (ZVI), which is well known to reduce different nitro-containing compounds (AGRAWAL; TRATNYEK, 1996; WANARATNA *et al.*, 2006), was shown to reduce DNAN to its corresponding aromatic amines under regular temperature and pH. A previous study

observed that Fe/Cu particles could reduce DNAN; however, under acidic conditions (pH < 3) (KOUTSOSPYROS *et al.*, 2012). Additionally, sulfate green rust ($Fe^{2+}_4Fe^{3+}_2(OH)_{12}SO_4 \cdot 2H_2O$) can reduce both DNAN and NTO while being oxidized to lepidocrocite (γ-$Fe^{3+}O(OH)$)-like minerals at room temperature and pH 8.4 (KHATIWADA *et al.*, 2018c).

FeS minerals are the most abundant form of sulfide on Earth's lithosphere (MUYZER; STAMS, 2008) and one of the most common sulfides in aquatic sediments (MORSE *et al.*, 1987). Moreover, FeS minerals are often found coating the surfaces of soil minerals (RICKARD; MORSE, 2005). Mackinawite ($Fe_{0.995\text{-}1.023}S$) is a ubiquitous FeS mineral (BERNER, 1964; MORSE *et al.*, 1987). Amorphous mackinawite can be formed in sediments by the reaction between the biogenic ions S^{2-} and Fe^{2+} (MORSE *et al.*, 1987). Then, the initial precipitate transforms into a crystalline tetragonal iron sulfide with a layered structure that is stable under anoxic conditions and mild temperatures (JEONG *et al.*, 2008; RICKARD, 1995; TAYLOR; FINGER, 1970). The potential of FeS minerals to be used for remediation of contaminants has been extensively reported (GONG *et al.*, 2016), especially concerning heavy metals (COLES *et al.*, 2000), oxyanions (GALLEGOS *et al.*, 2007), radioisotopes (HYUN *et al.*, 2012), engineered nanoparticles (GONZALEZ-ESTRELLA *et al.*, 2016), and chlorinated organic compounds (CHEN *et al.*, 2017; JEONG *et al.*, 2007). Nevertheless, FeS minerals were not investigated for the reduction of IMCs yet. In fact, only one study (OH *et al.*, 2011) has indicated that FeS could reduce a nitro-containing compound (2,4-dinitrotoluene).

Herein, we describe for the first time the reduction of DNAN and NTO by FeS minerals (a mineralogically pure mackinawite and a commercially available FeS product). Additionally, we show that the reduction is surface-mediated and the DNAN reduced products can be partially adsorbed into mackinawite. This is also the first study demonstrating the reduction of a nitro-heterocyclic compound (NTO) by FeS.

3.3 MATERIALS AND METHODS

3.3.1 Chemicals

NTO (CAS # 932-64-9, purity > 95%) was purchased from Interchim (Montluçon, France). 3-Amino-1,2,4-triazol-5-one (ATO, CAS # 1003-35-6, purity > 95%) was purchased from PrincetonBio (Monmouth Junction, NJ, USA). DNAN (CAS # 119-37-7, purity = 98%) was purchased from Santa Cruz Biotechnology (Dallas, TX, USA). 4-Methoxy-3-nitroaniline (iMENA, CAS # 577-72-0, purity = 97%) was purchased from Accela (San Diego, CA, USA).

2-Methoxy-5-nitroaniline (MENA, CAS # 99-59-2, purity = 98%) and 2,4-diaminoanisole (DAAN, CAS # 615-05-4, purity > 98%) were purchased from Sigma-Aldrich (Saint Luis, MO, USA). Commercial FeS (CAS # 1317-37-9, purity = 99%) was purchased from Alfa Aesar (Haverhill, MA, USA).

3.3.2 Mackinawite synthesis

A synthetic, and mineralogically pure, mackinawite was prepared following Jeong *et al.* (2008). We performed the synthesis inside an anaerobic chamber (Coy Inc., Grass Lake, MI, USA) filled with 95-98% N_2 and 2-5% H_2. The Milli-Q water used was sparged with N_2 for 60 min before solutions preparation. Combining 1.2 L of a 1.10 M Na_2S solution with 2.0 L of a 0.57 M $FeCl_2$ solution produced a black FeS precipitate (BUTLER; HAYES, 1998), which was kept under vigorous mixing with a magnetic stirrer inside the anaerobic chamber for three days. The precipitated mackinawite was separated from the supernatant by centrifugation at 10,000 rpm for 15 min and then washed eight times with deoxygenated Mili-Q water and centrifugation. Later, we freeze-dried the synthesized mackinawite at -45°C under vacuum at < 0.150 mbar, grounded it in a mortar to break up any aggregates, and stored it inside sealed glass septa vials under anoxic conditions for subsequent assays.

3.3.3 Experiments

3.3.3.1 Mineral-surface reactivity

We tested the ability of the mineralogically pure mackinawite and the commercial FeS to reduce NTO and DNAN dissolved in ultra-pure water under anoxic conditions using 160-mL serum bottles with a liquid volume of 50 mL. We purged the oxygen by flushing the liquid for 4 min with 80% N_2 and 20% CO_2. Then, we closed the test tubes with t-butyl caps and aluminum seals and needle flushed the headspace for an additional 4 min with the same gas mixture. We calculated the solids/solution ratio (SSR) for the mineral-surface reactivity experiments based on the SSAs measured, so the total surface area (SA) was the same in all assays. The experiments were performed with either 4.280 g L^{-1} of mackinawite or 5.000 g L^{-1} of commercial FeS paired with either 1000 µM NTO or 400 µM DNAN. We also tested two pH conditions: 6.5 (buffer: 8.5 mM $NaHCO_3$ and 20% CO_2 in the headspace) and 7.6 (buffer: 95.2 mM $NaHCO_3$ and 20% CO_2 in the headspace). Bottles were incubated in the dark in an orbital shaker at 130 rpm and 30ºC. Subsamples (0.5 mL) for HPLC-DAD were collected at

different time intervals using syringes and needles then filtered through a 0.22-µm membrane to halt any reactions between the minerals and the compounds. The experiments were performed in triplicates.

We extracted DNAN and its reduced products adsorbed into mackinawite via sonication in acetonitrile, an adaptation of the EPA SW-846 Method 8330, originally developed for soils. After a 5-h reaction, the entire content of the bottle was filtered through a 0.22-µm membrane. The membrane with mackinawite was then placed inside a 50-mL falcon tube with 10-mL of acetonitrile, vortexed for 1 min, and sonicated for 1 h at room temperature. Then, samples of the diluted extracted were collected, filtered through a 0.22-µm membrane, and analyzed in the HPLC-DAD.

3.3.3.2 Controls

We assayed controls with NTO and DNAN to verify whether the reactions were surface-mediated or dependent on dissolved Fe^{2+} or S^{2-}. Fe^{2+} or S^{2-} concentrations were calculated as two times the stoichiometric concentration to reduce the nitro groups of NTO or DNAN to amino groups. Thus, in the controls with dissolved Fe^{2+}, we used $(NH_4)_2Fe(SO_4)_2 \cdot 6H_2O$ at concentrations of 4000 µM (for the control with 1000 µM NTO) or 3200 µM (for the control with 400 µM DNAN). In the controls with dissolved S^{2-}, the concentrations of aqueous S^{2-} (as $Na_2S \cdot 9H_2O$) were 1500 µM (for the control with 1000 µ NTO) or 1200 µM (for the control with 400 µM DNAN). Dissolved Fe^{2+} or S^{2-} were delivered as 1 mL of 50-folds concentrated solutions prepared inside the anaerobic chamber. Due to the sulfide volatility, the total amount of sodium sulfide nonahydrate was 2.74 times higher than the target concentration in the aqueous solution, calculated using Henry's law and ideal gas law for the experimental condition. In the control with dissolved Fe^{2+}, flushing was performed as described in section 3.3.3.1. In the control with dissolved S^{2-}, flushing was performed before injecting the S^{2-} concentrated solution with a syringe and needle. Incubation and sampling followed the described in section 3.3.3.1.

3.3.4 Analytical techniques

3.3.4.1 Surface area

Specific surface areas (SSA) of the commercial FeS and mackinawite were analyzed by multipoint BET (Brunauer Emmett Teller method) from dried samples with nitrogen purging at -196^{o}C (Micromeritics Gemini VII 2390t, Norcross, GA, USA).

3.3.4.2 XANES

The commercial FeS was characterized by X-ray absorption near-edge spectroscopy (XANES). Iron and sulfur K-edge spectra were collected at Stanford Synchrotron Radiation Lightsource (SSRL) beamline 11-2 and 4-3, respectively. Energy was calibrated for iron with a thin iron foil with the first inflection of the white line absorbance defined as 7112 eV. Sulfur was calibrated with sodium thiosulfate with the first peak assigned 2472.04 eV. Freeze-dried unreacted and reacted samples were ground, loaded into Al sample holders, sealed with Kapton tape, and placed in a liquid nitrogen (LN_2) cryostat. All scans ($n \geq 4$) were averaged using the SIXPACK software package, spectra were background-subtracted, normalized, and quantitatively analyzed by linear combinations fitting (LCF) using reference minerals collected under similar conditions using the Athena software package (RAVEL; NEWVILLE, 2005).

3.3.4.3 XRD

Mackinawite and commercial FeS were analyzed by X-ray diffraction (XRD). Mackinawite was analyzed at the University of Arizona. The sample was placed on zero background silicon wafers. The diffractogram was collected (λ = 1.5405 Å) from 4 degrees to 68 degrees 2θ at 0.01-degree 2θ steps (PANanalytical X'Pert PRO with an ultra-fast X'Celerator detector, Malvern Panalytical, Malvern, UK). The commercial FeS was analyzed at the Stanford Synchrotron Radiation Laboratory. The sample was placed between two layers of acrylate polymer adhesive tape (Magic Tape, Scotch, St. Paul, MN, USA) and collected at the SSRL beam line 11-3, in transmission mode with (λ = 0.9753 Å) with a MAR345 image plate with a focused spot size of 150 μm, and calibrated with a LaB_6 standard. The tape was collected as a background that was subtracted from the data. Data analysis, peak identification, and assignment of crystalline phase were performed using the X'Pert HighScore Plus (Malvern Panalytical, Malvern, UK) software with ICCD PDF-2 diffraction reference files.

Diffractograms collected at different X-ray energies were all converted to Cu-Kα radiation for conventional comparisons.

3.3.4.4 HPLC-DAD

Liquid samples were analyzed by high-performance liquid chromatography (HPLC). NTO and ATO were analyzed using an Agilent 1290 Infinity HPLC coupled to a diode array detector (DAD). A Hypercarb column (Thermo Scientific, Waltham, MA, USA) was exposed to a gradient of water with 0.1% trifluoroacetic acid and acetonitrile, as described by MADEIRA *et al.* (2017).

DNAN, MENA, iMENA, and DAAN were analyzed using a Shimadzu LC-20AT (Kyoto, Japan) HPLC-DAD equipped with a Zorbax Eclipse XDB-C18 column (5 µm, 4.6 × 250 nm) (Agilent, Santa Clara, CA, USA). The mobile phase was a methanol/5-mM phosphate buffer (46/54% v/v) running isocratically (0.6 mL min-1) at 30 ºC. The injection volume was 100 µL. The method detected DNAN, MENA, iMENA, and DAAN at 300, 254, 254, and 210 nm, respectively. The retention times were 16.0 min for DNAN, 11.6 min for MENA, 8.7 min for iMENA, and 6.4 min for DAAN.

3.4 RESULTS AND DISCUSSION

3.4.1 Characterization of FeS minerals

The mackinawite and the commercial FeS presented similar specific surface areas (SSAs), as shown in Table 2. Successful mackinawite's synthesis was confirmed by an XRD analysis, as shown in Appendix A.

We also analyzed the commercial FeS on XANES, an element-specific analysis, as seen in Figure 6. Results showed that, although the stoichiometry of the commercial FeS was probably correct, the material was composed of a mixture of different compounds containing Fe and S, with mineral FeS forms being predominant. XRD, a qualitative non-element-specific technique able to identify crystalline structures, confirmed the presence of FeS mineral forms and indicated the occurrence of pyrite (FeS_2) in the commercial FeS (Figure 7). The predominant minerals in the commercial FeS were pyrrhotite and troilite. The fitting in the XANES analysis could not differentiate between those minerals due to their high similarity. Equally good fits could be obtained within a range of each (pyrrhotite and troilite), so results are presented as a sum of both minerals. Pyrrhotite exhibits the composition $F_{1-x}S$. The most

iron-deficient forms, which have a monoclinic crystalline structure, presents x = 0.125. The pyrrhotite has a hexagonal crystalline structure when $x \leq 0.1$. Troilite is the stoichiometric form of pyrrhotite, with x = 0, also presenting hexagonal symmetry (BELZILE *et al.*, 2004). Pyrrhotite is the most abundant iron sulfide in the Earth. It is widespread in hydrothermal deposits but, differently from mackinawite, very rare in aquatic sediments. In contrast, naturally occurring troilite is rare in the Earth and is mainly found in meteorites (RICKARD; LUTHER, 2007). Thus, the characterization of the commercial FeS indicates that its reactivity towards IMCs can be evaluated for the development of mineral-packed reactors. On the other hand, the evaluation of mackinawite has applications on both mineral-packed reactors and the assessment of IMCs' fate in soils and aquatic sediments.

Figure 6 – S and Fe Kα XANES spectra with relative abundances of each mineral form detected. XANES is an element-specific technique. Panel A: Sulfur (S) XANES. Panel B: Iron (Fe) XANES. The black line labeled as "commercial FeS" represents the collected data, whereas the dashed red line represents the fit to the model (sum of the different mineral forms in the sample).

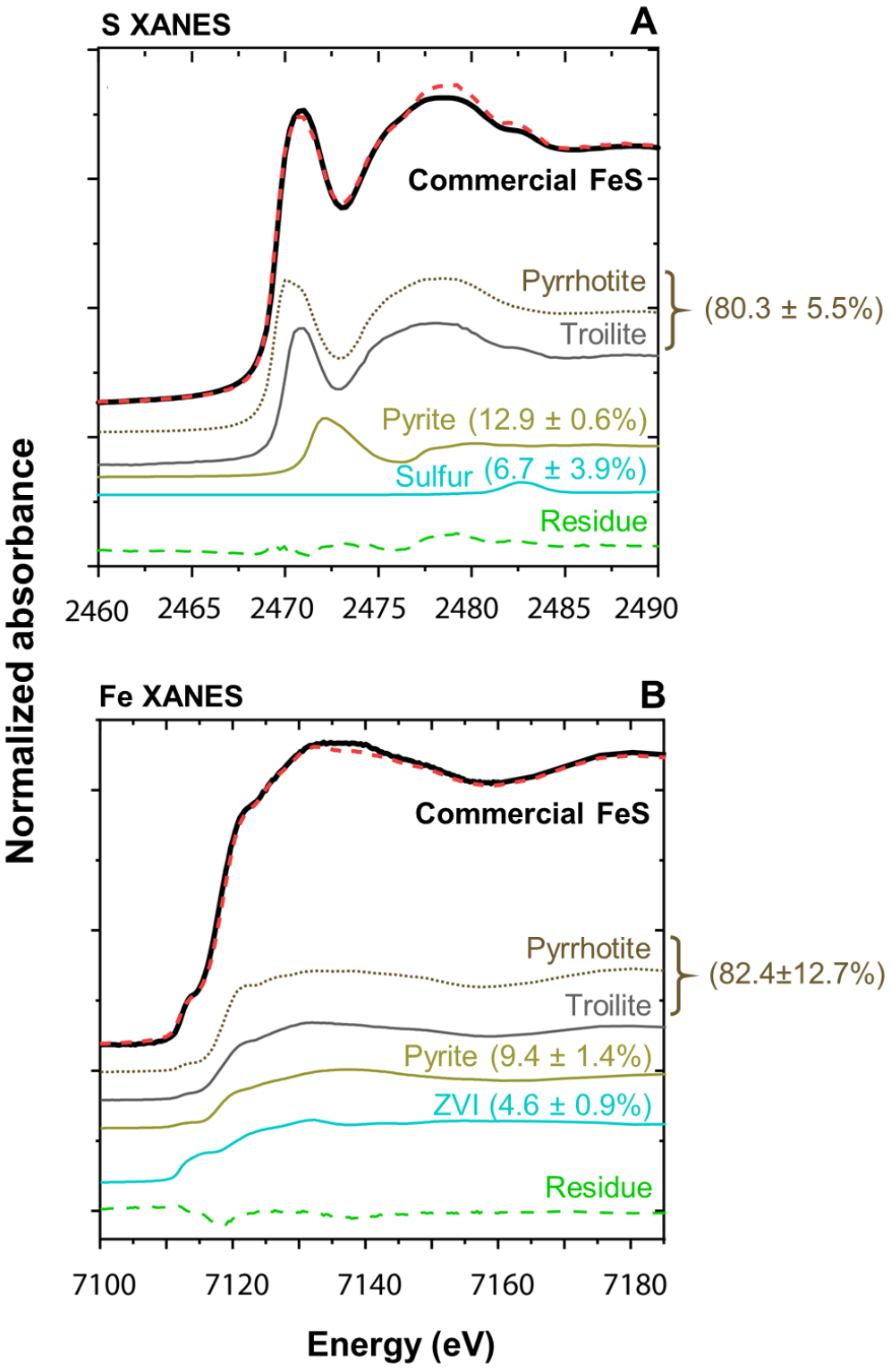

Figure 7 – XRD spectrum for commercial FeS. XRD is a qualitative analysis able to detect crystal structures. The vertical lines labeled as “troilite”, “pyrrhotite”, “pyrite”, and “ZVI” represent the expected peaks exhibited by the respective minerals in XRD.

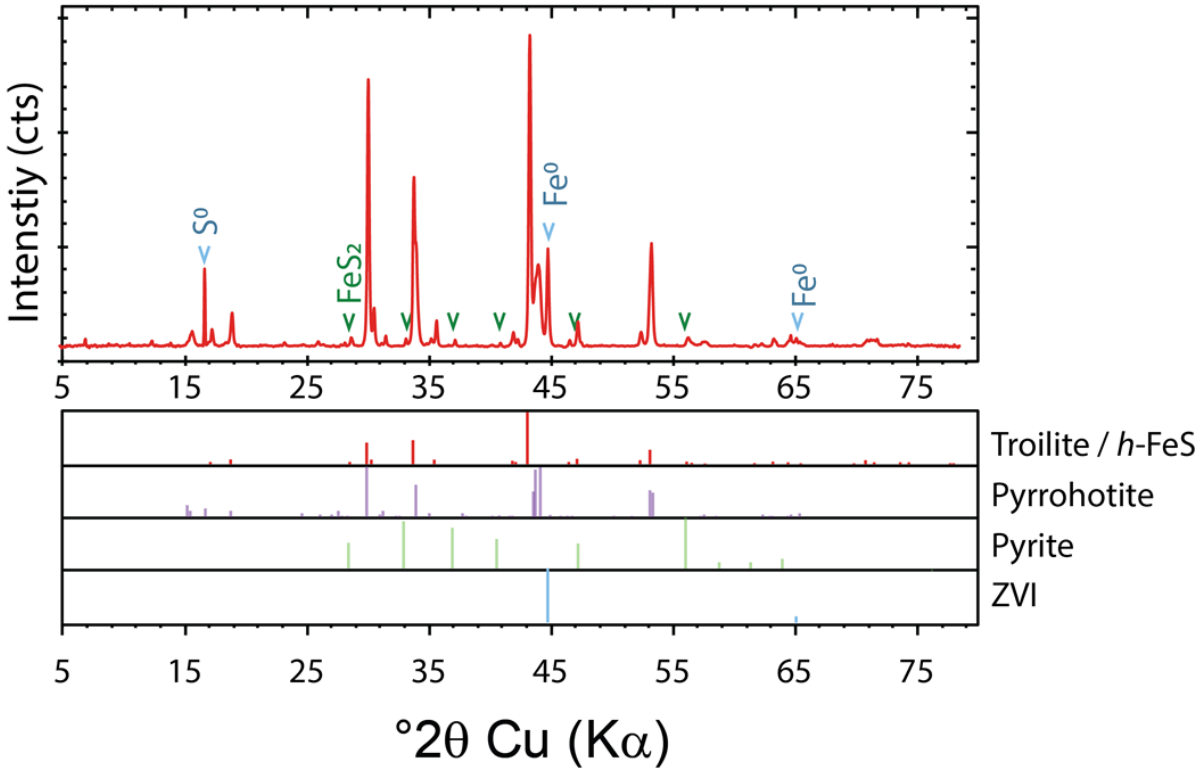

3.4.2 FeS minerals reactivity

Both the mackinawite and the commercial FeS reduced the IMCs tested (Table 2, Figures 8 and 9). DNAN was reduced in two steps (Figure 8). Firstly, the nitro group in the ortho position was reduced to an amino group, forming 2-methoxy-5-nitroaniline (MENA). Then, MENA’s nitro group in the para position was reduced, forming 2,4-diaminoanisole (DAAN). As an alternative pathway, we observed the formation of a minor intermediate, 4-methoxy-3-nitroaniline (iMENA), which resulted from the reduction of the DNAN’s nitro group in the para position. iMENA was also further reduced to DAAN. The maximum concentration observed for iMENA was only 16 µM (0.9 h, DNAN + commercial FeS at pH = 6.5), corresponding to 4.2% of the initial DNAN concentration and 10.8% of MENA concentration in the same sample. Thus, DNAN’s reduction by FeS minerals was regioselective towards the ortho nitro group. Curiously, DNAN’s reduction by sulfate green rust produced almost equivalent concentrations of MENA and iMENA (KHATIWADA *et al.*, 2018c). Ahn *et al.* (2011) mention the occurrence of both MENA and iMENA as intermediates of DNAN’s reduction by ZVI without differentiating between the isomers. In agreement with our observations, other studies with ZVI show that MENA was indeed the major intermediate

(HAWARI *et al.*, 2015; OU *et al.*, 2015). Additionally, MENA was reported as the only detectable intermediate of DNAN's biological reduction (HAWARI *et al.*, 2015; OLIVARES *et al.*, 2013; OLIVARES *et al.*, 2016a).

Although both mackinawite and commercial FeS reduced DNAN, those FeS minerals behaved differently. The final products of DNAN reduction by mackinawite were MENA (percentage of initial DNAN concentration: 11.4 ± 2.4% at pH 6.5 and 22.8 ± 3.7% at pH 7.6) and DAAN (5.6 ± 0.3% at pH 6.5 and 19.7 ± 6.6% at pH 7.6). However, the reduction by commercial FeS did not accumulate MENA, forming only DAAN as the final product.

Since we observed a poor yield of reduced products in the solution after DNAN's reaction with mackinawite, we performed an extraction of possibly adsorbed products from the reacted mackinawite using sonication with acetonitrile. We could recover adsorbed MENA (percentage of initial DNAN concentration: 31.6 ± 0.2% at pH 6.5 and 33.6 ± 7.2% at pH 7.6) and DAAN (30.4 ± 5.8% at pH 6.5 and 20.1 ± 3.6% at pH 7.6) from mackinawite, and not DNAN, which indicates that DNAN was fully reduced and not merely adsorbed. The surface excess (q_{ads}), representing the amount of compound recovered per mass of mackinawite, was 28.5 ± 0.2 and 29.7 ± 6.3 7.6 for MENA at pH 6.5 and 7.6, respectively, and 27.5 ± 5.2 mmol kg^{-1} and 17.7 ± 3.2 mmol kg^{-1} for DAAN at pH 6.5 and 7.6, respectively. The adsorption may be related to the layered structure of mackinawite, as opposed to the three-dimensional structure of pyrrhotite and troilite (main components of the commercial FeS). Linker *et al.* (2015) observed that a clay mineral with a layered structure (montmorillonite) could adsorb MENA in a process involving interlayer intrusion of the compound. Mackinawite exhibit layers spaced approximately at 5 Å (JEONG *et al.*, 2008), a similar spacing to that occurring between montmorillonite layers (≈ 9.5 – 10.0 Å) (BRINDLEY, 1951). This similarity suggests an influence of the layered structure in the mackinawite's adsorption capacity.

Table 2 – Parameters of NTO and DNAN reduction on FeS mineral surfaces.

IMC	Mineral surface	SSA ($m^2 g^{-1}$) [(i)]	SSR ($g L^{-1}$) [(ii)]	Total SA (m^2) [(iii)]	pH	k_{IMC} (h^{-1}) [(iv)]	Recovery of reduced products (%)
DNAN	Mackinawite	0.25	4.28	0.0535	6.5	13.7 ± 2.2	79.0 ± 5.3 [(v)]
					7.6	10.1 ± 1.7	96.2 ± 10.9 [(v)]
	Commercial FeS	0.214	5.00	0.0535	6.5	5.0 ± 0.1	74.8 ± 4.0
					7.6	10.2 ± 0.2	109.5 ± 15.8
NTO	Mackinawite	0.25	4.28	0.0535	6.5	7.3 ± 0.7	88.8 ± 0.5
					7.6	4.4 ± 1.9	96.5 ± 1.4
	Commercial FeS	0.214	5.00	0.0535	6.5	5.1 ± 0.9	89.5 ± 0.6
					7.6	3.8 ± 1.6	87.8 ± 0.8

[(i)] Specific surface area.

[(ii)] Solids solution ratio.

[(iii)] Total surface area.

[(iv)] All R^2 (correlation coefficient) values were above 0.95.

[(v)] The values include the products recovered by extraction from the mackinawite with acetonitrile.

Figure 8 – DNAN reduction on FeS mineral surfaces at different pH values. Panel A: DNAN + mackinawite at pH 6.5. Panel B: DNAN + commercial FeS at pH 6.5. Panel C: DNAN + mackinawite at pH 7.6. Panel D: DNAN + commercial FeS at pH 7.6. Legend: DNAN (●), MENA (▲), iMENA (△), DAAN (○), and DNAN + MENA + iMENA + DAAN (dashed line). Symbols represent the average of three replicates, and error bars represent the standard deviation.

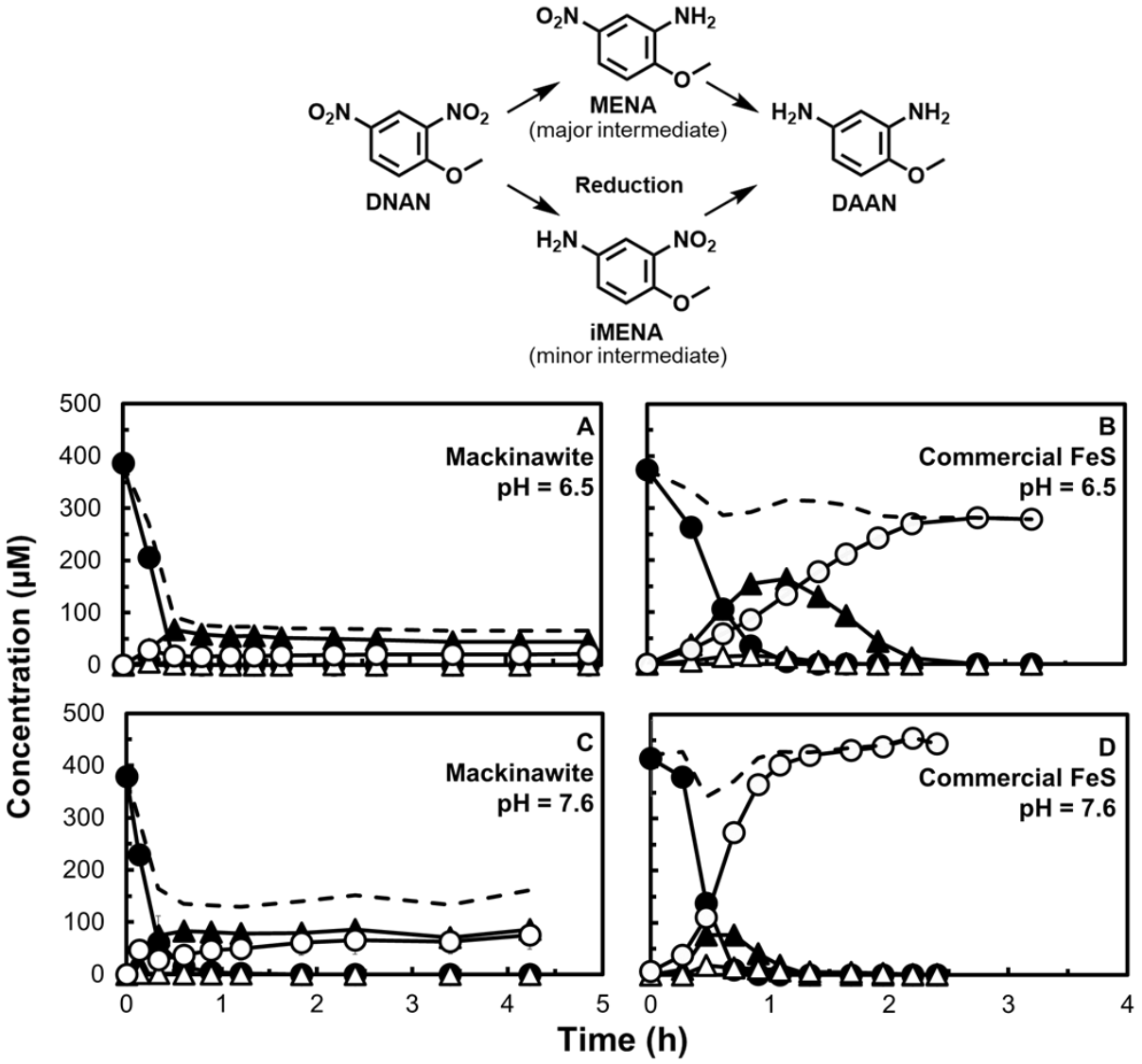

Unlike DNAN, NTO was utterly reduced to 3-amino-1,2,4-triazol-5-one (ATO) by both mackinawite and commercial FeS without significant adsorption (Figure 9). ATO is also the product of the biological reduction of NTO (KRZMARZICK *et al.*, 2015; LE CAMPION 1999b). So far, only Khatiwada *et al.* (2018c) have observed the reduction of NTO to ATO by a reactive mineral (sulfate green rust). Other studies have observed NTO disappearance in Fe/Cu bimetal systems at acidic conditions (KOUTSOSPYROS *et al.*, 2012), with the formation of urea (KITCHER *et al.*, 2017). However, unlike in our study, ATO was not detected.

Figure 9 – NTO reduction on FeS mineral surfaces at different pH values. Panel A: NTO + mackinawite at pH 6.5. Panel B: NTO + commercial FeS at pH 6.5. Panel C: NTO + mackinawite at pH 7.6. Panel D: NTO + commercial FeS at pH 7.6. Legend: NTO (⧫), ATO (◊), and NTO + ATO (dashed line). Symbols represent the average of three replicates, and error bars represent the standard deviation.

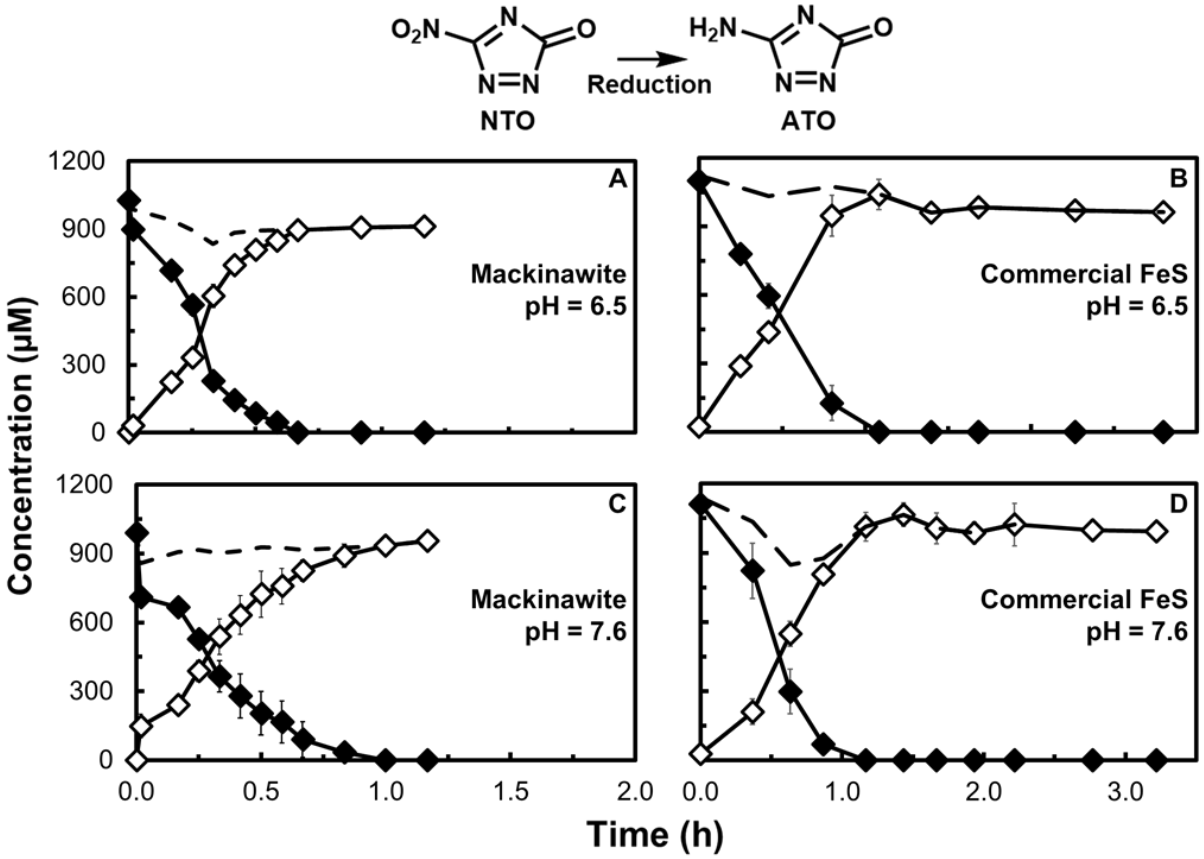

Variations on the pH in the range evaluated in this study were not a game-changer. However, varying the pH may have influenced the reactions in two ways. Firstly, by changing the pH from 6.5 to 7.6 using a sodium bicarbonate/CO_2 buffer, Na^+ concentration severely increased in the system, going from 8.5 mM Na^+ to 95.2 mM Na^+. Cations such as Na^+ can cause the desorption of compounds from the minerals (KHATIWADA *et al.*, 2018c; LINKER *et al.*, 2015), which may explain the higher concentration of MENA and DAAN in the solution after DNAN's reaction with mackinawite at pH 7.6 compared to mackinawite at pH 6.5. Therefore, this effect was probably due to Na^+ concentration and not to pH changes. Secondly, at pH 7.6, dissolved Fe^{2+} precipitated, forming a surface that partially reduced DNAN and NTO, as discussed in section 3.4.3.

3.4.3 Were the reactions surface-mediated?

To test whether the reduction of IMCs occurred on the surface of the FeS minerals or by reactions with the dissolved ions, we combined DNAN and NTO with dissolved Fe^{2+} and S^{2-} in separated assays. We observe that both IMCs were stable when paired with S^{2-} regardless of the pH condition. Nonetheless, a pH effect was observed for the control with dissolved Fe^{2+}. At pH 6.5, no precipitate was formed and both DNAN and NTO were stable. At pH 7.6, however, a precipitate was formed, generating a surface that probably contained Fe^{2+}. This precipitate exhibited reactivity towards the IMCs, partially reducing these compounds for a limited interval (approximately 4.5 h for DNAN and 2.0 h for NTO). DNAN was reduced mostly to MENA (91.4 ± 4.1%), whereas NTO was partially reduced to ATO (59.9 ± 2.2%). Our results indicate that the reductions of DNAN and NTO are, indeed, surface-mediated. In the assays with the FeS minerals at pH 7.6, the precipitate with Fe^{2+} may have contributed with the FeS minerals for the IMCs' reduction. However, at pH 6.5, the mackinawite and the commercial FeS were the only responsible for the IMCs reduction since no precipitate is formed.

4 CONCLUSIONS

Mackinawite and commercial FeS can abiotically reduce DNAN and NTO to their respective amino-containing daughter products under anoxic conditions and at environmentally occurring pH and temperature. The reductive transformation is surface-mediated, not taking place when only dissolved Fe^{2+} and S^{2-} are present. As opposed to the three-dimensional structure of pyrrhotite and troilite (main components of the commercial FeS), the layered structure of mackinawite makes it more suitable for adsorption reactions with DNAN's aromatic amines reduced products. The reduction of IMCs by FeS minerals contributes to understanding the geochemical transformations of IMCs in soils and aquatic sediments. Our results also suggest that mackinawite and commercial FeS can be applied for the engineered remediation of DNAN and NTO. Further experiments will focus on the products of FeS minerals oxidation due to their exposure to IMCs.

4 NTO MICROBIAL RESPIRATION

Resulting publication: MADEIRA, C. L.*; MENEZES, O.*; PARK, D*.; HATT, J.; GAVAZZA, S. KRZMARZICK, M. J.; SIERRA-ALVAREZ, R.; SPAIN, J.; KONSTANTINIDIS, K. T.; FIELD, J. A. Bacteria make a living breathing the insensitive munitions compound 3-Nitro-1,2,4-triazol-5-one (NTO). Submitted for publication. *Shared co-first authorship.

Figure 10 – Graphical abstract for section 4.

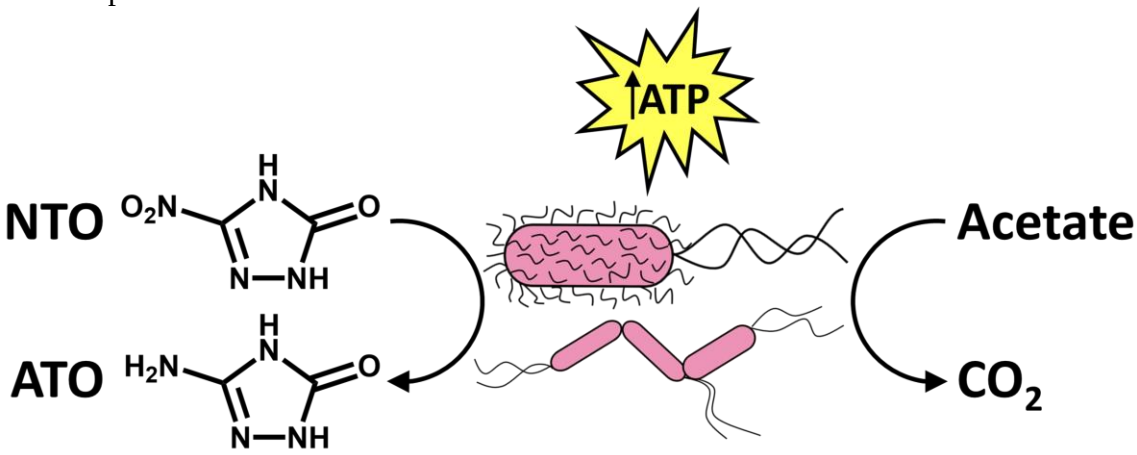

4.1 ABSTRACT

The nitro-heterocyclic 3-nitro-1,2,4-triazol-5-one (NTO) is an ingredient of insensitive explosives increasingly used by the military, becoming an emergent environmental pollutant. Cometabolic biotransformation of NTO occurs in mixed microbial cultures in soils and sludges with an excess of electron-donating substrates. Herein we present the unusual energy-yielding metabolic process of NTO respiration, in which the NTO reduction to 3-amino-1,2,4-triazol-5-one (ATO) is linked to the anoxic acetate oxidation to CO_2 by a culture enriched from municipal anaerobic digester sludge. Cell growth was observed simultaneously with NTO reduction, whereas the culture was unable to grow in the presence of acetate only. Extremely low concentrations (0.06 mg L^{-1}) of the uncoupler carbonyl cyanide m-chlorophenyl hydrazone inhibited NTO reduction, indicating that the process was linked to ATP formation. The ultimate evidence of NTO respiration was ATP production due to simultaneous exposure to NTO and acetate. Metagenome sequencing revealed that the main microorganisms (and relative abundances) were *Geobacter anodireducens* (89.3%) and *Thauera* sp. (5.5%). Possible mechanisms involved in NTO reduction, e.g., nitroreductases and cytochromes, are discussed.

This study is the first description of a nitro-heterocyclic compound being reduced in anaerobic respiration, shedding light on creative microbial processes that enable bacteria to make a living reducing NTO.

4.2 INTRODUCTION

To mitigate the inadvertent initiation of conventional munitions, explosive compounds with lower sensitivity to shock and thermal decomposition, such as the nitro-heterocyclic 3-nitro-1,2,4-triazol-5-one (NTO), have been selected as ingredients of insensitive munitions (POWELL, 2016). The development of insensitive munitions formulations has led to an increase in the manufacture and use of NTO, causing the potential for release of the compound in wastewater from manufacturing sites and the natural environment through the detonation of explosives in military training ranges (TAYLOR *et al.*, 2015b). Due to its high solubility (16,642 mg L^{-1}) and low pK_a (3.76), NTO can dissolve in water quickly upon entering the soil and potentially cause the acidification of the soil solution, affecting the aquatic biota and mobilizing metals (TAYLOR *et al.*, 2015a). Additionally, NTO was reported to cause toxic effects to several organisms, such as testicular toxicity in male rats (CROUSE *et al.*, 2015; LENT *et al.*, 2020), neuromuscular anomalies in Japanese quail (JACKOVITZ *et al.*, 2018), and abnormal swimming behavior in zebrafish embryos (MADEIRA *et al.*, 2018). Therefore, strategies for removing NTO in non-target environments such as soils, groundwater, and wastewater should be developed.

Microorganisms are known for playing an essential role in remediation strategies to remove anthropogenic xenobiotic contaminants. In typical aerobic respiration, contaminants are used by microorganisms as electron donors, and oxygen is used as the electron acceptor (HAYAISHI, 2012; STAMS *et al.*, 2006). However, compounds containing electron-withdrawing functional groups, such as halogens, carbonyl, sulfonyl, cyano, and nitro groups, are very persistent in aerobic environments since they are less prone to microbial-catalyzed oxidation. Under anaerobic conditions, certain microorganisms can perform creative reductive processes, using xenobiotic compounds as the final electron acceptors in respiration. The reduction of halogenated benzoates by an anaerobic consortium was discovered in 1982 (SUFLITA *et al.*, 1982). Then, 3-chlorobenzoate was found to be degraded by an anaerobic coculture containing a dechlorinator (which reduced 3-chlorobenzoate to benzoate), a benzoate degrader (which oxidized benzoate to acetate, CO_2, and H_2), and a methanogen (which reduced CO_2 to CH_4). Both the dechlorinator and the methanogen used the H_2 generated by the benzoate

degraders as the electron donor. Increases in adenosine triphosphate (ATP) production and cell growth were coupled to the addition of 3-chlorobenzoate, indicating that energy was derived from using 3-chlorobenzoate as an electron acceptor (DOLFING; TIEDJE, 1987). The use of organohalogens as terminal electron acceptors in anaerobic respiration is now a well-established microbial reaction (BOMMER *et al.*, 2014), and it has been widely applied in bioremediation of sites contaminated with chlorinated compounds, such as tetrachloroethene (PCE) (MAYMOGATELL *et al.*, 1997) and trichloroethene (TCE) (EDWARDS, 2014).

Other contaminants with oxidized functional groups are also reduced by microorganisms providing energy for cell growth. Certain compounds containing a sulfonate functional group can serve as the terminal electron acceptor for anaerobic respiration (LIE *et al.*, 1996). The cell growth of sulfate-reducing bacteria was linked to the transformation of 2-hydroxyethanesulfonate, where the sulfonate moiety was reduced and released as sulfide, and the carbon skeleton functioned as the electron donor. Nitroaromatics also participate in the respiration of anaerobic bacteria. The reduction of the explosive 2,4,6-trinitrotoluene (TNT) was coupled to proton translocation in a *Pseudomonas* sp. strain JLR11, indicating that the reduction of its nitro groups may have contributed to a transmembrane proton gradient driving ATP synthesis. As a second cue of TNT respiration, bacteria grew in minimal medium with acetate as the electron donor and TNT as the only possible electron acceptor under anoxic conditions (ESTEVE-NUÑEZ *et al.*, 2000). Similarly, the marine bacterium *Shewanella marisflavi* EP1 anaerobically reduced 2,4-dinitrotoluene (2,4-DNT) via a respiratory process, demonstrated by the inhibition of 2,4-DNT reduction by the electron transport chain inhibitors Cu^{2+}, dicumarol, and metyrapone (HUANG *et al.*, 2015). However, microorganisms able to make a living respiring nitro-heterocyclic compounds such as NTO have not been reported to date.

In this study, we enriched from a municipal anaerobic digester sludge a culture that reduces NTO to 3-amino-1,2,4-triazol-5-one (ATO) under anaerobic conditions using acetate as the electron donor. Cell growth and ATP production were linked to NTO reduction, a process that could be inhibited by a respiratory uncoupler, indicating that NTO was used as the terminal electron acceptor in respiration. Additionally, we performed shotgun metagenome sequencing of the enrichment culture to identify the microorganisms present in the culture.

4.3 MATERIALS AND METHODS

4.3.1 Inoculum

The enrichment culture was originally developed using anaerobic digester sludge from the Tres Rios Wastewater Reclamation Facility in Tucson, Arizona, as inoculum. The volatile suspended solids (VSS) content of the sludge was 1.60% (w/w), determined according to Standard Methods (APHA, 2017).

4.3.2 Chemicals

NTO (CAS# 932-64-9, purity > 95%) was purchased from Interchim (Montluçon, France), ATO (CAS# 1003-35-6, purity > 95%) was purchased from PrincetonBio (Monmouth Junction, NJ, USA), sodium acetate (CAS# 127-09-3, purity = 99.7%) was purchased from Fisher Scientific (Hampton, NH, USA), ferric citrate (CAS# 3522-50-7, 18-20% of Fe^{3+} content) was purchased from Chem-Impex International (Wood Dale, IL, USA), and carbonyl cyanide *m*-chlorophenyl hydrazone (CCCP, CAS# 555-60-2, purity = 98%) was purchased from Acros Organics (Geel, Belgium).

4.3.3 Experiments

4.3.3.1 Enrichment culture development

An NTO-reducing culture was enriched from municipal anaerobic digester sludge (1.0 g VSS L^{-1}) with acetate as the electron donor and carbon source under anaerobic conditions. The mineral medium contained the following ingredients (in mg L^{-1}): K_2HPO_4 (250), $CaCl_2.2H_2O$ (10), $MgSO_4.7H_2O$ (100), NH_4Cl (20), $NaHCO_3$ (4,000), and trace element solution (1 mL L^{-1}). The solution of trace elements contained (in mg L^{-1}): H_3BO_3 (50), $FeCl_2.4H_2O$ (2,000), $ZnCl_2$ (50), $MnCl_2.4H_2O$ (50), $(NH_4)_6Mo_7O_{24}.4H_2O$ (50), $AlCl_3.6H_2O$ (90), $CoCl_2.6H_2O$ (2,000), $NiCl_2.6H_2O$ (50), $CuCl_2.2H_2O$ (30), $NaSeO_3.5H_2O$ (100), EDTA (1,000), 36% HCl (1 mL). NTO and sodium acetate concentrations were, respectively, 500 and 2000 µM, unless otherwise specified, and the total suspension volume was 50 mL. The experiments were performed in closed 160-mL serum bottles flushed with 80% N_2 / 20% CO_2 and kept in the dark in an orbital shaker at 130 rpm and 30°C. When NTO disappeared, we

transferred 5% (v/v) of the suspension to different bottles containing NTO, acetate, and mineral medium.

After 54 transfers, two dilutions-to-extinction were carried out to enrich the culture further. This experiment consisted of serial dilutions of 10% (v/v) prepared under the same conditions described for the transfers, except that 25-mL assay tubes with 10 mL of liquid volume were used. In the first dilution-to-extinction, NTO reduction was observed in all the triplicates up to the 8^{th} dilution (10^{-8} of the original volume), which was used as inoculum in a second dilution-to-extinction. In the second experiment, NTO reduction was observed in all the triplicates up to the 5^{th} dilution (10^{-5} of the original volume), which was used to re-inoculate serum bottles for further experiments and microbial community characterization.

4.3.3.2 NTO reduction by the enrichment culture

The reduction of NTO simultaneous with acetate oxidation and cell growth was assessed in a closed-bottle experiment using the enrichment culture after the dilutions-to-extinction as the inoculum (4% v/v). The total volume of the suspension in the serum bottles was 50 mL. The gas phase was composed of 80% N_2 / 20% CO_2. The concentrations of NTO and acetate were 3 mM. Liquid samples were removed at selected time points for high-performance liquid chromatography (HPLC) and gas chromatography-flame ionization detector (GC-FID) analysis (0.6 mL sample diluted in 0.6 mL MilliQ water). The samples were clarified by centrifugation (13,000 rpm for 10 min). For acetate analysis, 10 µL of concentrated formic acid was added to the samples. Cell growth was measured by using optical density at 600 nm (OD600). A calibration curve correlating the OD600 and the volatile suspended solids (VSS) content of the biomass (expressed as mg VSS L^{-1}) is shown in Appendix B.

A similar closed-bottle experiment was carried out to assess the production of CO_2 linked to acetate removal. In this experiment, bicarbonate and CO_2 were replaced with a phosphate buffer (798 mg L^{-1} KH_2PO_4 and 1596 mg L^{-1} K_2HPO_4, pH 7.2), and the bottles were flushed with 100% He to eliminate background CO_2. The biomass was washed before inoculation to remove residual bicarbonate present in the medium. The total suspension volume was 100 mL, and the concentrations of NTO and acetate were 2 mM. The total concentrations of CO_2 in the system were calculated based on the ideal gas law, Henry's law, and acid-base equilibrium.

4.3.3.3 NTO reduction under limiting-acetate conditions

The NTO reduction by the enrichment culture was tested using limiting concentrations of acetate. The enrichment culture was inoculated at a rate of 4% (v/v) in a mineral medium containing 1000 µM NTO and different concentrations of acetate (0, 225, 450, 675, and 900 µM). The total volume of the suspension was 50 mL. The bottles were flushed with 80% N_2 / 20% CO_2 and incubated as previously described. Liquid samples were clarified by centrifugation for HPLC and GC-FID analyses of NTO and acetate concentrations, respectively.

4.3.3.4 Inhibition of NTO reduction by CCCP

We assessed the CCCP effect on the NTO reduction by the enrichment culture to verify if NTO reduction was linked to microbial respiration. Serum bottles were inoculated with 2% (v/v) of the enrichment culture. CCCP concentrations varied from 0.006 to 6.000 mg L^{-1}, and were delivered using 0.5 mL of ethanol. Controls were assayed without CCCP but with ethanol addition. The remaining experimental conditions were the same as described for the enrichment culture transfers. HPLC samples were clarified and analyzed as previously described.

4.3.3.5 ATP measurement

We grew cells for ATP measurements by cultivating the enrichment culture in 500 mL of mineral medium containing 4 mM NTO and 4 mM acetate distributed in 10 serum bottles. After complete NTO reduction, we concentrated the cells by centrifuging the content of the bottles for 20 min at 4000 rpm. The cell suspension was washed two times with fresh medium without NTO or acetate, followed by centrifugation. Then, we transferred 1.5 mL of the concentrated cell suspension to different 25-mL assay tubes in triplicates. Tubes were sealed with t-butyl caps and aluminum seals and flushed with 80% N_2 / 20% CO_2. We added NTO and acetate (1000 µM) into the sacrificial assay tubes 3.5 h before ATP measurement. We also performed controls with NTO only, with acetate only, without NTO and acetate (both at 0.0 or 3.5 h), and abiotic (medium only with NTO and acetate). The incubation was carried out under the same conditions as described for the transfers. We measured the ATP production by the enrichment culture using an ATP Assay Kit from Millipore Sigma (Burlington, MA, USA) following the manufacturer's protocol. More information about ATP measurement is described in the Supporting information (SI). We also measured NTO concentration and OD600.

4.3.3.6 Use of alternative electron acceptors and electron donors

We assessed the ability of our enrichment culture to use different combinations of electron acceptors and electron donors in closed-bottle experiments. For the experiments using alternative electron acceptors, the enrichment culture (4% v/v) was incubated in mineral medium containing 2000 µM acetate, except for the experiment with ferric citrate, in which we used 1000 µM acetate. All the bottles were flushed with 80% N_2 / 20% CO_2. The electron acceptors were added to the bottles through concentrated stock solutions to final concentrations of 1000 µM for 4-nitroimidasole, 2-methyl-4(5)-nitroimidasole, 4-nitroanisole, 4-nitrophenol, 2,4-dinitrotoluene, nitroguanidine, 3-nitrotriazole, and 3-nitripyrazole. In the experiments using alternative electron acceptors, the disappearance of the nitro-containing compounds was assessed via HPLC measurements.

We tested the ability of our enrichment culture to reduce Fe^{3+} in the form of soluble ferric citrate. The enrichment culture (2% v/v) was incubated in mineral medium containing 500 µM ferric citrate and 1000 µM acetate. The total volume of the suspension was 50 mL, and the headspace was flushed with 80% N_2 / 20% CO_2 to create anaerobic conditions. Additionally, we had a control without acetate (Fe^{3+} + EC) and an abiotic control (Fe^{3+} + Ac). The bottles were kept in the dark in a shaker at 130 rpm and 30ºC. Samples taken over time were acidified to prevent Fe^{2+} oxidation and then clarified by centrifugation. The increase in Fe^{2+} concentration over time was assessed using the Ferrozine method (STOOKEY, 1970).

For the experiments using alternative electron donors, the enrichment culture (4% v/v) was incubated in mineral medium containing 1000 µM NTO. Glucose and ethanol were added through stock solutions to final concentrations of 500 and 1000 µM, respectively. In the treatment containing hydrogen, 10 mL of pure H_2 were added to the sealed bottles using a syringe. The total suspension volume was 50 mL, and the bottles were kept in the dark in an orbital shaker at 130 rpm and 30ºC. In the experiments testing the use of alternative electron donors, we assessed the disappearance of NTO over time. All the samples were clarified by centrifugation prior to analysis.

4.3.3.7 Effect of iron concentration on NTO reduction rate

To investigate the use of Fe by the enrichment culture (2% v/v) as a redox mediator for NTO reduction, we conducted an experiment with different added Fe^{2+} concentrations in the

medium (0.0, 0.6, and 1.8 mg L^{-1}) as ferrous chloride. The NTO and acetate concentrations were both 1000 µM. The experiment was conducted in closed bottles as previously described, and the NTO concentration was measured over time. Liquid samples were taken after the complete removal of NTO for soluble Fe analysis by inductively coupled plasma–optical emission spectrometry (5100 SVDV ICP-OES, Agilent Technologies, Santa Clara, CA, USA) using the parameters described by Nguyen *et al.* (2020) in the wavelength 238.2 nm. These samples were clarified and acidified to a final concentration of 2% (v/v) nitric acid prior to the analysis.

4.3.4 Analytical methods

4.3.4.1 HPLC

The concentrations of NTO and ATO were measured using high performance liquid chromatography (HPLC). An Agilent 1290 Infinity HPLC (Santa Clara, CA, USA) coupled with a diode array detector (DAD) was equipped with a Hypercarb column (Thermo Scientific, Waltham, MA, USA), and the mobile phase consisted of a gradient of water with 0.1% trifluoroacetic acid and acetonitrile, as previously described (MADEIRA *et al*., 2017).

4.3.4.2 GC-TCD and GC-FID

For CO_2 and acetate analyses, we used a gas chromatograph GC 7890A (Agilent Technologies, Santa Clara, CA, USA) equipped with two detectors and two columns. For CO_2, we used a Carboxen 1010 Plot column (30 m × 0.32 mm, Sigma-Aldrich, Saint Louis, MO, USA) and a thermal conductivity detector (TCD) at 230ºC. The inlet was operated in splitless mode at 100ºC, and the oven temperature was also 100ºC. Helium was used as carrier gas at a flow rate of 7 mL/min, and the gas injections of 100 µL were performed with a gastight syringe. For acetate, we used a fused silica Stabilwax®-DA column (30 m × 0.53 mm, Restek, State College, PA, USA) and a flame ionization detector (FID) at 280ºC, with air and hydrogen as the flame source. The inlet temperature was 280ºC, and the oven temperature started at 100ºC, increased to 150ºC at a rate of 8ºC/min. Helium was used as the carrier gas at a flow rate of 5.2 mL/min, and the injection volume was 1 µL.

4.3.4.3 OD600

The optical density at 600 nm (OD600) was measured at the wavelength of 600 nm using a UV-1800 UV-VIS spectrophotometer (Shimadzu, Kyoto, Japan).

4.3.4.4 ATP

We measured the bioluminescence produced in the ATP assay using a FlexStation 3 multi-mode microplate reader (Molecular Devices, San Jose, CA, USA). The data was analyzed with the ready-to-glow protocol from the software SoftMax Pro 5.2 (also from Molecular Devices) with an integration time of 1500 ms.

4.3.5 Sample preparation for metagenomic analysis

After the dilutions-to-extinction were performed, cells grown in 160-mL serum bottles with a 100-mL liquid volume containing 4 mM NTO and 4 mM acetate were retrieved by filtration using syringes rinsed with DNase/RNase-free water and autoclaved, attached to Sterivex-GP Pressure filter units (0.22 µm pore size, MilliporeSigma, Burlington, Massachusetts, USA). The filters were then rinsed with DNase/RNase-free phosphate-buffered saline, placed into 50-mL sterile centrifuge tubes, flash-frozen with liquid nitrogen, and stored at -80^{o}C. The experiment was conducted in triplicate. DNA extraction, metagenomic analysis, and interpretation of metagenomic data were performed by Doyoung Park and Dr. Janet K. Hatt and supervised by Dr. Konstantinos T. Konstantinidis at Georgia Institute of Technology (Atlanta, GA, USA) (PARK, 2020).

4.4 RESULTS

4.4.1 NTO Reduction

The microbial culture enriched from municipal anaerobic digester sludge reduced NTO to ATO using acetate as the electron donor and carbon source (Figure 11, Panel A). After an initial lag-phase of approximately 0.6 days, NTO was completely reduced to ATO within 2.0 days. The conversion of 3300 µM NTO was accompanied by the consumption of 2840 µM acetate. Biomass increased in parallel with NTO conversion to ATO, indicating that the enrichment culture sustained growth in the presence of acetate as the electron donor and NTO

as the electron acceptor. The cell yield of the enrichment culture was 0.174 g biomass g acetate^{-1}. The doubling time was 1.2 days, calculated based on the VSS increase during NTO reduction. No significant acetate consumption occurred when NTO was absent (Figure 11, Panel B). The biomass increase during incubation of the treatment lacking NTO was only 13.7% of the biomass increase in the treatment with both NTO and acetate.

Figure 11 – NTO and acetate consumption by anaerobic enrichment culture concurrently to ATO and biomass formation. Panel A: Enrichment culture incubated with NTO and acetate in mineral medium. Panel B: Enrichment culture incubated with acetate in mineral medium (without NTO). Legend: NTO (●), ATO (○), biomass (▲), and acetate (■). Symbols represent the average of three replicates, and error bars represent the standard deviation.

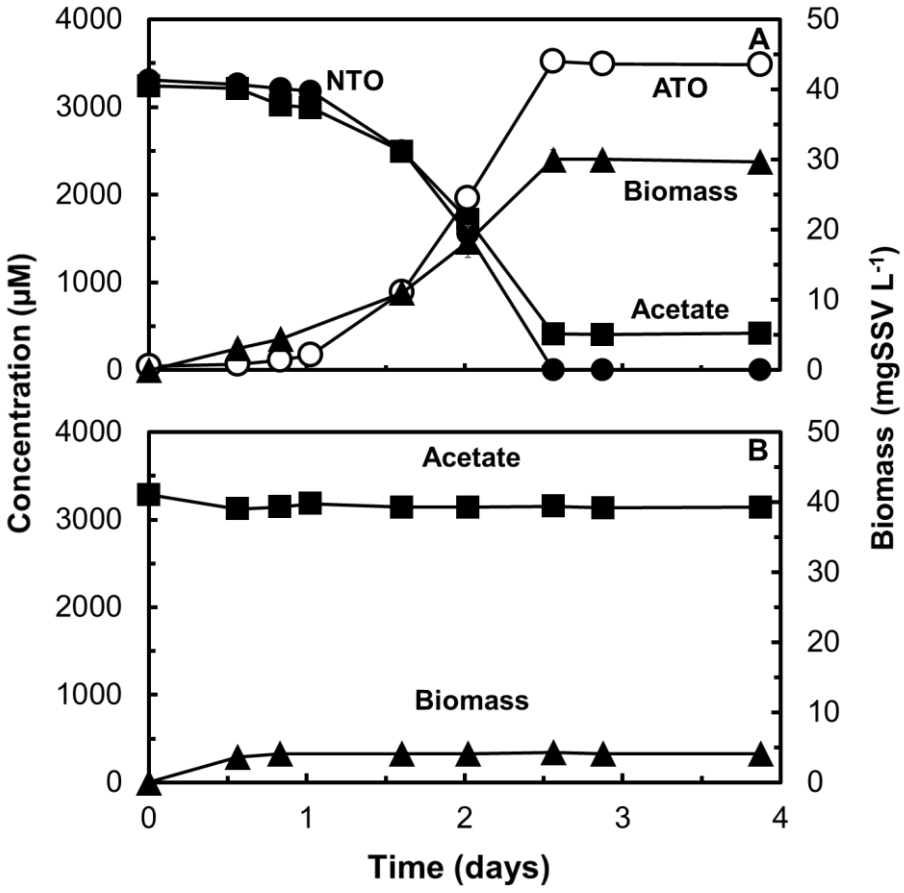

The production of CO_2 from acetate oxidation corresponded to the theoretical concentration needed to reduce 2000 µM NTO (Figure 12). As the NTO reduction began, the CO_2 level started to increase. The complete removal of NTO resulted in the production of approximately 3000 µmol CO_2 L_{medium}^{-1}. For each mole of NTO reduced to ATO, 0.75 moles of acetate were oxidized to CO_2. Since each acetate molecule contains 2 carbons, we expected the formation of 3000 µmol CO_2 L_{medium}^{-1} for an initial concentration of 2000 µM NTO. There was no CO_2 production when NTO was absent nor in the abiotic control.

Figure 12 – NTO consumption by anaerobic enrichment culture concurrently to ATO and CO_2 formation. Legend: NTO (●), ATO (□), and CO_2 (⧫). Symbols represent the average of three replicates, and error bars represent the standard deviation.

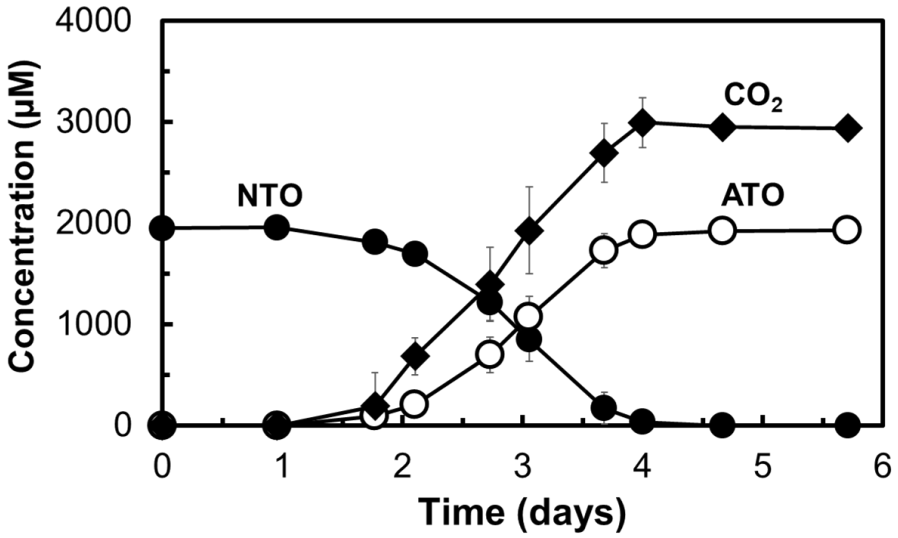

The dependence of NTO reduction on the presence of acetate was further demonstrated in an experiment testing several limiting concentrations of acetate for NTO reduction . The NTO reduction was proportional to the amount of acetate present in the medium, indicating that the reaction stopped once all the electron-donating substrate was consumed (Figure 13, panel A). In the treatment without acetate, no NTO reduction was observed within five days. In all the treatments containing acetate, partial NTO reduction occurred until the acetate was completely depleted (Figure 13, panel B). Reduction of 20%, 39%, 75%, and 89% of the initial concentration of NTO (1000 µM) in the treatments containing 225, 450, 675, and 900 µM acetate indicated that the NTO reduction depended upon the availability of acetate.

Figure 13 – NTO and acetate consumption by anaerobic enrichment culture under limiting acetate concentrations. Panel A: NTO concentration over time. Panel B: Acetate concentration over time. Legend based on different initial concentrations of acetate: 0 (✕), 225 (○), 450 (⧫), 675 (△), and 900 µM (■). Symbols represent the average of three replicates, and error bars represent the standard deviation.

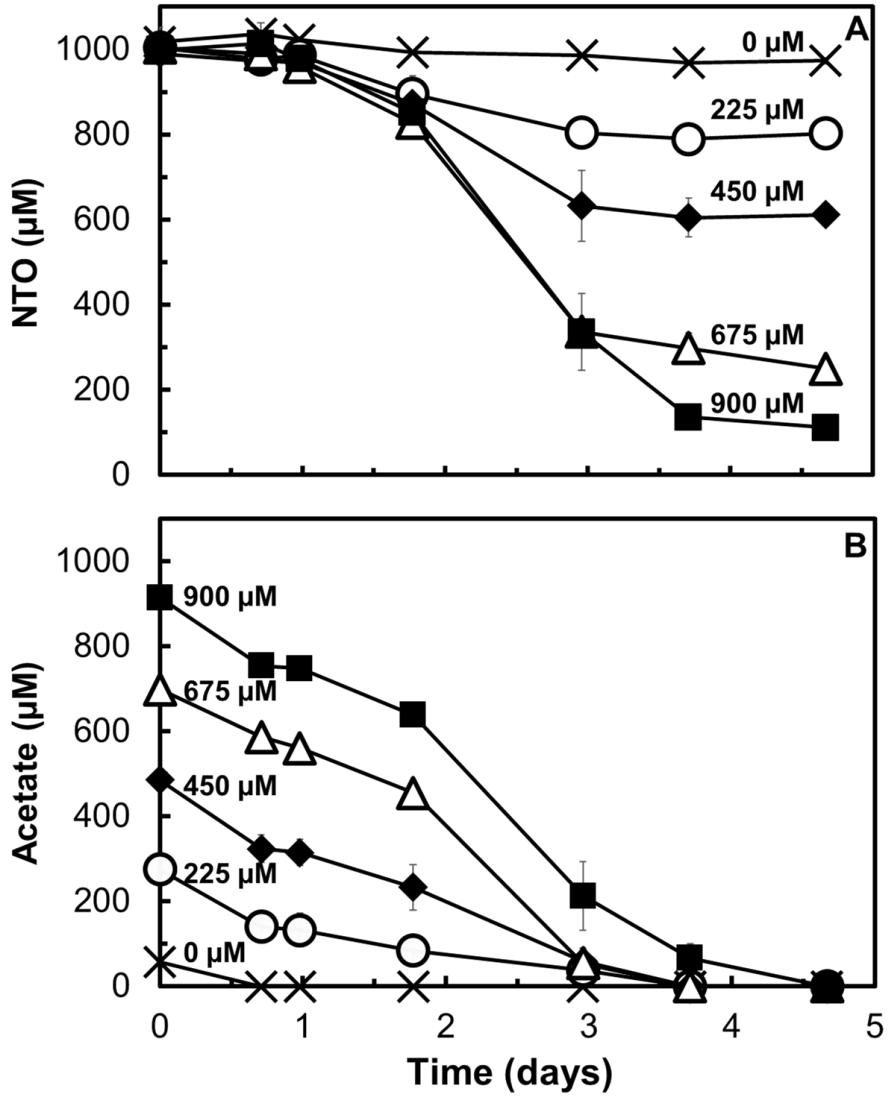

4.4.2 Uncoupler effects and ATP production

CCCP is an uncoupler of oxidative phosphorylation (LEWIS *et al.*, 1994). Therefore, the effect of CCCP on the NTO reduction by the enrichment culture was evaluated (Figure 14). CCCP caused complete inhibition of NTO reduction at concentrations as low as 0.600 mg L^{-1} and had measurable impacts at 0.060 mg L^{-1}.

Figure 14 – Inhibition of NTO reduction by different concentrations of CCCP using the NTO-acetate enrichment culture as inoculum. Panel A: NTO concentration over time. Panel B: ATO concentration over time. Legend based on different concentrations of CCCP: 6.000 (■), 0.600 (△), 0.060 (⧫), 0.006 (○), and 0.000 mg L^{-1} (✕). Symbols represent the average of three replicates, and error bars represent the standard deviation.

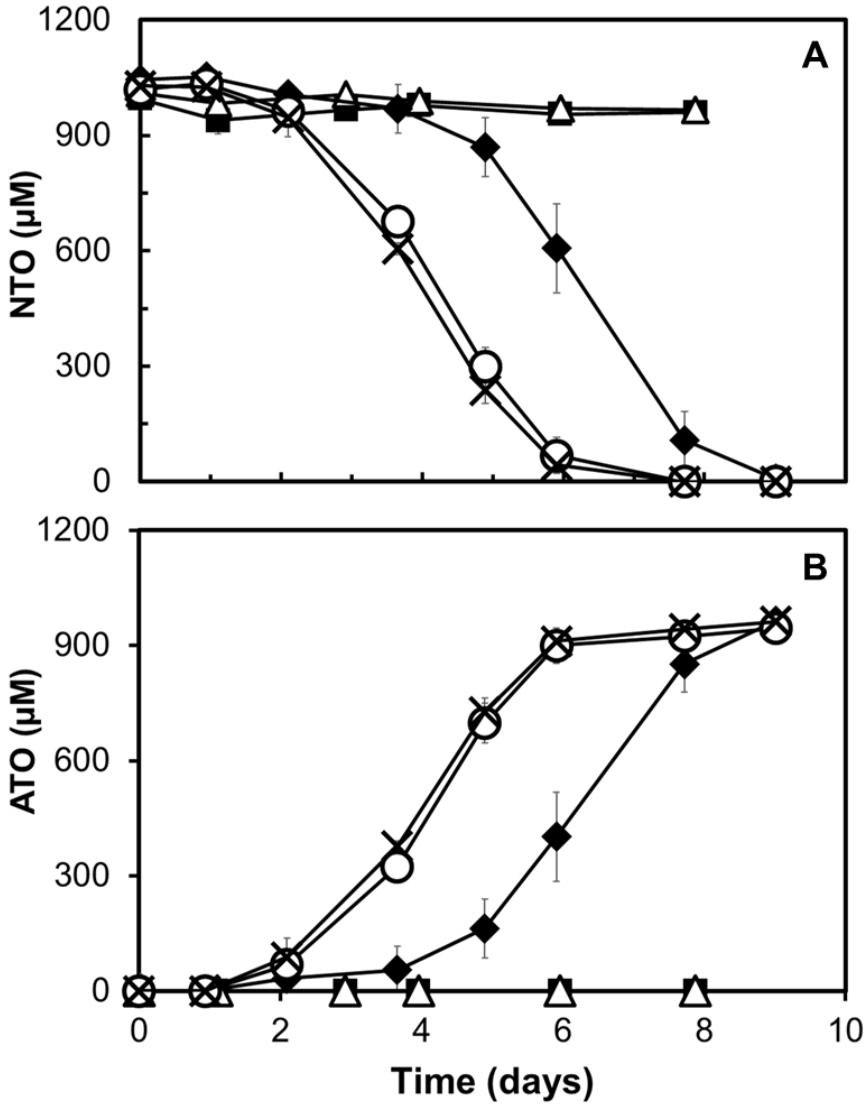

The next step was to assess the ATP production by the enrichment culture using NTO as the electron acceptor and acetate as the electron donor. ATP production normalized by the biomass concentration was significantly higher in the treatment containing both NTO and acetate, indicating that NTO reduction supported energy production and cell growth (Figure 15). ATP was not significantly produced in the treatments containing only the enrichment culture or the enrichment culture with NTO only or acetate only after 3.5 h of incubation. The results indicate that ATP production was linked to the presence of the NTO/acetate pair. The ATP production over time in all the different treatments is shown in Appendix B.

Figure 15 – ATP production by enrichment culture before and after addition of NTO and acetate. Bars represent the average of 3 replicates, and error bars represent the standard deviation. Same letters indicate no significant difference between different treatments (Student's t-test with 95% confidence intervals).

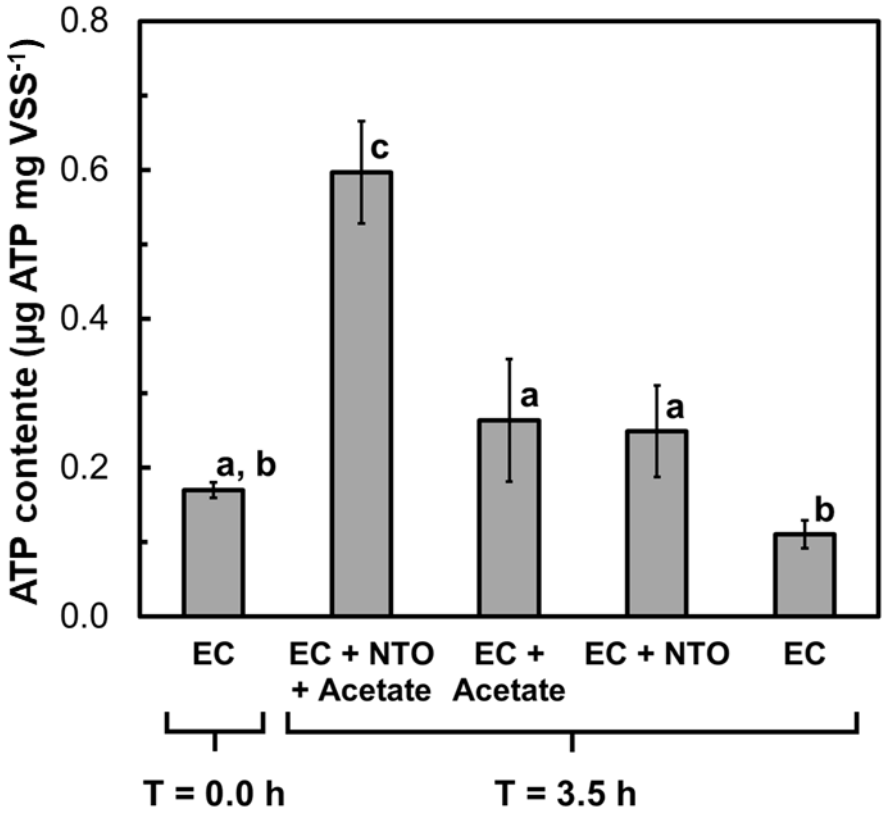

4.4.3 Enrichment culture metagenome

Metagenome sequencing revealed that the main microorganisms (and relative abundances) were *Geobacter anodireducens* (89.3%) and *Thauera* sp. (5.5%). Genes encoding proteins possibly involved in NTO reduction, e.g., nitroreductases and cytochromes, were found in the metagenome and are discussed in section 4.5. For an in-depth description of metagenome results, please consult Park (2020).

4.5 DISCUSSION (AND COMPLEMENTARY RESULTS)

The biological reduction of NTO to ATO has already been demonstrated in a few studies using soil microorganisms (KRZMARZICK *et al.*, 2015; MADEIRA *et al.*, 2017) and a pure culture of *Bacillus licheniformis* strain (LE CAMPION *et al.*, 1999b) with an excess of electron-donating substrates. However, this is the first study to report cell growth linked to NTO transformation. The results provide strong evidence that members of the culture utilized NTO as the final electron acceptor in anaerobic respiration. The oxidation of acetate only occurred

in the presence of NTO, as demonstrated by the lack of acetate consumption in the treatment where NTO was absent (Figure 11, panel B). Furthermore, limiting acetate concentrations led to a cessation in the NTO reduction (Figure 13), providing more evidence that the NTO reduction was coupled to the acetate oxidation.

Cell growth was observed in parallel with NTO reduction and acetate oxidation (Figure 11, panel A). The reduction of the NTO nitro group to amine requires 6 e^- eq, whereas the oxidation of acetate to CO_2 provides 8 e^- eq. According to this stoichiometry, 2475 µM acetate would be needed to reduce 3300 µM NTO. However, we observed the disappearance of 2840 µM acetate, indicating that part of the acetate-carbon was used for cell growth. In treatments lacking NTO, only a minor increment in biomass was observed during the first 14 hours (Figure 11, panel B).

The strong inhibition of the enrichment culture by CCCP provides additional evidence that NTO served as a final electron acceptor in anaerobic respiration. CCCP unlinks ATP formation from the electron transport system due to a disruption in the proton gradient (OTTEN *et al.*, 1999). Instead of returning through the pore in the ATPase, the protons bypass the pore, uncoupling oxidative phosphorylation from the respiratory process (MITCHELL, 1966). The complete inhibition of NTO reduction when the enrichment culture was exposed to CCCP suggests that NTO reduction was linked to ATP production. Indeed, the ATP content of cells significantly increased only when the enrichment culture was exposed to the NTO/acetate pair, providing evidence of NTO respiration.

The metagenome results indicate that two species, *Geobacter anodireducens* and *Thauera* sp., predominate in the enrichment culture (PARK, 2020). Two possible mechanisms for NTO reduction were identified. Firstly, several homologs of nitroreductases were observed. Nitroreductases are widely distributed among bacteria and can reduce various nitroaromatics (ROLDÁN *et al.*, 2008). Additionally, nitroreductases produced by rat tissues were observed to reduce nitro-heterocyclic compounds (BARTEL *et al.*, 2009; WALTON; WORKMAN, 1987). Nevertheless, literature examples suggest that the reduction of nitro-compounds by nitroreductases is not linked to energy production (LIU *et al.*, 2017), even when the enzyme's true physiological role was proven to be the reduction of a nitroaromatic compound (nitrobenzene) (FIORELLA; SPAIN, 1997; SOMERVILLE *et al.*, 1995).

The second possible mechanism behind NTO reduction is the extracellular electron transfer (EET), inferred by the presence of cytochrome protein families in the metagenome of the *Geobacter anodireducens*. *Geobacter* species along with *Shewanella*, *Desulfovibrio*, and *Enterobacter* can release intracellular electrons to the cell exterior via an electron transfer chain, reducing exogenous compounds (ZHANG *et al.*, 2018). This process is linked to energy

production, conferring electroactive bacteria the ability of respiring nitroaromatic compounds. As an example, 2,6-dinitrotoluene (2,6-DNT) was reduced by *Shewanella oneidensis* MR-1, and an investigation at the gene level revealed that the Mtr respiratory pathway, in which electrons are transferred from cytochrome proteins attached to the cytoplasmic membrane to an external electron acceptor, had a key role in 2,6-DNT reduction. Besides, the oxygen insensitive nitroreductase NfnB was also linked to 2,6-DNT reduction, indicating that both mechanisms can co-occur (LIU *et al.*, 2017).

Although the EET system offers an explanation for the energy derived from the reduction of NTO, both EET and nitroreductases do not reduce nitroaromatic compounds by substrate-specific reactions (ZHOU *et al.*, 2020). The members of the NTO-respiring enrichment culture could not reduce any other nitro-containing compound we tested, such as 3-nitrotriazole, 3-nitropyrazole, 4-nitroimidasole, and 4-nitrophenol (Table 3). Thus, it is tempting to suggest that, unlike the possibilities previously described for nitroaromatics, a non-conventional substrate-specific mechanism could be involved in NTO reduction. Further studies will focus on the transformation process at the gene level.

Table 3 – Activity of the NTO-acetate enrichment culture incubated with different combinations of electron donors and electron acceptors.

e^- **Acceptor**	e^- **Donor**	e^- **Acceptor reduction observed**
NTO	Acetate	Yes
4-Nitroimidasole	Acetate	No
2-Methyl-4(5)-nitroimidazole	Acetate	No
4-Nitroanisole	Acetate	No
4-Nitrophenol	Acetate	No
2,4-Dinitrotoluene	Acetate	No
Nitroguanidine	Acetate	No
3-Nitrotriazole	Acetate	No
3-Nitropyrazole	Acetate	No
Ferric citrate	Acetate	Yes
NTO	Glucose	Yes
NTO	H_2	No
NTO	Ethanol	No

The reduction of hexahydro-1,3,5-trinitro-1,3,5-triazine (RDX) by *Geobacter metallireducens* was also observed (KWON; FINNERAN, 2006), and the fastest reduction rate was achieved when anthraquinone-2,6-disulfonate (AQDS), Fe, and purified humic substances were used as electron shuttles, indicating that the RDX transformation was not biologically-catalyzed, but catalyzed by the reducing chemical compounds. Since our enrichment culture was able to reduce Fe^{3+} added to the medium in the form of ferric citrate (Figure 16), we evaluated a possible electron shuttle effect of Fe on the NTO reduction (Figure 17) by adding different concentrations of Fe to the culture medium. The enrichment culture could still reduce NTO to ATO when Fe was not added to the medium, with only residual trace amounts present (0.02 mg Fe L^{-1}). Tripling the concentration of Fe in the medium, compared to the usual 0.60 mg L^{-1} used, did not increase the NTO reduction rate, indicating that soluble Fe did not act as an electron shuttle in our experiments. The minor inhibition caused by the lack of Fe was probably due to the role of Fe as a cofactor for a variety of cellular processes, since Fe deficiency has been associated with downregulation of genes related to respiratory functions in *Geobacter* sp (EMBREE *et al.*, 2014).

Figure 16 – Production of Fe^{2+} (△) by the enrichment culture incubated with ferric citrate (500 µM) and acetate (1000 µM). Symbols represent the average of three replicates, and error bars represent the standard deviation.

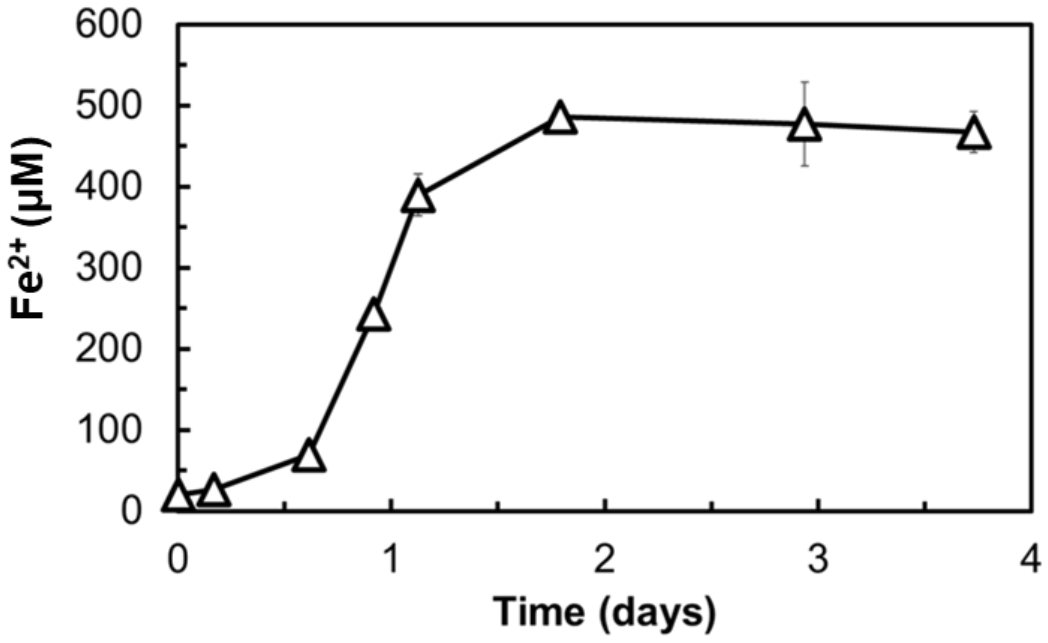

Figure 17 – Rate of NTO reduction by the enrichment culture versus total Fe concentration measured in the medium. The added Fe concentrations were 0.0, 0.6, and 1.8 mg L^{-1}. Symbols represent the average of three replicates, and error bars represent the standard deviation.

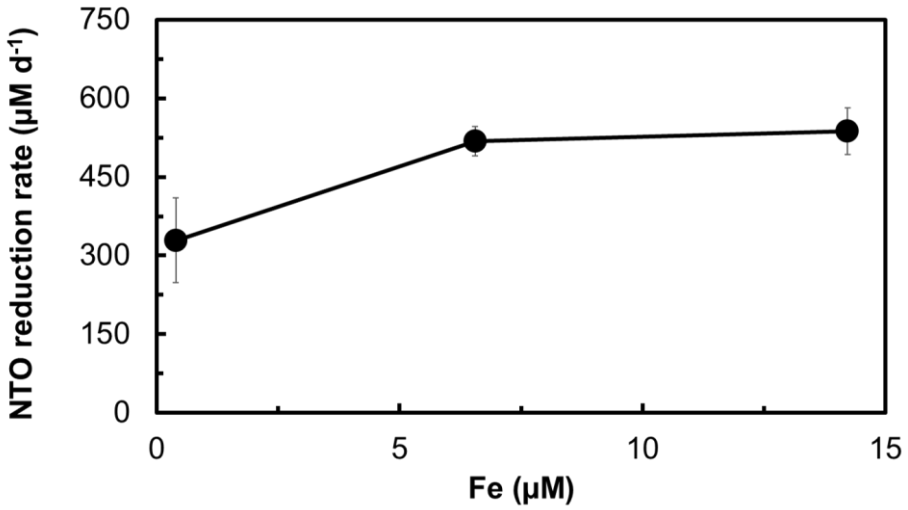

This work shows multiple lines of evidence of the novel NTO respiration: (i) the growth of the enrichment culture was dependent on the presence of NTO and acetate; (ii) acetate was not consumed when NTO was absent; (iii) the enrichment culture exhibited high specificity to NTO, as evidenced by the lack of ability to reduce the other nitro-containing compounds tested; (iv) CCCP strongly inhibited the NTO reduction in the enrichment culture; and (v) the cells' ATP content increased when simultaneously exposed to NTO and acetate but not when individually exposed. Evidence of TNT respiration (ESTEVE-NUÑEZ *et al.*, 2000), as well as the use of 2,4-DNT as electron acceptor in anaerobic respiration (HUANG *et al.*, 2015), has already been reported in the literature. Nevertheless, this is the first time a nitro-heterocyclic compound was shown to be used as the final electron acceptor in anaerobic respiration. The findings presented here regarding the physiological role of NTO in the enrichment culture respiration can be applied in the development of bioremediation strategies to clean up training ranges contaminated with NTO, and in the assessment of natural attenuation in anaerobic environments. However, more studies are necessary to fully elucidate the enzymatic mechanism of the NTO reduction by *Geobacter anodireducens* and *Thauera* sp.

5 DAAN REMOVAL IN SLUDGE UNDER DIFFERENT ELECTRON ACCEPTOR CONDITIONS

Resulting publication: MENEZES, O.; MELO, N.; PARAISO, M.; FREITAS, D.; FLORÊNCIO, L.; KATO, M. T.; GAVAZZA, S. The key role of oxygen in the bioremoval of 2,4-diaminoanisole (DAAN), the biotransformation product of the insensitive munitions compound 2,4-dinitroanisole (DNAN), over other electron acceptors. Chemosphere, p. 128862, 2020.

Figure 18 – Graphical abstract for section 5.

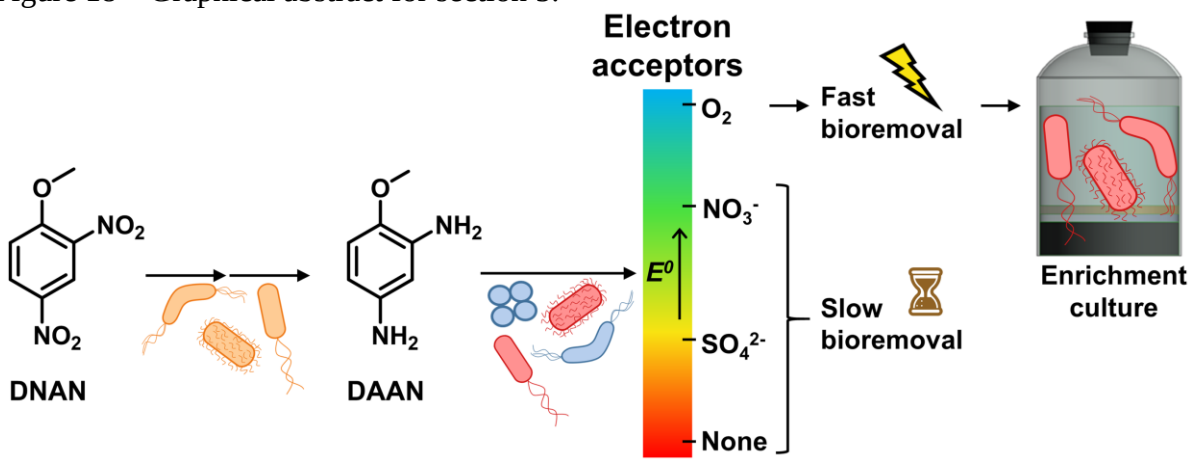

5.1 ABSTRACT

Insensitive munitions compounds, such as 2,4-dinitroanisole (DNAN), are replacing conventional explosives. DNAN is anaerobically reduced to 2,4-diaminoanisole (DAAN), a toxic aromatic amine. However, the removal of DAAN under different redox conditions is yet to be elucidated. Herein, we analyzed DAAN consumption in biotic and abiotic microcosms when exposed to different redox conditions (without added electron acceptor, without added electron acceptor but with pyruvate as a co-substrate, with sulfate, with nitrate, and with oxygen), using an anaerobic sludge as inoculum. We observed that DAAN autoxidation, an abiotic reaction, was significant in aerobic environments. DAAN also reacted abiotically with heat-killed sludge up to a saturation limit of 67.4 µmol DAAN (g VSS heat-killed sludge)$^{-1}$. Oxygen caused the fastest removal of DAAN in live sludge among the conditions tested. Treatments without added electron acceptors (with or without pyruvate) presented similar DAAN removal performances, although slower than the treatment with oxygen. Sulfate did not exhibit any effect on DAAN removal compared to the treatment without added electron

acceptors. Nitrate, however, inhibited the process. An enrichment culture from the microcosms exposed to oxygen could be developed using DAAN as the sole substrate in aerobic conditions. The enrichment profoundly changed the microbial community. Unclassified microorganisms accounted for 85% of the relative abundance in the enrichment culture, suggesting that DAAN aerobic removal might have involved organisms that were not yet described. Our results suggest that DAAN aerobic treatment can be coupled to DNAN anaerobic reduction in sludge, improving the treatment of DNAN-containing wastewaters.

5.2 INTRODUCTION

Recently, insensitive munitions compounds (IMC) began to be applied for munitions production, due to their higher stability and smaller proneness to accidental explosions compared to conventional explosives (BODDU *et al.*, 2008). Environmental contamination by munitions compounds can occur via pieces of undetonated explosives on the soil or industrial wastewater discharge into water bodies. The remediation of these pollutants is imperative to environmental protection since they and their biotransformation products are known to be toxic, potentially mutagenic, and strong methanogenic inhibitors (KOVACIC; SOMANATHAN, 2014; OLIVARES *et al.*, 2016b; OLIVARES *et al.*, 2016c). One of the most important IMC is 2,4-dinitroanisole (DNAN), a major replacer of the conventional explosive 2,4,6-trinitrotoluene (TNT) (DAVIES; PROVATAS, 2006) and a component of the insensitive munitions formulations IMC101, IMC104, and PAX21, with percentages varying from 32 to 43% of the formulations' weight (TAYLOR *et al.*, 2015b).

Previous studies have explored different remediation strategies for DNAN contamination, such as adsorption to activate carbon (BODDU *et al.*, 2009), photo-transformation (HALASZ *et al.*, 2018; TAYLOR *et al.*, 2017), phytoremediation (RICHARD; WEIDHAAS, 2014b), aerobic biodegradation (FIDA *et al.*, 2014; RICHARD; WEIDHAAS, 2014a), reduction by reactive minerals (KHATIWADA *et al.*, 2018c), and anaerobic biotransformation (NIEDZWIECKA *et al.*, 2017; OLIVARES *et al.*, 2016a; PLATTEN *et al.*, 2013). In the latter case, during the anaerobic treatment of DNAN-containing wastewater (OLIVARES *et al.*, 2013) or in a saturated soil subsurface with depleted oxygen (TAYLOR *et al.*, 2015a), the two nitro groups of DNAN can be reduced to amino groups. The first reduced product of DNAN is 2-methoxy-5-nitroaniline (MENA), as a result of the reduction of nitro groups at the ortho position. Some studies reported 4-methoxy-3-nitroaniline (iMENA) as a minor product of DNAN reduction at para position (HAWARI *et al.*, 2015; OLIVARES *et al.*,

2016a). 2,4-Diaminoanisole (DAAN) is the aromatic amine formed when both nitro groups of DNAN are reduced.

The physicochemical properties of the reduced product DAAN are very different from those of DNAN. DNAN exhibits a water solubility of 213 mg L^{-1}. On the other hand, the solubility of the reduced product DAAN is higher than 40,000 mg L^{-1} (HAWARI *et al.*, 2015). With an octanol/water partition coefficient ($LogK_{ow}$) at 25 °C of 1.612 (BODDU *et al.*, 2008), DNAN is more hydrophobic than DAAN ($LogK_{ow}$ at 25 °C < -1) (HAWARI *et al.*, 2015). DAAN is also toxic to the environment, exhibiting a 50% inhibitory concentration of 155 µM in Microtox tests and 176 µM in methanogenic assays (LIANG *et al.*, 2013), as well as carcinogenic to mammals (AMES *et al.*, 1975; AUNE; DYBING, 1979).

DAAN was reported to undergo different abiotic reactions after DNAN anaerobic biotransformation: autoxidation to azo dimers in aerobic environments (HAWARI *et al.*, 2015), coupling reactions with other DNAN biotransformation products in anaerobic environments (KADOYA *et al.*, 2019; KADOYA *et al.*, 2018), and incorporation reactions into soil natural organic matter (OLIVARES *et al.*, 2017).

In the treatment of nitroaromatic-containing wastewater, some reduced products (aromatic amines) were found to be biodegraded in methanogenic environments (FUCHS, 2008; RAZO-FLORES *et al.*, 1999) or using different electron acceptors (FIELD *et al.*, 1995; FUCHS *et al.*, 2011). Nevertheless, how different electron acceptors affect DAAN removal in sludge and whether biodegradation can still occur despite the abiotic reactions that DAAN can undergo are still open questions.

The present study aimed to evaluate DAAN removal in biological sludge under different electron acceptor conditions, assessing the contributions of biotic and abiotic pathways for this process. Additional objectives were to observe how DAAN exposure affects the microbial community and to develop an enrichment culture with microorganisms adapted to the best condition tested.

5.3 MATERIALS AND METHODS

5.3.1 Medium composition and inoculum

DAAN ($C_7H_{10}N_2O$, molecular weight: 138.17 g mol^{-1}, CAS # 615-05-4, analytical standard) was purchased from Sigma-Aldrich (Saint Louis, MO, USA). The composition of the mineral medium used was (mg L^{-1}): K_2HPO_4 (250), $CaCl_2.2H_2O$ (10), $MgSO_4.7H_2O$ (100),

$MgCl_2.6H_2O$ (100), NH_4Cl (280), $NaHCO_3$ (1100) and 1 mL L^{-1} of trace elements solution. Trace elements solution was composed of (mg/L): H_3BO_3 (50), $FeCl_2.4H_2O$ (2000), $ZnCl_2$ (50), $MnCl_2.4H_2O$ (2000), $(NH_4)_6Mo_7O_{24}.4H_2O$ (50), $AlCl_3.6H_2O$ (90), $CoCl_2.6H_2O$ (2000), $NiCl_2.6H_2O$ (50), $CuCl_2.2H_2O$ (100), EDTA (1000), resazurin (2000), HCl 36% (1 mL/L). We used ultra-pure water in the preparation.

The inoculum used in this study was a mixture in a 1:2 proportion of an anaerobic-microaerobic sludge from a lab-scale sequencing batch reactor treating textile effluent (MENEZES *et al.*, 2019) and an anaerobic granular sludge from a full-scale upflow anaerobic sludge blanket (UASB) treating petrochemical wastewater (Suape Port, Ipojuca, PE, Brazil), respectively. We elutriated the sludge five times in 50-mL falcon tubes by adding deionized water and centrifuging at 3500 rpm for 10 min. We then measured the volatile suspended solids (VSS) content of the sludge according to APHA (2017). A sludge concentration of 5 g VSS L^{-1} was used in the microcosms.

5.3.2 Biotic and abiotic assays

We evaluated the removal of DAAN (24 mg L^{-1}, 176 µM) using different electron acceptor conditions in biotic microcosms with sludge: no added electron acceptor (no added e^- acceptor), no added e^- acceptor with pyruvate addition (100 mg L^{-1}, 1136 µM), nitrate (80 mg L^{-1}, 1290 µM), sulfate (100 mg L^{-1}, 1041 µM), and atmospheric oxygen. The headspaces for the conditions with no added e^- acceptor, no added e^- acceptor with pyruvate addition, nitrate, and sulfate were composed of 80% of N_2 and 20% of CO_2. We tested all microcosms in triplicate and incubated them in the dark at 27 ± 2 °C.

Serum flasks (100 mL) with t-butyl caps and aluminum seals were used as biotic and abiotic microcosms for the anaerobic conditions (i.e., using no e^- added acceptor, no added e^- acceptor + pyruvate, sulfate, or nitrate). The liquid volume was 80 mL, as a 20-mL headspace was kept. We purged the oxygen by flushing the medium and the headspace with an N_2/CO_2 mixture (80/20%) for 4 min. The anaerobic microcosms were incubated upside-down in a glove box (818-GB, Plas-Labs, Lansing, MI, USA) filled with the same N_2/CO_2 mixture. Differently, microcosms with oxygen had a total volume of 120 mL, with 40 mL of headspace, and were kept upturned in regular atmospheric air. A 0.45-µm filter attached to an ordinary hypodermic needle connected the inside of the flask to the air, assuring oxygen exposure.

We refilled the microcosms with mineral medium, DAAN, and electron acceptors every time 12 mL of liquid volume had been withdrawn by sampling. At every refilling, we flushed

the headspace once more as previously described, except for the condition with oxygen. We spiked DAAN again in all biotic microcosms after total consumption for two more times. We also reestablished pyruvate, nitrate, and sulfate concentrations whenever they were completely consumed.

Abiotic microcosms without sludge with the same DAAN concentration and electron acceptor conditions as the biotic microcosms were assayed. We also tested abiotic microcosms with heat-killed sludge and without added electron acceptors. Heat-killed sludge was autoclaved for three consecutive days (1 h in the first and 30 min the next days). The abiotic microcosms were also assayed in triplicates. Other experimental conditions were the same as in the biotic microcosms.

The materials used in all biotic and abiotic assays were sterilized by autoclaving for 30 min. The medium was filtered using a 0.22-µL membrane.

5.3.3 Development of enrichment cultures

After the assays with biotic and abiotic microcosms, we developed enrichment cultures from the sludge of the microcosms without added electron acceptors and with oxygen. Once DAAN was completely consumed, we transferred 10% of the mixed suspension volume of the microcosms to a fresh medium. The transfers were performed in duplicates, except when specified otherwise. Medium composition, DAAN concentration, and incubation conditions were the same as in the biotic assays previously described. After nine transfers, we performed a 10^{-4} dilution to extinction of the enrichment culture from the condition with oxygen to further select the specific microorganisms responsible for DAAN removal. We used a DAAN concentration of 500 µM. The dilution to extinction was carried out in 25-mL assay tubes, in which 10 mL corresponded to the liquid volume and 15 mL to the headspace. The headspace was connected to the atmosphere by the same filter-needle system described for the microcosms with oxygen. The bottles were incubated in the shaker at 1300 rpm for seven days. We used the suspended volume of the 10^{-4} dilution as the inoculum to further transfers.

5.3.4 Analytical methods

We analyzed the samples using a Shimadzu LC-20AT (Kyoto, Japan) high-pressure liquid chromatograph coupled to a diode array detector (HPLC-DAD). For DAAN quantification, a Zorbax Eclipse XDB-C18 column (5 µm, 4.6 × 250 nm) (Agilent, Santa Clara,

CA, USA) was exposed to methanol/5-mM phosphate buffer (46/54% v/v) as a mobile phase, running isocratically (0.6 mL min^{-1}) at 30 ºC. The injection volume was 100 µL. The method detected DAAN at 210 nm in a retention time of 5.3 min.

The method for pyruvate quantification applied an Aminex HPX-87H column (7.8 × 300 mm) (Bio-Rad, Hercules, CA, USA) at 64 ºC, with a mobile phase of sulfuric acid (5 mM) running isocratically (0.8 mL min^{-1}, 31 min). The injection volume was 20 µL. Pyruvate was detected at 208 nm at 6.6 min of retention time.

We measured nitrate and sulfate using a Dionex ICS 2100 (Thermo Fisher Scientific, Waltham, MA, USA) ion chromatography (IC), with a Dionex Ion PacTM AS23 (Thermo Fisher Scientific) (2 × 250 nm), operated with a mobile phase of sodium carbonate (4.5 mM) and sodium bicarbonate (0.8 mM) at a flow rate of 0.25 mL min^{-1} during 20 min. Nitrate and sulfate were detected at retention times of 14.0 and 19.8 min, respectively. Oxygen was measured in the biotic and abiotic aerobic-microcosms using an Intellical^{TM} LDO101 sensor (Hach, Loveland, CO, USA).

We measured dissolved total Fe and Fe^{2+} in samples from the supernatants of live and heat-killed sludges using the phenanthroline method, according to APHA (2017). The samples were previously filtered in 0.22-µm membranes. Fe^{3+} concentration was calculated by subtracting the Fe^{2+} concentration from the total Fe concentration.

5.3.5 Microbial community analyses

We collected sludge samples (500 µL) for DNA extraction from the inoculum using a sterile syringe in technical triplicates before starting the experiments and from each biotic microcosm in biological triplicates after the removal of DAAN for three times. We homogenized the inoculum container and microcosms immediately before sampling. Cell samples were collected from the enrichment culture of the condition with oxygen using a different approach. We performed the 6^{th} transfer after the 10^{-4} dilution to extinction in triplicate with 50 mL of liquid volume and with a 500-µM DAAN concentration. After DAAN removal, we centrifuged the bottles' liquid volume in sterilized tubes at 4,000 rpm for 15 min and discarded the supernatant. We repeated this process three times until the final cell suspension volume was 500 µL, which we used for DNA extraction.

DNA was extracted from the samples using a PowerSoil® DNA isolation kit (MoBio Laboratories Inc., Carlsbad, CA, USA) according to the manufacturer's protocol. DNA quality, measured by ND-2000 spectrophotometer (Nanodrop Inc., Wilmington, DE, USA), was

accepted when the 260/280 nm ratio was higher than 1.8. After that, DNA samples were stored at -20°C. Then, 16S rRNA sequencing was carried out using V3-V4 primers 341F-806R and performed by a MiSeq System (Illumina, San Diego, CA, USA) at NeoProspecta (Florianópolis, SC, Brazil).

The datasets in FastQ format were preprocessed and annotated by MG-Rast server 3.5 (KEEGAN *et al.*, 2016) with default parameters. Sequence data were deposited at MG-Rast under the project number mgp94601. We normalized output data using the Microbiome Analyst server (DHARIWAL *et al.*, 2017). Principal Component Analysis of the relative abundance data of genera in the samples was performed using the software STAMP (PARKS *et al.*, 2014).

5.4 RESULTS AND DISCUSSION

5.4.1 DAAN in abiotic microcosms

The first step was to investigate DAAN stability when incubated with different electron acceptors in abiotic microcosms (without sludge). DAAN loss under oxygen exposure in abiotic conditions occurred at a rate of 0.14 d^{-1} (Figure 19, panel E). Previous studies about DAAN stability in aerobic environments reported a consumption rate of 0.08 d^{-1} (HAWARI *et al.*, 2015). The difference is possibly related to distinct dissolved oxygen concentrations in both experiments. When exposed to oxygen, DAAN autoxidizes to an azo dimer ($C_{14}H_{16}N_4O_2$) and a demethylated azo dimer derivate ($C_{13}H_{14}N_4O_2$) (HAWARI *et al.*, 2015; PLATTEN *et al.*, 2010). These autoxidation products, however, are not environmentally safe. Mixtures rich in DAAN azo dimers were reported to be toxic to *Allivibrio fischeri* (50%-inhibition concentration of 41 µM) (OLIVARES *et al.*, 2016c). Thus, a single-step chemical removal of DAAN by autoxidation to azo dimers is not enough to promote DNAN-containing wastewaters' detoxification after DNAN reduction to DAAN. A biological process may be necessary, as discussed later.

Additionally, we investigated DAAN removal due to nitrate exposure because aniline (another aromatic amine) was reported to undergo oxidation reactions in the presence of nitrate, forming azo compounds (PEREIRA *et al.*, 2011). Nitrate exposure partially and slowly removed DAAN in the absence of sludge, as shown in Appendix B. We only observed changes in DAAN concentrations after 40 days at a rate of 0.01 d^{-1}. DAAN loss was 30.8% after 127 days. Nitrate concentration, however, remained stable throughout the entire experiment.

Figure 19 – DAAN consumption under different redox conditions. Panel A: without added e^- acceptors in live sludge. Panel B: without added e^- acceptors and with pyruvate as a co-substrate in live sludge. Panel C: with sulfate in live sludge. Panel D: with nitrate in live sludge. Panel E: with oxygen in live sludge and abiotic (without sludge). Panel F: in heat-killed sludge. For the experiments showed in all panels, except panel E, the headspace was 80% N_2 and 20% CO_2. For the experiment showed in panel E, the headspace was atmospheric air. Legend: DAAN (●), pyruvate (◊), sulfate (□), nitrate (△), and DAAN abiotic autoxidation control with oxygen (○). Symbols represent the average of three replicates, and error bars represent the standard deviation. Closed arrows indicate new spikes of DAAN, and * means that DAAN from a different batch was used. Open arrows indicate new spikes of pyruvate, sulfate, or nitrate.

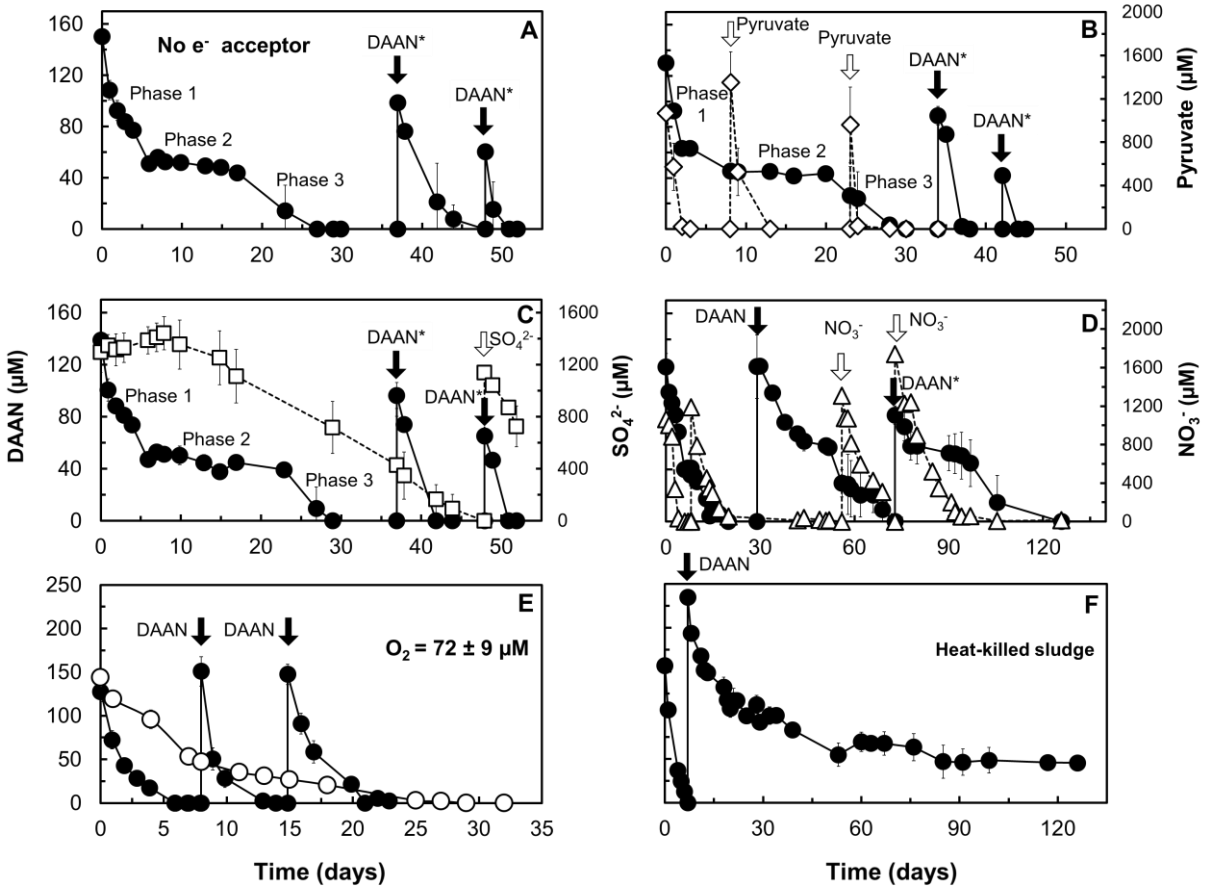

DAAN remained unreacted in the abiotic microcosms without added e^- acceptor (with or without pyruvate addition) and with sulfate. Sulfate and pyruvate concentrations also remained stable during the abiotic assays, as shown Appendix C.

We also tested whether DAAN could abiotically react with heat-killed sludge (Figure 19, panel F). In this condition, we observed complete DAAN loss in only seven days at a rate of 0.39 d^{-1} after the first spike. However, after the second spike, we observed a slower and incomplete removal of DAAN at a rate of 0.06 d^{-1}. The sludge became saturated with DAAN after 53 days, with a total consumption of 67.4 µmol DAAN (g VSS heat-killed sludge)$^{-1}$. Between 53 and 126 days, DAAN concentration did not significantly change. Hawari *et al.*

(2015) observed DAAN being completely and irreversibly adsorbed or reacted in two different soils in less than one day, which was ascribed to reactions with the soils' organic matter. We discussed reactions between DAAN and possible humic and fulvic acids extracted from sludge in section 5.4.3. Additionally, since DAAN was suggested to undergo abiotic oligomerization reactions in the presence of oxidized metals in anaerobic conditions (PLATTEN *et al.*, 2010), we investigated if autoclaving would increase the concentrations of dissolved total Fe and Fe^{3+} in the sludge. In the live sludge used as inoculum, dissolved total Fe and Fe^{3+} concentrations were 7.9 and 3.6 mg L^{-1}, respectively. After autoclaving, these concentrations increased to 155.4 and 65.2 mg L^{-1}, respectively. These values suggest that abiotic azo oligomerization caused by oxidated metals might have contributed to DAAN anaerobic consumption in heat-killed sludge. The next step was to determine if live sludge could continuously remove DAAN.

5.4.2 DAAN in biotic microcosms

DAAN was utterly consumed in all treatments with live sludge (Figure 19). A summary table describing first-order consumption rates is shown in Appendix C. DAAN consumption rates under anaerobic conditions without added e^- acceptor (i.e. fermentative with or without pyruvate) and with sulfate presented three distinct phases, according to Figure 19 (panels A to C): (i) phase 1: DAAN was consumed during 6 to 8 days; (ii) phase 2: DAAN concentration remained stable during 9 to 17 days, depending on the treatment; (iii) phase 3: DAAN started to be consumed once more. Phase 1 can be attributed to DAAN abiotic reactions with the sludge, as it reached a plateau after some days (phase 2). However, DAAN loss during phase 1 (85 to 99 µM, depending on the treatment) was lower than the DAAN loss in heat-killed sludge after seven days of incubation (157 µM). The higher loss in heat-killed sludge was probably related to differences in the adsorption properties of live and dead biomasses (TSEZOS; BELL, 1989), possibly being the heat-killed sludge structure more suitable for reactions with DAAN. After phase 2, DAAN restarted to be consumed, which was probably due to biological activity (phase 3). Thus, phases 1 and 2 together comprise the lag phase, which lasted 17, 20, and 23 days, for the conditions without added e^- acceptor, without added e^- acceptor + pyruvate, and with sulfate, respectively. After the second and third DAAN spikes, DAAN consumption started immediately.

The addition of pyruvate as a co-substrate in microcosms without added e^- acceptors to enhance fermentative conditions (Figure 19, panel B) did not represent a benefit for DAAN consumption compared to the treatment without pyruvate (Figure 19, panel A). Similarly,

sulfate as a possible electron acceptor (Figure 19, panel C) also did not affect DAAN removal when compared to the condition without added e^- acceptors (Figure 19, panel A). Further evidence that sulfate was not coupled to DAAN removal is that microbial community started to consume sulfate after eight days, while the lag phase for DAAN consumption lasted 23 days. Additionally, the resazurin (used as a redox indicator) turned colorless in the bottles without added e^- acceptor, without added e^- acceptor + pyruvate, and with sulfate, indicating that the redox potential values in those treatments were lower than -111 mV (JACOB, 1970). Thus, the similarity in redox conditions suggests that the same reactions leading to DAAN removal in the treatment without added e^- acceptor also drove DAAN consumption in the treatments without added e^- acceptor + pyruvate and with sulfate.

Differently from what we observed for heat-killed sludge, the anaerobic reactions with live sludge completely removed DAAN three times, showing that biological activity played a role in DAAN consumption. Although DAAN's amino groups can represent a problem for nucleophilic attack by anaerobes (FIELD *et al.*, 1995), some aromatic amines are known to be degraded under methanogenic conditions. Those include 5-aminosalicylate and 4-aminobenzoate (RAZO-FLORES *et al.*, 1999), anthranilic acid (RAZO-FLORES *et al.*, 1999), and 2-aminobenzoic acid (LIN'KOVA *et al.*, 2011).

We also tested nitrate as a possible electron acceptor for DAAN removal (Figure 19, panel D). After the first DAAN spike, DAAN was consumed faster than in the other anaerobic conditions and without a lag phase. This observation raised the question whether nitrate could have been used as an electron acceptor and DAAN as an electron donor since aniline was reported to be degraded under denitrifying conditions (KAHNG *et al.*, 2000; PEREIRA *et al.*, 2011; VAZQUEZ-RODRIGUEZ *et al.*, 2008; WU *et al.*, 2007). Additionally, DAAN rapid transformation rate might have been due to the redox potential of nitrate-reducing conditions, which is higher than the sulfate-reducing or fermentative conditions and closer to aerobic conditions. However, when we maintained the microbial community without nitrate from day 20 to day 56, DAAN was removed at a similar rate, which did not change when nitrate was added again for two times (days 56 and 73). After the third DAAN spike, the treatment showed the slower consumption rate observed for all treatments with live sludge. Despite the slow DAAN consumption, the community was still active, as it was able to remove nitrate during the entire experiment. Instead of using DAAN, denitrifiers probably used residual organic matter in sludge as their carbon and energy source. Therefore, denitrifying conditions did not favor DAAN removal.

The fastest DAAN removal among the treatments was observed under oxygen exposure (Figure 19, panel E). The aerobic microcosms did not exhibit a lag phase. We spiked DAAN three times and observed consumption rates ranging from 0.47 to 0.88 d^{-1}. Live sludge under aerobic conditions entirely removed DAAN in only six days after each DAAN spike, while the DAAN abiotic removal by oxygen took 27 days to be completed (Figure 19, panel E). This observation evidences the importance of microorganisms on the DAAN aerobic removal.

5.4.3 Development of DAAN-consuming enrichment cultures

After screening different electron acceptor conditions, we selected biotic microcosms to develop DAAN-consuming enrichment cultures. Since pyruvate, sulfate, or nitrate addition did not improve DAAN removal in anaerobic microcosms, we decided to enrich the microbial community from the treatment without added e^- acceptors. On the other hand, the DAAN aerobic removal in live sludge was remarkably faster than DAAN autoxidation in abiotic conditions. Hence, we also enriched the microbial community from the microcosms with oxygen to degrade DAAN.

Figure 20 (panel A) shows that DAAN consumption became slower at each transfer of the microbial community from the microcosms without added e^- acceptors. DAAN stopped being removed after three transfers, even with an incubation time of 119 days. Nevertheless, previous studies suggested that DAAN could become anaerobically covalently incorporated into soil organic matter (OLIVARES et al., 2017). Weber *et al.* (1996) reported aniline, the simplest aromatic amine, to react with humic and fulvic acids dissolved in river water. Thus, we evaluated three possible causes for the lack of DAAN removal: (i) the transfers caused the microorganisms to lose their ability to remove DAAN; (ii) instead of a biological process, DAAN removal was happening by chemical reactions with natural organic matter possibly present in sludge, which was being diluted ten times at each transfer; or (iii) electron acceptors naturally present in the sludge were coupled to DAAN removal and became diluted 1000x by the three consecutive transfers, causing the process to stop. To test alternative (ii), we incubated DAAN with possible humic and fulvic acids extracted from sludge for over 76 days, as shown in Appendix C. However, no relevant DAAN consumption was observed, which ruled out alternative (ii). We tested alternative (iii) by measuring the concentration of nitrite, nitrate, and sulfate in our inoculum using IC. However, this alternative was also ruled out because the concentrations of those electron acceptors in the inoculum were below the detection limit of 0.5 mg L^{-1}. We concluded that, although anaerobic sludge could actively remove DAAN, the

microorganisms in our inoculum were not able to grow using DAAN as their sole substrate in anaerobic conditions.

Figure 20 – DAAN consumption by the enrichment cultures. Panel A: enrichment culture from the condition without added e^- acceptors. Panel B: enrichment culture from the condition with oxygen. Legend: DAAN incubated with the enrichment culture (●) and DAAN in an abiotic autoxidation control with oxygen (○). Symbols represent the average of two replicates in panel A and three replicates in panel B, and error bars represent the standard deviation.

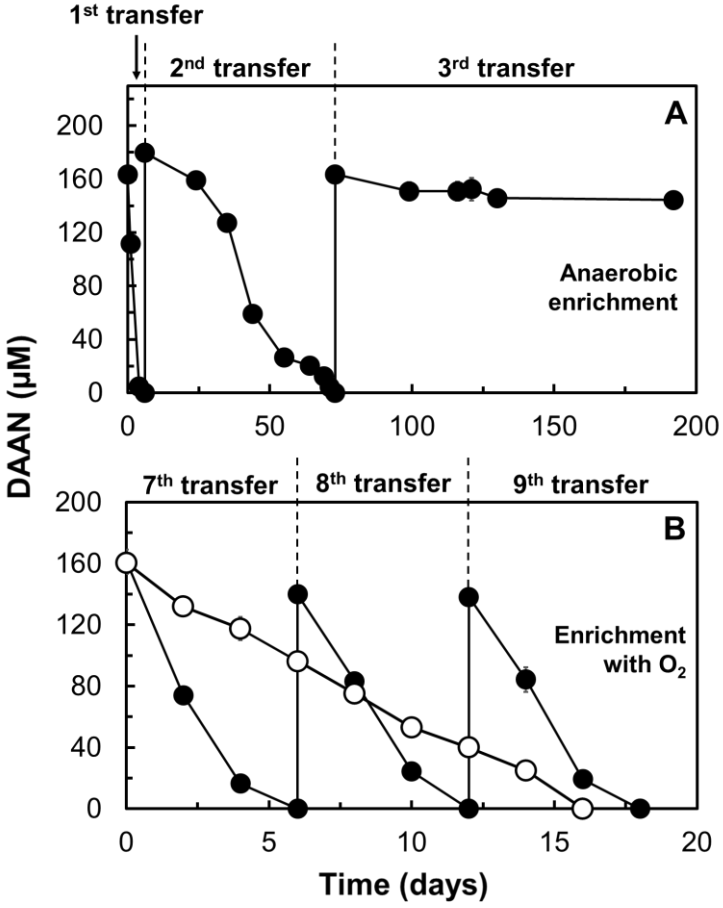

On the other hand, microorganisms could be enriched to remove DAAN in the presence of oxygen, as shown in Figure 20 (panel B). DAAN consumption by the culture was best described by a zero-order rate, except for the 7th transfer. Differently from what is observed for sludge, the limiting step in more selected and diluted cultures tends to be the enzymatic production, not the concentration of the target compound (DAAN, in our case) (VAN DER ZEE *et al.*, 2001). Thus, the transfers caused the degradation rate to become independent from DAAN concentration, fitting in a zero-order model. The zero-order consumption rates were 30.7, 25.3, and 25.2 µM d^{-1} for the 7th, 8th, and 9th transfers, respectively, with R^2 values ranging from 0.92 to 0.97. DAAN removal by the enrichment culture was 2.5 to 3.0 times faster than that of the abiotic control, which exhibited a rate of 10.1 µM d^{-1} (R^2 = 0.99). Our findings show

for the first time that not only DAAN can be bioremoved despite all abiotic reactions it can undergo, but also microorganisms might have used DAAN as a substrate in the presence of oxygen. We further enriched the culture by performing a 10^{-4} dilution to extinction and six more transfers before sequencing the microbial community.

5.4.4 Changes in the microbial community

To assess the effects of DAAN exposure in the sludge microbial community, we performed 16S rRNA sequencing in the inoculum and live sludge from microcosms after total DAAN consumption for three times. We also sequenced the community from the DAAN-removing aerobic enrichment culture. Rarefaction curves (shown in Appendix C) reached apparent asymptotes, indicating that the sampling represented the microbial communities well. In agreement with that, Chao1 values (SI) were higher than 90%, implying good coverage of our sequencing. Among all samples, the number of genera changed the most in the enrichment culture, decreasing to 22 compared to 354 in the inoculum. The values of diversity and evenness indexes are detailed in Appendix C.

Figure 21 illustrates the similarity between the microbial communities studied. Panel A shows a Principal Component Analysis of the abundance data (genus level), in which the first (PC1) and the second (PC2) principal components explained 92.4 and 5.1% of data variance, respectively. Closer values of PC1 and PC2 indicate stronger similarity between samples. Panel B shows a dendrogram based on Bray-Curtis Index, also comparing genera distribution within microbial communities. The communities from all microcosms distanced themselves from the inoculum, reflecting the possible effect of DAAN or electron acceptors. The communities in the microcosms without added e^- acceptor (with or without pyruvate) were the most similar, being both close to the community exposed to sulfate. This similarity contributes to our hypothesis that the mechanism of DAAN consumption in those treatments was the same. On the other hand, the aerobic enrichment culture exhibited the most distinct microbial community among all the samples, including the microcosms exposed to oxygen. The profound changes might have been a result of the selection of microorganisms adapted to DAAN aerobic removal.

Figure 21 – Similarity between the microbial communities from the inoculum, the sludge microcosms after exposure to different redox conditions during DAAN consumption, and the enrichment culture from the condition with oxygen. Panel A: principal component analysis applied to the normalized abundance of genera of the different microbial communities. Other principal components together explained only 2.5% of the data variance and were neglected. Panel B: dendrogram representing the taxonomic divergence at the genus level. Legend based on different microbial communities: inoculum (●), no added e- acceptor (◊), no added e- acceptor + pyruvate (□), sulfate (△), nitrate (▲), oxygen (+), and enrichment culture from the condition with oxygen (★).

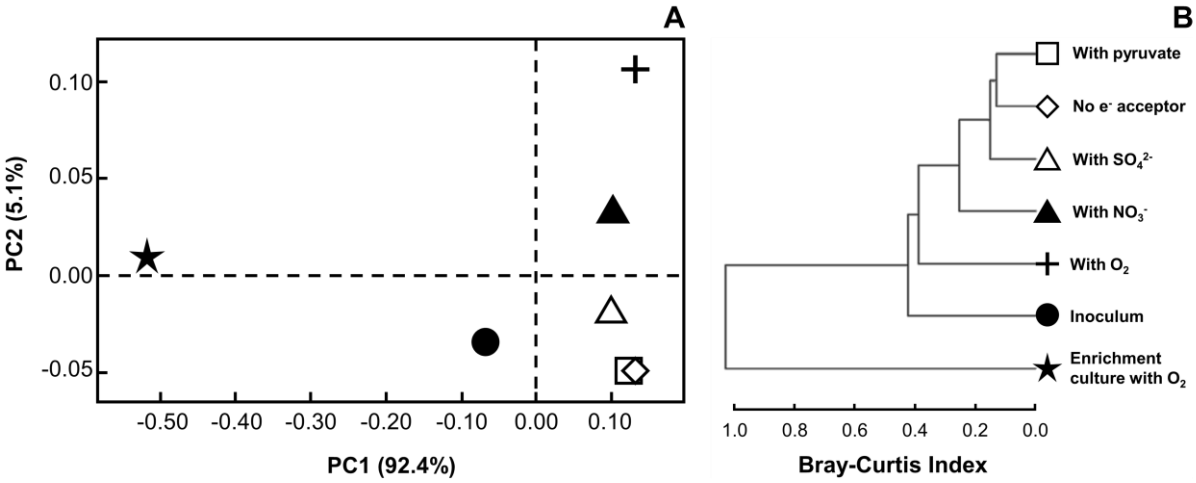

Figure 22 shows the taxonomic profiles at the genus and family levels of the samples. Since the inoculum was a mixture of sludges from textile and petrochemical wastewater treatments, we expected to find aromatic-degrading microorganisms. Indeed, some of the most abundant genera in the inoculum and the sludge microcosms were reported to grow on aromatic compounds. Some species of *Clostridium*, one of the most abundant genera in our samples, were observed to anaerobically degrade methoxylated aromatic compounds (MECHICHI *et al.*, 2005) and completely mineralize sulfonated aromatics to methane (SHCHERBAKOVA *et al.*, 2015). Some *Bacteroides* were reported to anaerobically convert aromatic amino acids to carboxylic acid (VAN DER MEULEN *et al.*, 2008), removing the aromatic character and the amino group from compounds similar to DAAN. Other genera reported to grow on aromatic compounds anaerobically were *Porphyromonas* (PRAJAPATI *et al.*, 2016), *Methanocella* (KATO *et al.*, 2015), *Geobacter* (WISCHGOLL *et al.*, 2005), and *Parabacteroides* (MESLE *et al.*, 2015). Additionally, *Rhodococcus* species were shown to degrade xylenes using oxygen as an electron acceptor (KIM *et al.*, 2002).

In our study, the microbial communities of the sludge microcosms changed to adapt to DAAN exposure or the redox conditions in the microcosms. *Bacteroides*, *Parabacteroides*, and *Rhodococcus* became relatively more abundant in all microcosms compared to the inoculum,

although *Rhodococcus* particularly thrived in aerobic conditions (7.8 times more abundant than in the inoculum). The growth of anaerobes, such as *Bacteroides* and *Parabacteroides*, in the microcosms with oxygen probably occurred in micro-zones with low oxygen availability. These micro-zones are possible since the initial dissolved oxygen concentration in the microcosms (2.33 ± 0.3 mg L^{-1}) was far from saturation (8.0 mg L^{-1} for 27 °C). The relative abundance of *Geobacter*, which presents facultative species (LIN et al., 2004), also increased in the microcosms with oxygen. Moreover, *Porphyromonas* became more abundant in all anaerobic microcosms, while *Clostridium* exhibited a relative abundance increase in the microcosms without added e^- acceptor (with and without pyruvate addition). Despite this diversity, the microorganisms could not support the development of an DAAN-removing anaerobic enrichment culture. Additionally, none of those genera was predominantly present in the aerobic enrichment culture.

Unclassified microorganisms derived from the domain *Bacteria* were abundant in the inoculum (42.0%) and the sludge microcosms with oxygen (22.8%). After enriching the culture using DAAN as the sole substrate in the presence of oxygen, the relative abundance of those unclassified microorganisms increased to 84.7%. Such increasing suggests that the DAAN aerobic bioremoval might have been carried out by microorganisms not characterized by previous studies, reflecting the process novelty. The other 15.3% was formed mainly by anaerobic bacteria (e.g., *Paenibacillus* and *Escherichia*), which are probably related to the inoculum source. The remarkable difference between the communities from the sludge microcosm with oxygen and the aerobic enrichment culture means that many microorganisms in the inoculum could survive under DAAN exposure, but only a few could grow possibly using DAAN as substrate.

Figure 22 – Taxonomic profiles of the microbial communities from the inoculum, the sludge microcosms after exposure to different redox conditions during DAAN consumption, and the enrichment culture from the condition with oxygen. Panels show the top 15 more abundant taxa for each level. Less abundant taxa were grouped as “Others”. Panel A: family level. Panel B: genus level.

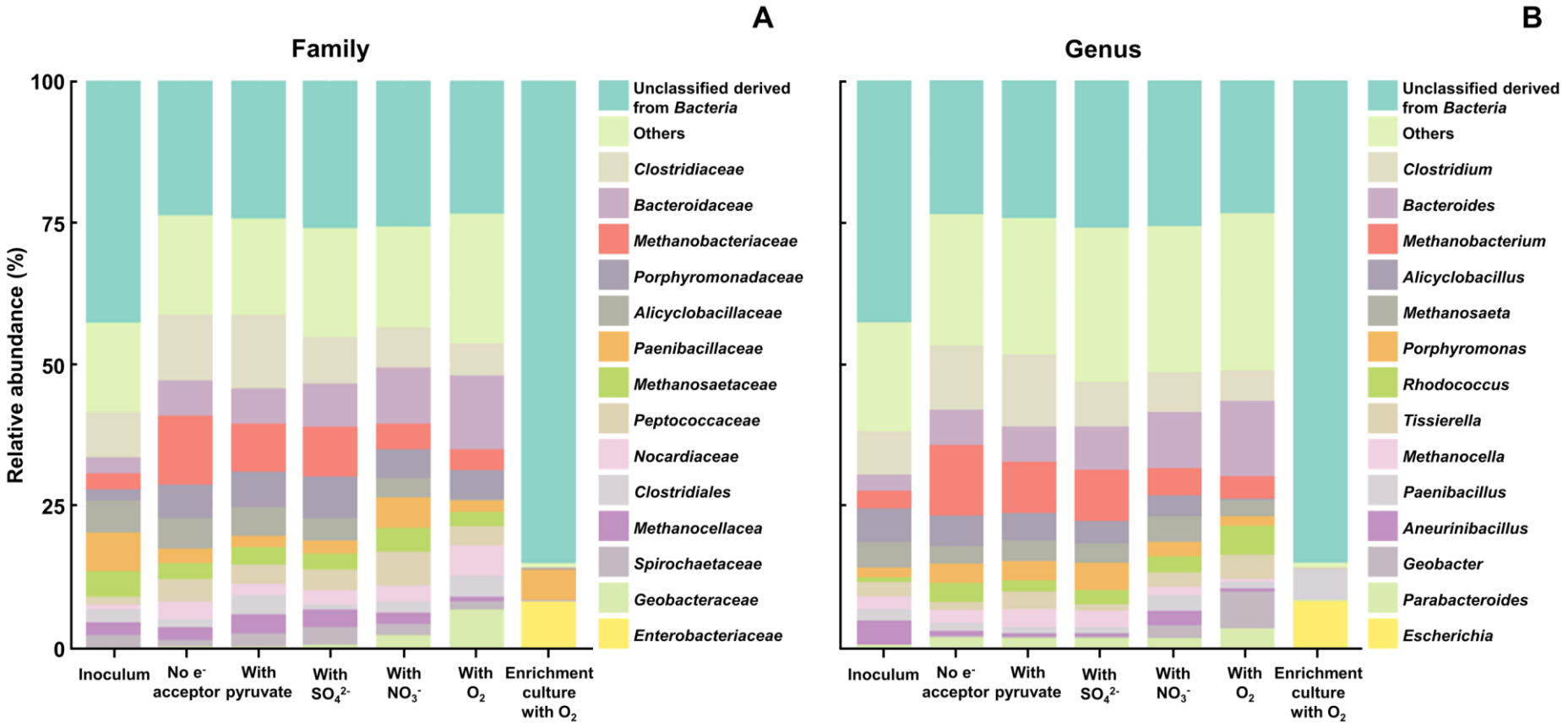

5.5 CONCLUSIONS

We screened different electron acceptor conditions to promote DAAN removal in sludge, assessing the contributions of different biotic and abiotic processes. Adding pyruvate (as a co-substrate), sulfate, or nitrate (as electron acceptors) does not improve DAAN removal compared to the fermentative condition without added electron acceptors or co-substrates. On the other hand, aerobic conditions can remarkably favor DAAN's removal, with contributions of both autoxidation and biotic pathways. Our findings suggest that an aerobic DAAN-removing step may be implemented after DNAN anaerobic biotransformation to improve DNAN-containing wastewater treatment. Future work should focus on the metagenome and by-products of DAAN aerobic transformation.

6 DAAN INCORPORATION INTO MODEL HUMIC COMPOUNDS

Resulting publication: MENEZES, O.; KADOYA, W.; GAVAZZA, S.; SIERRA-ALVAREZ, R.; MASH, E.; ABRELL, L.; FIELD, J. A. Oligomerization with model quinone compounds unveils the environmental fate of the insensitive munitions reduced product 2,4-diaminoanisole (DAAN) under anoxic conditions. Submitted for publication.

Figure 23 – Graphical abstract for section 6.

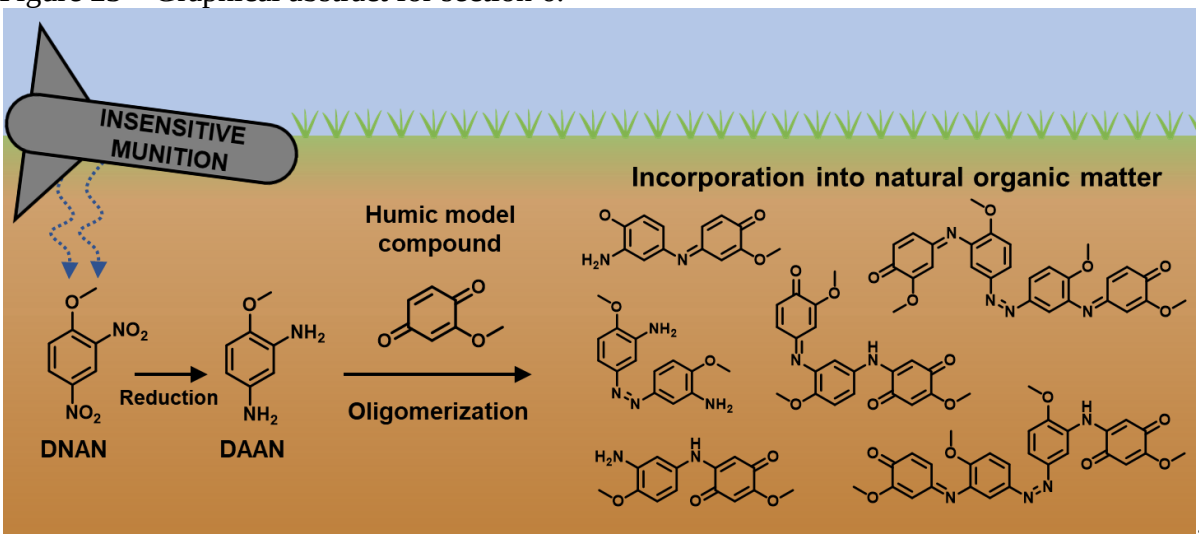

6.1 ABSTRACT

2,4-Dinitroanisole (DNAN) is an insensitive munitions compound expected to replace 2,4,6-trinitrotoluene (TNT). The product of DNAN's reduction in the environment is 2,4-diaminoanisole (DAAN), a toxic and carcinogenic aromatic amine. DAAN is known to become irreversibly incorporated into soil natural organic matter (NOM) after DNAN's reduction. Herein, we investigate the reactions between DAAN and NOM under anoxic conditions, using 1,4-benzoquinone (BQ) and methoxybenzoquinone (MBQ) as model humic moieties of NOM. A new method stopped the fast reactions between DAAN and quinones, capturing the fleeting intermediates. We observed that DAAN incorporation into NOM (represented by BQ and MBQ models) is quinone-dependent and occurs via Michael addition, imine (Schiff-base) formation, and azo bond formation. After dimers are formed, incorporation reactions continue, resulting in trimers and tetramers. After 20 days, 56.4% of dissolved organic carbon from a mixture of DAAN (1 mM) and MBQ (3 mM) had precipitated, indicating an extensive polymerization, with DAAN becoming incorporated into high-molecular-weight humic-like compounds. Our

findings shed light on abiotic mechanisms of DAAN incorporation into NOM, showing that this process does not require aerobic conditions nor a specific catalyst. The incorporation of DAAN into NOM can potentially be applied as a remediation strategy coupled with DNAN anaerobic biotransformation.

6.2 INTRODUCTION

The defense industry is replacing conventional explosives with insensitive munitions compounds (IMCs). “Insensitive” means that those compounds are more resistant to unintentional detonation caused by mechanical shocks or high temperatures than conventional explosive constituents (BODDU *et al.*, 2008; SIKDER; SIKDER, 2004). One of the most important IMCs is 2,4-dinitroanisole (DNAN), which has been replacing 2,4,6-trinitrotoluene (TNT) in munitions formulations (DAVIES; PROVATAS, 2006). Unfortunately, DNAN represents an environmental threat, being reported to be toxic to methanogens, nitrifying bacteria, bioluminescent bacteria (LIANG *et al.*, 2013), algae, ryegrass, earthworms (DODARD *et al.*, 2013), and zebrafish (OLIVARES *et al.*, 2016b).

At military firing ranges, chunks of undetonated ordnance can remain in the soil, be dissolved by precipitation, and reach ground and surface water (TAYLOR *et al.*, 2015a). The solubility of DNAN (276 mg L^{-1}) (BODDU *et al.*, 2008) is in the same order of magnitude as that of TNT (100 mg L^{-1}) (BRANNON; PENNINGTON, 2002). Such contamination can last for long periods since the decomposition of nitroaromatic compounds under aerobic conditions is not reliable (AMARAL *et al.*, 2009). On the other hand, a diversity of microorganisms (HAWARI *et al.*, 2015; OLIVARES *et al.*, 2016a) and some reactive minerals (KHATIWADA *et al.*, 2018c; SHEN *et al.*, 2013) can promote the reduction of nitro groups under anaerobic conditions, producing aromatic amines. This transformation has crucial implications for DNAN’s environmental fate.

The reduction of DNAN’s ortho nitro group produces 2-methoxy-5-nitroaniline (MENA), while the reduction of the para nitro group produces 4-methoxy-5-nitroaniline (iMENA) (HAWARI *et al.*, 2015; OLIVARES *et al.*, 2016a). Further reduction of the remaining nitro group of MENA or iMENA forms 2,4-diaminoanisole (DAAN), an aromatic amine toxic to many microorganisms (LIANG *et al.*, 2013; OLIVARES *et al.*, 2016c) and carcinogenic to mammals (AMES *et al.*, 1975; AUNE; DYBING, 1979). Although DNAN reduction to DAAN by biotic and abiotic pathways is well known, DAAN’s ultimate environmental fate is not well understood.

In many soil experiments, DAAN does not accumulate after MENA or iMENA reduction. Instead, this compound disappears after a few days (HAWARI *et al.*, 2015; LIANG *et al.*, 2013; OLIVARES *et al.*, 2016a). Attempts to recover sorbed DAAN in soil failed, indicating covalent incorporation (HAWARI *et al.*, 2015). Furthermore, ^{14}C from ^{14}C radiolabeled DNAN was shown to become irreversibly incorporated into the soil's humin fraction after anaerobic reduction (OLIVARES *et al.*, 2017). A possible explanation is that the amino groups on DAAN covalently react with quinone moieties of natural organic matter (NOM), as shown for other aromatic amines (GULKOWSKA *et al.*, 2012; THORN *et al.*, 1996a). The reactions that govern aromatic amines coupling with quinones are Michael addition and imine formation (KUTYREV, 1991; PARRIS, 1980). Previous works illustrate these mechanisms by showing that benzidine or 4-methylaniline (aromatic amines) reacted with the quinone compound 2,6-dimethyl-1,4-benzoquinone, producing the corresponding Michael adducts and imines (ONONYE; GRAVEEL, 1994; ONONYE *et al.*, 1989). Indeed, quinone groups of NOM seem to drive many environmentally relevant redox reactions (UCHIMIYA; STONE, 2009).

Strong evidence demonstrates that quinones are important moieties of NOM (UCHIMIYA; STONE, 2009). Firstly, NOM can undergo reversible redox reactions quantified with electron carrier capacity (RATASUK; NANNY, 2007; UCHIMIYA; STONE, 2009). Secondly, cyclic voltammetry of NOM has been shown to behave very similarly to cyclic voltammetry of model quinone compounds (NURMI; TRATNYEK, 2002). Semiquinone radicals derived from the one-electron reduction of quinones or the one-electron oxidation of hydroquinones can be detected in NOM by electron paramagnetic resonance (SCOTT *et al.*, 1998). Such detection is correlated with the reversible redox capacity of the NOM. Additionally, hydroxylamine-treated NOM generates resonances consistent with monoximes attributable to the tautomeric equilibrium between the nitrosophenol and monoxime derivatives of quinones (THORN *et al.*, 1992), constituting strong evidence for quinones in NOM.

Due to the complexity of NOM, the use of small molecules as models is an efficient way to assess the substitution reactions between aromatic amines, such as DAAN, and quinone moieties present in NOM. Model quinone compounds share similar redox properties, and the results of studies applying one of them can be extrapolated to the others. Methoxybenzoquinone (MBQ) is a model quinone compound worthy of special attention since it is an intermediate of lignin degradation and a potential constituent of NOM (BUSWELL *et al.*, 1979; KIRK; LORENZ, 1973; YUAN *et al.*, 2016). Also, MBQ was the most susceptible to oxidoreductase enzymes activity among a group of humic model quinones (BUSWELL *et al.*, 1979).

This study's objective was to investigate the abiotic pathways of DAAN irreversible incorporation into NOM via anoxic reactions with quinones. To this end, we evaluated the formation of oligomers from reactions between DAAN and two model humic constituents, 1,4-benzoquinone (BQ) and methoxybenzoquinone (MBQ). However, those reactions take place in seconds. To work around this problem, we developed a new method to capture fleeting intermediates for examination. This new approach allowed for the first time a comprehensive look at the mechanisms leading to DAAN disappearance in the environment. An additional objective was to assess the formation of high-molecular-weight insoluble polymers from DAAN reactions with quinones.

6.3 MATERIALS AND METHODS

6.3.1 Chemicals

We purchased 2,4-diaminoanisole (DAAN, CAS # 615-05-4, 98+% purity) and 1,4-benzoquinone (BQ, CAS # 106-51-4, 98+% purity) from Sigma-Aldrich (Saint Louis, MO, USA). DAAN was purified by thin-layer chromatography. 1,4-Hydroquinone (HQ, CAS # 123-31-9, 99.5% purity) was purchased from Acros Organics (Morris Plains, NJ, USA). Methoxybenzoquinone (MBQ, CAS # 2880-58-2, 99% purity) and methoxyhydroquinone (MHQ, CAS # 824-46-4, 98% purity) were purchased from TCI America (Portland, OR, USA).

6.3.2 DAAN incorporation assays

6.3.2.1 Pairing DAAN and quinones

We performed experiments pairing DAAN with BQ or MBQ using sacrificial test tubes. In all experiments, the pH was held at 5 using a phosphate buffer (13.8 mM of KH_2PO_4 and 16.2 mM of K_2HPO_4). We added 4.5 mL of BQ or MBQ concentrated aqueous solutions (final concentration ranging from 0.3 to 3 mM depending on the experiment) into 25 mL test tubes. We purged the oxygen by flushing the liquid for 4 min with N_2. Then we closed the test tubes with t-butyl caps and aluminum seals and needle flushed the headspace for an additional 4 min. DAAN concentrated solution was prepared and stored in a serum bottle, also flushed with N_2, and sealed to avoid oxygen contamination. The reaction started when we added 0.5 mL of

DAAN concentrated solution into the test tubes containing either BQ or MBQ and vortexed immediately. DAAN's added concentration varied from 0.3 to 3.0 mM in our experiments.

To stop the reaction, we added 15 mL of acetonitrile after the appropriate reaction time, vortexed, and froze the sacrificial test tubes at −80 °C until analysis. Control experiments to verify this method's ability to stop the reactions were performed and can be found in Appendix D. The reaction times varied from 6 s to 15 min. We also performed control experiments with separated DAAN, BQ, HQ, MBQ, and MHQ, and paired DAAN and HQ, or DAAN and MHQ.

6.3.2.2 Polymerization assay

We performed an experiment pairing DAAN and MBQ to assess the reaction products' precipitation after more extended periods (20 days). We added 26 mL of MBQ concentrated solution with the same phosphate buffer described in section 6.3.2.1 to 45 mL serum bottles in which oxygen was also purged by flushing with N_2. Then, 4 mL of DAAN concentrated solution (previously stored under anoxic conditions) was added to the bottles, which were kept in the dark. Subsamples were removed at appropriate times and filtered immediately using a 0.22 µm membrane to remove suspended organic carbon. The filter was coupled to the syringe used to collect samples to minimize sample exposure to oxygen before filtration. We diluted the filtered samples four times with ultrapure water and froze them at –80 °C until analysis. Anoxic control experiments with separated DAAN and MBQ, and paired DAAN and MHQ were also performed. All experiments were performed in duplicate at 23 ± 1 °C.

6.3.3 Analytical methods

6.3.3.1 UHPLC – DAD

We analyzed the samples from DAAN-BQ and DAAN-MBQ pairing experiments with UHPLC-DAD (Agilent 1290 Infinity, Santa Clara, CA, USA). We used a Zorbax SB-C18 column (4.6 × 150 mm, 5 µm; Agilent, Santa Clara, CA, USA). The mobile phase ran isocratically (0.5 mL min^{-1}) at 36 °C for 31.0 min with a gradient of acetonitrile/H_2O (v/v%) in as follows: from 0.0 to 3.0 min held at 5/95, from 3.0 to 18.0 min increasing to 90/10, from 18.0 to 18.5 increasing to 98/2, from 18.5 to 26.0 held at 98/2, from 26.0 to 27.0 decreasing to 5/95, and from 27.0 to 31.0 held at 5/95. The sample injection volume was 20 µL. The compounds were detected at the following retention times and wavelengths: DAAN (10.8 min,

300 nm), BQ (10.6 min, 300 nm), HQ (8.0 min, 290 nm), MBQ (11.0 min, 400 nm), and MHQ (9.3 min, 290 nm). We prepared standards using a 75/25% mixture of acetonitrile/H_2O.

6.3.3.2 UHPLC-HRAM-MS/MS

We prepared a comprehensive compound library using ChemDraw (PerkinElmer Informatics) including masses of products from different hypothetical reactions between DAAN and quinones to be used in a targeted UHPLC-HRAM-MS/MS analysis of reaction mixtures. Imine formation, Michael addition (KUTYREV, 1991; PARRIS, 1980), and azo bond formation (HAWARI *et al.*, 2015) were the main reactions considered. Derived compounds from DAAN previously found during DNAN biotransformation in soil or sludge were also included (LIANG *et al.*, 2013; OLIVARES *et al.*, 2016a), as well as the possible products of reactions between those compounds and DAAN or quinones. The library included structures ranging from dimers to heptamers (seven monomer units), which totaled 167 different masses.

UHPLC-HRAM-MS/MS (UltiMate 3000 UHPLC, Dionex, Sunnyvale, CA, USA coupled to a Q Exactive Focus Orbitrap mass spectrometer, Thermo Scientific, San Jose, CA, USA) was used to detect targeted compounds in our samples. Chromatographic conditions are described in section 6.3.3.1. Positive mode electrospray ionization at 380 °C with a capillary setting of 4.0 kV was used with N_2 at flow rates at 60 for sheath gas and 20 for auxiliary gas in the mass spectrometer ion source. Product ion spectra were acquired using a collision energy of 10 eV. High resolution (35 K) accurate mass measurements for precursors ions $[M + H]^+$ were sought in a survey scan (m/z 90 – 900 Da). We used Excalibur 4.1.31.9 and TraceFinder 4.1 to process data and identify mass chromatogram peaks.

6.3.3.3 DOC measurements

We measured dissolved organic carbon (DOC) using a Shimadzu Total Carbon Analyzer VCSH (Columbia, MD, USA). We added concentrated hydrochloric acid (HCl) to the samples to adjust the pH to 2. Inorganic carbon was purged by sparging the samples with air using the equipment default configuration. Then, the samples' organic carbon content (filtered immediately after sampling) was combusted at 680 °C and quantified. Standards were prepared using potassium hydrogen phthalate ($C_8H_5KO_4$) in the appropriate concentration range.

6.4 RESULTS AND DISCUSSION

6.4.1 Transformation of DAAN and quinones

Initially, we tested the reactions between DAAN and BQ (Figure 24). BQ was partially reduced to HQ. The combination of DAAN and BQ seemed highly reactive since we did not detect DAAN after 6 s nor BQ and HQ after 3 min. We also observed an increase in color and turbidity within the first seconds of reaction. In parallel, we performed controls with DAAN, BQ, and HQ incubated individually, and with DAAN and HQ incubated together (shown in Appendix D). The concentrations of DAAN, BQ, and HQ were stable in the controls.

Figure 24 – Concentrations of DAAN (●, ○) BQ (▲, △), and HQ (■, □) incubated in anaerobic conditions. Open shapes refer to the added concentrations of the compounds, while closed shapes refer to measured concentrations. The dashed line represents the sum of BQ and HQ. DAAN was entirely consumed in less than 6 s.

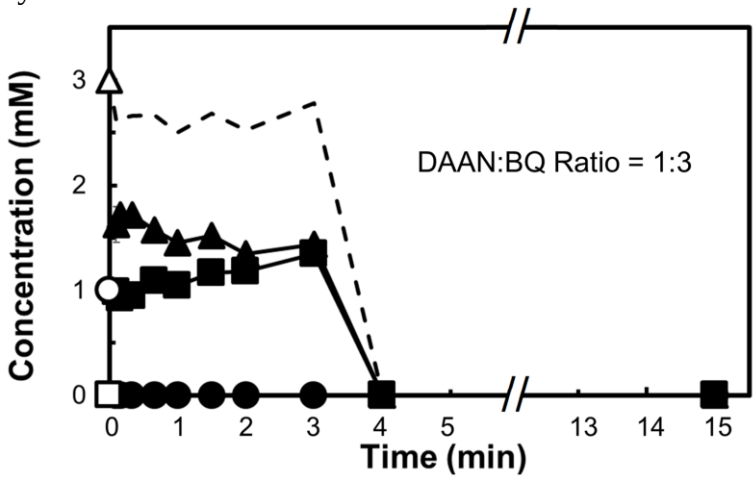

To seek a less reactive system than the combination of DAAN and BQ, we tested the DAAN reaction with MBQ, a quinone compound with fewer atoms available for nucleophilic attack than BQ. Additionally, there is strong evidence that MBQ is a reliable model for NOM (BUSWELL *et al.*, 1979; KIRK; LORENZ, 1973; YUAN *et al.*, 2016). We reacted DAAN with MBQ in three different molar ratios, as seen in Figure 25. When the DAAN:MBQ molar ratio was 1:3 or 1:10, DAAN was again entirely consumed in 6 s or less, while MHQ was formed as a product of MBQ reduction. When the DAAN:MBQ molar ratio was 3:1, the reaction entirely consumed MBQ within 6 s, and MHQ was not detected. In the latter case, DAAN was partially consumed in 6 s, then formed again, possibly due to reversible reactions discussed in section 6.4.2. The gradual formation of colored reaction mixtures (shown in Appendix D) was

observed. Controls with MBQ and MHQ incubated individually and with DAAN and MHQ incubated together did not exhibit a change in the concentration of the analyzed compounds (shown in Appendix D).

Figure 25 – Concentrations of DAAN (●, ○) MBQ (▲, △) and MHQ (■, □) incubated in anaerobic conditions. Open shapes refer to the added concentrations of the compounds, while closed shapes refer to measured concentrations. The dashed line represents MBQ and MHQ summed. DAAN was entirely consumed in less than 6 s when the DAAN:MBQ molar ratio was 1:3 (panel A) or 1:10 (panel B). MBQ was totally consumed in less than 6 s when the DAAN:MBQ molar ratio was 10:1.

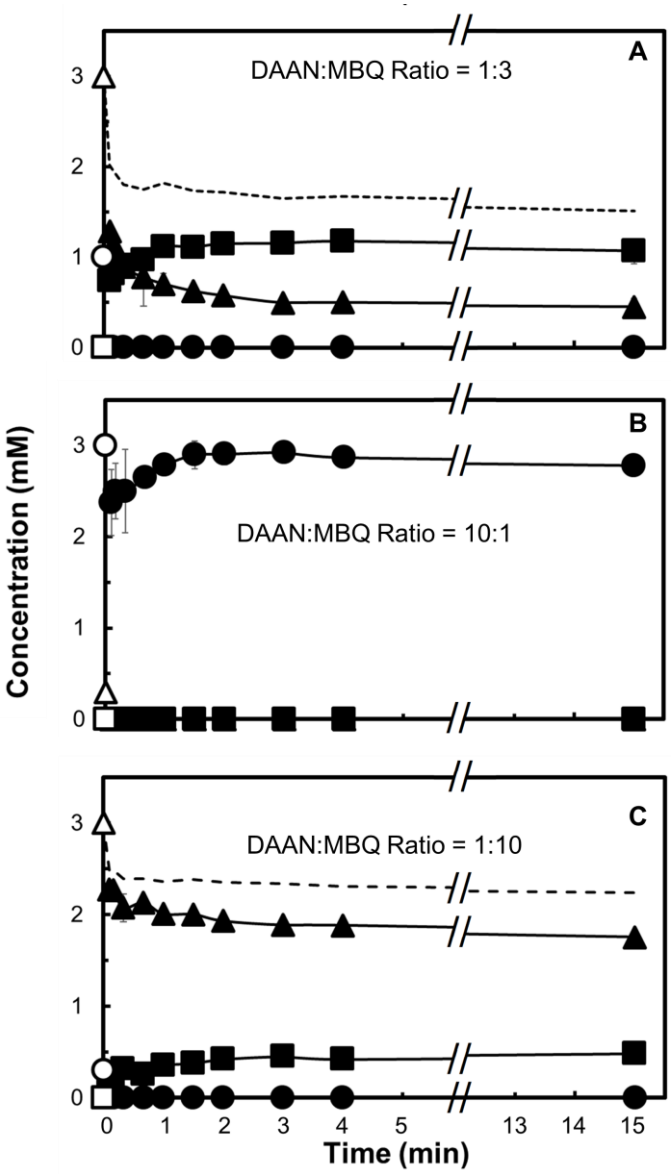

We observed that the DAAN anoxic disappearance was quinone-dependent since pairing DAAN with the reduced forms HQ or MHQ did not lead to DAAN consumption. Moreover, the quinones were not wholly recovered as phenols (Figures 24 and 25), giving

further evidence that they participated in covalent coupling reactions with DAAN. For aerobic conditions, previous studies (GULKOWSKA *et al.*, 2012; GULKOWSKA *et al.*, 2013; THORN; KENNEDY, 2002; THORN *et al.*, 1996b) already indicated that aromatic amines covalently bind to carbonyl groups in NOM. These carbonyl groups are ketone and quinone moieties naturally present in NOM or produced by oxidation of phenolic groups by phenoloxidase enzymes or metal oxides. In this work, however, we studied the DAAN incorporation in anoxic conditions. Furthermore, we used the model quinone compounds directly, without enzymes or other oxidants. Our first results support the findings of Olivares *et al.* (2017), which suggested DAAN could anoxically bind with NOM in soil. Our next step was to analyze the products of such reactions.

6.4.2 Identified products and mechanisms of reactions

We analyzed the formed products of the DAAN reactions with BQ and MBQ using a UHPLC-HRAM-MS/MS (Tables 4 and 5). Our approach to stop the reactions at different time points allowed us to detect different products in a range of molecular weights from 229 to 529 g mol^{-1}. Such findings represent the first time that the products of DAAN reaction with quinones were identified. We tentatively assigned the identified products with the most probable structure based on previous studies with DAAN, a strong body of literature about other aromatic amines, and the steric effects expected from the molecules. Figures 26 and 27 show the proposed structures. The compounds **F** and **P** had masses that could be assigned to alternative structures (shown in Appendix D). However, in the literature, such alternative products have only been attested when nitroso intermediates of DNAN (DAAN's parent compound in the environment) are present in the system (KADOYA *et al.*, 2018; OLIVARES *et al.*, 2016a), which is not the case in this study.

As shown in Figures 26 and 27, the identified products originated from a mixture of reactions with multiple combinations. DAAN reacted with both BQ and MBQ resulting in Michael adducts, imines, and azo oligomers. We show semi-quantitative data corresponding to the peak areas in Appendix D.

Table 4 – Summary of adducts detected in anaerobic incubation of DAAN with benzoquinone (BQ) via UHPLC-HRAM-MS/MS.

Structure in Fig. 26	Molecular formula [M]	Monoisotopic mass [M+H][(i)]	Measured mass [M+H][(ii)]	Retention time (min)[(iii)]	|Delta| (ppm)[(iv)]	Spectral data (Int.)	Incubation times in which it was observed
(A)	$C_{13}H_{12}N_2O_2$	229.0972	229.0963-229.0970	14.1-14.2	0.98	213.0656 (24.2), 214.0736 (36.16), 228.0889 (41.92), 229.0969 (100.0)	6 s, 10 s, 20 s, 40 s, 1 min, 1 min 30 s, 2 min, 3 min, 4 min, 15 min
(B)	$C_{13}H_{12}N_2O_3$	245.0921	245.0914-245.0919	15.3-15.4	0.80	213.0655 (28.7), 214.0734 (77.7), 215.0770 (8.5), 231.0762 (7.1), 245.0916 (100.0)	6 s, 10 s, 20 s, 40 s, 1 min, 1 min 30 s, 2 min, 3 min, 4 min, 15 min
(C)	$C_{14}H_{16}N_4O_2$	273.1346	273.1340-273.1342	17.5-16.7	1.40	242.1155 (71.9), 243.1189 (8.6), 256.1076 (11.9), 273.1340 (100.0)	10 s, 20 s, 40 s, 1 min, 1 min 30 s, 2 min, 3 min, 4 min, 15 min
(D)	$C_{20}H_{18}N_4O_3$	363.1452	363.1425-363.1449	18.3-19.7	0.67	363.1440 (100.0)	6 s, 10 s, 40 s, 1 min, 1 min 30 s, 2 min, 3 min, 4 min, 15 min
(E)	$C_{20}H_{20}N_4O_3$	365.1608	365.1594-365.1602	14.1-14.3	1.57	138.0787 (5.1), 227.0810 (100.0), 228.0845 (10.41), 364.1520 (46.41), 365.1595 (61.0)	6 s, 10 s, 20 s, 40 s, 1 min 30 s

Table 4 – Summary of adducts detected in anaerobic incubation of DAAN with benzoquinone (BQ) via UHPLC-HRAM-MS/MS (conclusion).

Structure in Fig. 26	Molecular formula [M]	Monoisotopic mass [M+H][(i)]	Measured mass [M+H][(ii)]	Retention time (min)[(iii)]	|Delta| (ppm)[(iv)]	Spectral data (Int.)	Incubation times in which it was observed
(F)	$C_{20}H_{18}N_4O_4$	379.1401	379.1389-379.1409	17.3-17.6	0.31	272.1263 (6.3), 349.1292 (9.7), 350.1366 (32.9), 351.1406 (5.1), 381.1552 (100.0)	6 s, 1 min 30 s, 2 min, 15 min
(G)	$C_{20}H_{20}N_4O_4$	381.1557	381.1543-381.1566	18.0-18.4	1.91	349.1288 (12.5), 350.1367 (42.6), 364.1288 (5.01), 381.1549 (100.0)	20 s, 40 s, 1 min 30 s, 2 min, 3 min, 4 min, 15 min

[(i)] Calculated in Xcalibur 4.1.31.9.
[(ii)] Range of masses measured in UHPLC-HRAM-MSMS from all time points.
[(iii)] Range of retention times observed in UHPLC-HRAM-MSMS from all time points.
[(iv)] Other observations matched the compound within 4.65 ppm of the calculated monoisotopic mass.

Table 5 – Summary of adducts detected in anaerobic incubation of DAAN with methoxybenzoquinone (MBQ) via UHPLC-HRAM-MS/MS.

Structure in Fig. 27	**Molecular formula [M]**	**Monoisotopic mass [M+H]$^{(i)}$**	**Measured mass [M+H]$^{(ii)}$**	**Retention time (min)$^{(iii)}$**	**|Delta| (ppm)$^{(iv)}$**	**Spectral data (Int.)**	**Incubation times in which it was observed for different molar ratios (DAAN:MBQ)**		
							Ratio 1:3	**Ratio 1:10**	**Ratio 10:1**
(C)	$C_{14}H_{16}N_4O_2$	273.1346	273.1340-273.1342	17.5-16.7	0.27	242.1155 (71.9), 243.1189 (8.6), 256.1076 (11.9), 273.1340 (100.0)	n/d	n/d	6 s, 10 s, 20 s, 40 s, 1 min, 1 min 30 s, 3 min, 4 min, 15 min
(H)	$C_{14}H_{14}N_2O_3$	259.1077	259.1072-259.1075	14.25-14.37	0.68	243.0761 (15.5), 244.0840 (21.7), 258.0995 (48.4), 259.1073 (100.0)	6 s, 10 s, 20 s, 40 s, 1 min, 1 min 30 s, 2 min, 3 min, 4 min, 15 min	6 s, 10 s, 20 s, 40 s, 1 min, 1 min 30 s, 2 min, 3 min, 4 min, 15 min	6 s, 10 s, 40 s, 1 min, 1 min 30 s, 2 min, 3 min, 4 min, 15 min

Table 5 – Summary of adducts detected in anaerobic incubation of DAAN with methoxybenzoquinone (MBQ) via UHPLC-HRAM-MS/MS (continuation).

Structure in Fig. 27	Molecular formula [M]	Monoisotopic mass [M+H]$^{(i)}$	Measured mass [M+H]$^{(ii)}$	Retention time (min)$^{(iii)}$	|Delta| (ppm)$^{(iv)}$	Spectral data (Int.)	Incubation times in which it was observed for different molar ratios (DAAN:MBQ)		
							Ratio 1:3	Ratio 1:10	Ratio 10:1
(I)	$C_{14}H_{14}N_2O_4$	275.1026	275.1020-275.1022	14.85-14.92	1.22	244.0838 (29.5), 275.1020 (100.0)	6 s, 10 s, 20 s, 40 s, 1 min, 1 min 30 s, 2 min, 3 min, 4 min, 15 min	6 s, 10 s, 20 s, 40 s, 1 min, 1 min 30 s, 2 min, 3 min, 4 min, 15 min	6 s, 10 s, 20 s, 40 s, 1 min, 1 min 30 s, 2 min, 3 min, 4 min, 15 min
(J)	$C_{14}H_{16}N_2O_4$	277.1183	277.1159-277.1194	10.67-11.23	1.41	n/a	10 s, 20 s, 40 s, 1 min 30 s, 2 min, 3 min, 15 min	n/d	n/d
(K)	$C_{21}H_{20}N_4O_4$	383.1557	393.1539-393.1557	15.17-15.97	0.01	n/a	6 s, 10 s, 20 s, 40 s, 1 min, 2 min, 3 min, 4 min, 15 min	n/d	n/d

Table 5 – Summary of adducts detected in anaerobic incubation of DAAN with methoxybenzoquinone (MBQ) via UHPLC-HRAM-MS/MS (continuation).

Structure in Fig. 27	Molecular formula [M]	Monoisotopic mass [M+H]$^{(i)}$	Measured mass [M+H]$^{(ii)}$	Retention time (min)$^{(iii)}$	|Delta| (ppm)$^{(iv)}$	Spectral data (Int.)	Incubation times in which it was observed for different molar ratios (DAAN:MBQ)		
							Ratio 1:3	Ratio 1:10	Ratio 10:1
(L)	$C_{21}H_{18}N_2O_6$	395.1238	395.1222-395.1245	15.18-16.91	0.28	363.0968 (28.7), 364.1042 (28.7), 365.1082 (5.7), 394.1150 (25.2), 395.1229 (100.0)	6 s, 10 s, 20 s, 40 s, 1 min, 1 min 30 s, 2 min, 3 min, 4 min, 15 min	n/d	n/d
(M)	$C_{21}H_{18}N_2O_7$	411.1187	411.1175-411.1182	15.06-16.50	1.10	411.1176 (100.0)	6 s, 10 s, 20 s, 40 s, 1 min, 1 min 30 s, 2 min, 3 min, 4 min, 15 min	40 s, 1 min, 1 min 30 s, 3 min, 4 min	15 min
(N)	$C_{21}H_{22}N_2O_7$	415.1500	415.1481-415.1497	13.66-13.69	0.70	414.1412 (23.4), 415.1486 (100.0)	1 min, 1 min 30 s, 3 min, 15 min	n/d	n/d

Table 5 – Summary of adducts detected in anaerobic incubation of DAAN with methoxybenzoquinone (MBQ) via UHPLC-HRAM-MS/MS (conclusion).

Structure in Fig. 27	Molecular formula [M]	Monoisotopic mass [M+H][(i)]	Measured mass [M+H][(ii)]	Retention time (min)[(iii)]	|Delta| (ppm)[(iv)]	Spectral data (Int.)	Incubation times in which it was observed for different molar ratios (DAAN:MBQ)		
							Ratio 1:3	Ratio 1:10	Ratio 10:1
(O)	$C_{28}H_{24}N_4O_6$	513.1769	513.1755-513.1766	16.09-16.80	0.44	513.1762 (100.0)	6 s, 1 min 30 s, 3 min, 15 min	n/d	n/d
(P)	$C_{28}H_{24}N_4O_7$	529.1718	529.1712-529.1723	16.28-16.34	0.06	501.1765 (21.1), 528.1635 (7.6), 529.1711 (100.0)	6 s, 10 s, 20 s, 40 s, 1 min, 1 min 30 s, 2 min, 3 min, 4 min, 15 min	n/d	n/d

[(i)] Calculated in Xcalibur 4.1.31.9.
[(ii)] Range of masses measured in UHPLC-HRAM-MSMS from all time points.
[(iii)] Range of retention times observed in UHPLC-HRAM-MSMS from all time points.
[(iv)] Other observations matched the compound within 4.65 ppm of the calculated monoisotopic mass.
n/a means not available.
n/d means not detected.

Figure 26 – Proposed formation of oligomers from the incubation of DAAN with BQ.

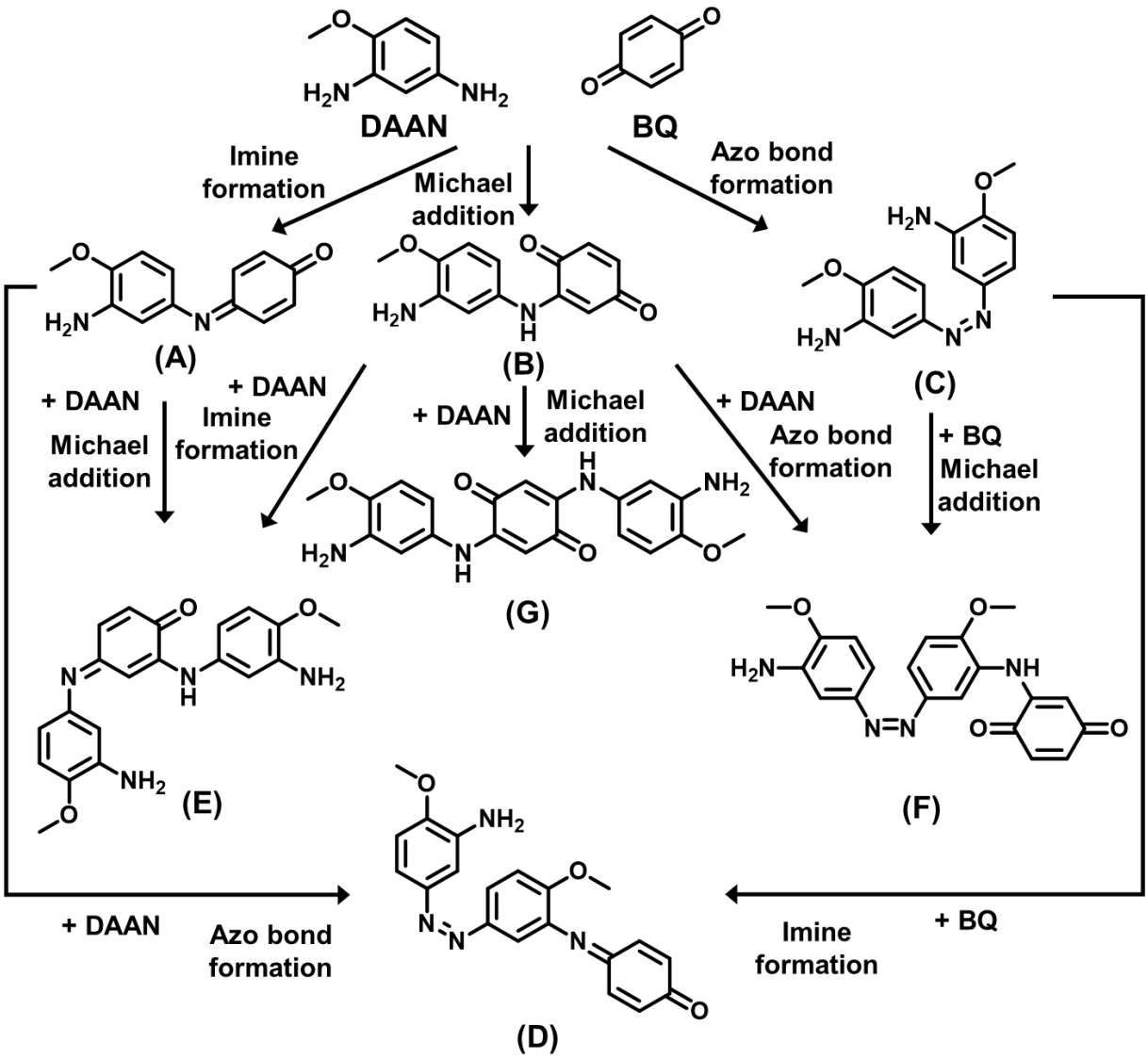

Figure 27 – Proposed formation of oligomers from the incubation of DAAN with MBQ.

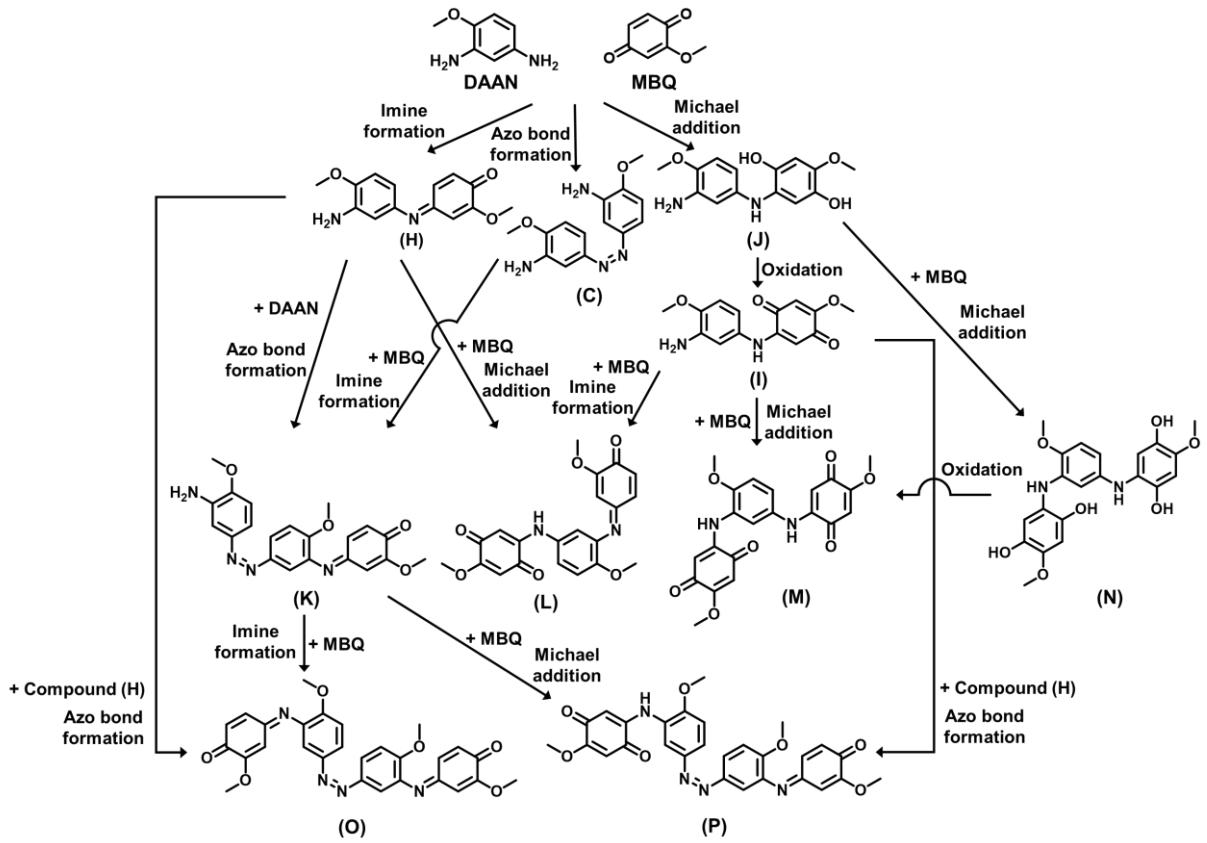

A proposed mechanism for the formation of Michael adducts (compounds **B**, **E**, **F**, **G**, **I**, **J**, **L**, **M**, **N**, and **P**) is shown in Figure 28 (scheme B). Michael addition forms strong bonds that are not easily reversible under environmental conditions (GULKOWSKA *et al.*, 2012; HSU; BARTHA, 1976; PARRIS, 1980). After the nucleophilic addition, the remaining quinones probably oxidized the phenol groups in the Michael adducts. This mechanism finds support from the work of Uchimiya and Stone (2006), which shows that quinones can oxidize hydroquinones. When DAAN reacted with BQ, compound **B** (Figure 26) was formed by Michael addition. The initially formed Michael Adduct was probably oxidized to compound **B** too fast to be detected. On the other hand, when DAAN reacted with MBQ, we could detect the initial Michael adduct in the system (compound **J** in Figure 27), as well as its oxidized product (compound **I** in Figure 27), giving evidence for the mechanism shown in Figure 28 (scheme B). Another example is compound **N** (Figure 27), a trimer formed by Michael additions that has the compound **M** as its oxidized product.

Figure 28 – Proposed mechanisms for the abiotic reactions between DAAN and MBQ under anaerobic conditions. Reversible chemistry of quinones (panel A) is the proposed source or sink of electrons and hydrogen for the other reactions. Imine formation (panel B) and Michael addition (panel C) occurred between DAAN and MBQ. Azo dimer formation (panel D) between two DAAN radicals in anaerobic conditions was quinone-dependent. Reactions between DAAN and BQ followed the same pathways.

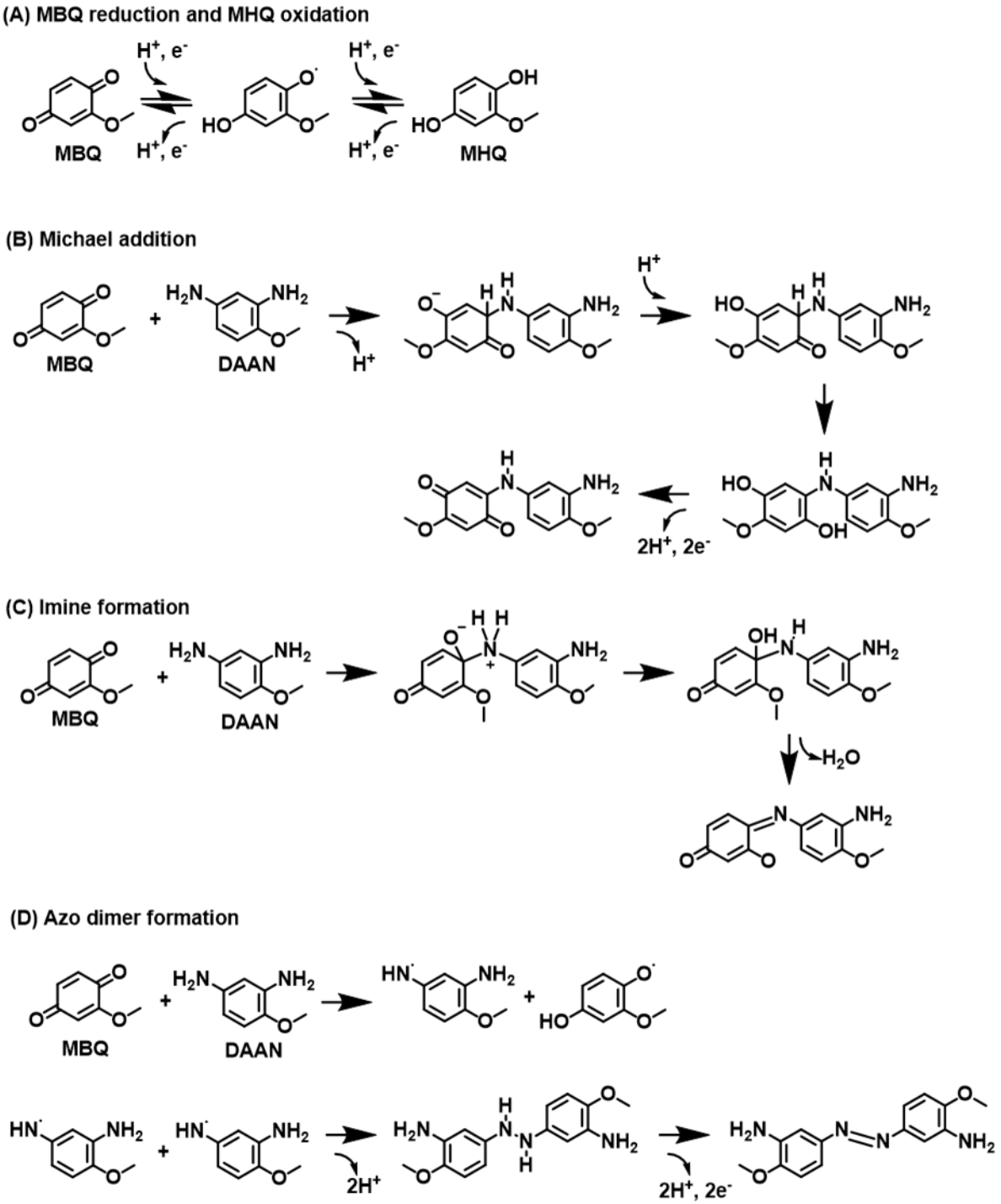

We also observed the formation of imines from the reaction of DAAN with MBQ (Figure 28, scheme C). This process is often seen as a fast and reversible reaction that does not

survive long incubations (PARRIS, 1980). The reversibility is true for anilines reacting with simple quinones since the equilibrium in aqueous systems favors hydrolysis (THORN *et al.*, 1996a). However, for aromatic amines reacting with substituted quinones, the imines are quite stable products and, in some instances, are the main form of nucleophilic addition (ONONYE; GRAVEEL, 1994; ONONYE *et al.*, 1989). Our study observed the highest concentration of imine dimers (compounds **A** and **H**) after only 6 s of reaction. After that, the peak areas due to imine products decreased over time, which may indicate that the imine dimers were going through the following processes: (i) being hydrolyzed back to DAAN and quinone, which could have participated in other reactions, (ii) being tautomerized to the Michael adducts, as hypothesized by Gulkowska *et al.* (2012), (iii) participating in reactions of further oligomerization, generating compounds with higher molecular weight, or (iv) undergoing a combination of these processes. The process (i) seems to be especially important when DAAN is in excess in the system (DAAN:MBQ molar ratio of 10:1), generating an increase in DAAN's concentration after the initial 6 s of reaction. Additionally, compounds **E**, **F**, **D**, **K**, **L**, **O**, and **P** were formed by the oligomerization of the initial dimers and presented imine bonds, which constitute evidence for the process (iii).

A third mechanism, the quinone-dependent formation of azo bonds from DAAN self-coupling in anoxic conditions (Figure 28, scheme D), is a novel finding. In our study, these nitrogen-nitrogen coupling products presented high peak areas in the UHPLC-HRAM-MS/MS analyses (plotted in Appendix D), comparable to the other main products (imines and Michael adducts). Azo bonds were present in a dimer (compound **C**) and in the trimers and tetramers found (compounds **D**, **F**, **K**, **O**, and **P**), indicating that azo bond formation was important for the polymerization process. Before our work, DAAN was believed to form azo dimers only in three conditions: (i) by auto-oxidation under oxygen exposure in aerobic environments (HAWARI *et al.*, 2015; PLATTEN *et al.*, 2010), which is common for other aromatic amines (KONAKA *et al.*, 1968), (ii) by coupling reactions with nitroso intermediates of DNAN reduction in anoxic conditions (KADOYA *et al.*, 2018; OLIVARES *et al.*, 2016a), or (iii) by one-electron oxidation of the amino group by manganese oxide, as described for other primary aromatic amines (LAHA; LUTHY, 1990). Thorn *et al.* (1996a) observed azo bonds forming between anilino radicals and free aromatic amino groups in fulvic acids, however with oxygen acting as the oxidant. For anoxic conditions, we propose that the quinone compounds could have acted as oxidants to form DAAN radicals. These DAAN radicals could have self-coupled, forming azo dimers. Similarly to DAAN, compounds **A**, **B**, **H**, and **I**, which are imines or

Michael adducts with free amino groups, could have been oxidized by quinones, forming radicals that could have self- or cross-coupled resulting in compounds **D**, **F**, **K**, **O**, and **P**.

Many studies described nucleophilic additions, and not radical reactions, as the most important mechanisms for the coupling of aromatic amines and quinones (BIALK *et al.*, 2007; COLON *et al.*, 2002; HSU; BARTHA, 1976; KIM *et al.*, 1997; PARK *et al.*, 1999; WANG *et al.*, 2002; WEBER *et al.*, 1996). To prove that, Gulkowska *et al.* (2012) reacted an aromatic amine with model humic constituents using the radical scavenger tert-butyl alcohol in the medium and observed the same coupling reactions as when no radical scavenger was used. Hence, we proposed the mechanisms governed by nucleophilic additions shown in Figure 28 (schemes B and C). However, we detected DAAN self-coupling products (Figure 28, scheme D), which indicates that the quinone compounds probably generated DAAN radicals. Additionally, the oxidation of hydroquinones by quinones can generate semi-quinone radicals (UCHIMIYA; STONE, 2006) (Figure 28, scheme A). Thus, some of the DAAN-quinone coupling products possibly originated from radical reactions. Previous studies have described the radical coupling reactions in aerobic environments (BOLLAG, 1992; CAMARERO *et al.*, 2008; CAMARERO *et al.*, 2005; CARUNCHIO *et al.*, 2001; DEC; BOLLAG, 2000; THORN *et al.*, 1996b; THORN; KENNEDY, 2002). Simmons *et al.* (1989) suggested that both radical and nucleophilic reactions led to the coupling of 4-chloroaniline and guaiacol under aerobic conditions, with the radical reactions being especially important for the oligomerization of the initial products. In our study, after the nucleophilic addition of DAAN and quinones, the reduced Michael adducts (e.g., compounds **J** and **N** in Figure 27) may have been oxidized by quinones under anoxic conditions. The oxidation may have formed radicals that could have undergone self- or cross-coupling reactions. Thus, nucleophilic additions initiated the coupling reactions between DAAN and quinones, but a combination of nucleophilic additions and radical couplings may have driven the oligomerization process.

The oligomerization process, combining the different reactions, caused the amino groups of DAAN to get locked inside the oligomers, such as in compounds **O** and **P** in Figure 27. The formation of imines or azo bonds, which are steps involved in the oligomerization, may be reversible. However, it is not the single steps but the progression along the sequence of reactions that determine the strength of the amino group incorporation into the humic-like polymers (GULKOWSKA *et al.*, 2012; PARRIS, 1980). Further polymerization is expected to create heterocyclic structures to lock the amino group (HSU; BARTHA, 1976; THORN *et al.*, 1996a). Nonetheless, we did not detect masses that corresponded to heterocyclic structures in

the range of molecular weights investigated in our study. We did observe, though, the precipitation of material during our assays, which we further investigated.

6.4.3 Formation of insoluble polymers

We set up an experiment to assess insoluble polymers' formation from DAAN reaction with quinones (Figure 29). We observed precipitation, expressed by the loss of DOC, only when DAAN and MBQ were incubated together. When DAAN was incubated with MHQ, the DOC remained very close to the theoretical value, evidencing that DAAN incorporation is quinone dependent also for long incubation times. After 20 days of incubation, the precipitation of organic carbon from the reaction of DAAN and MBQ was 58.4% of the theoretical total carbon. Such results indicate that the oligomerization process described in Figures 26 and 27 ultimately led to the formation of insoluble polymers. A polymerization process of this extent is expected to incorporate DAAN irreversibly, which reflects DAAN environmental fate.

Figure 29 – Dissolved organic carbon (DOC) of anaerobic incubation of paired DAAN + MBQ (●) in comparison to control experiments: separated DAAN + MBQ (○) and paired DAAN + MHQ (▲). Paired means the two compounds were incubated together. Separated means the two compounds were incubated individually, and their DOC contents were measured separately and summed in the graph. Precipitated organic carbon represents the loss of DOC by the polymerization reactions when DAAN and MBQ were paired, and it was calculated by subtracting DOC values of separated DAAN + MBQ from paired DAAN + MBQ.

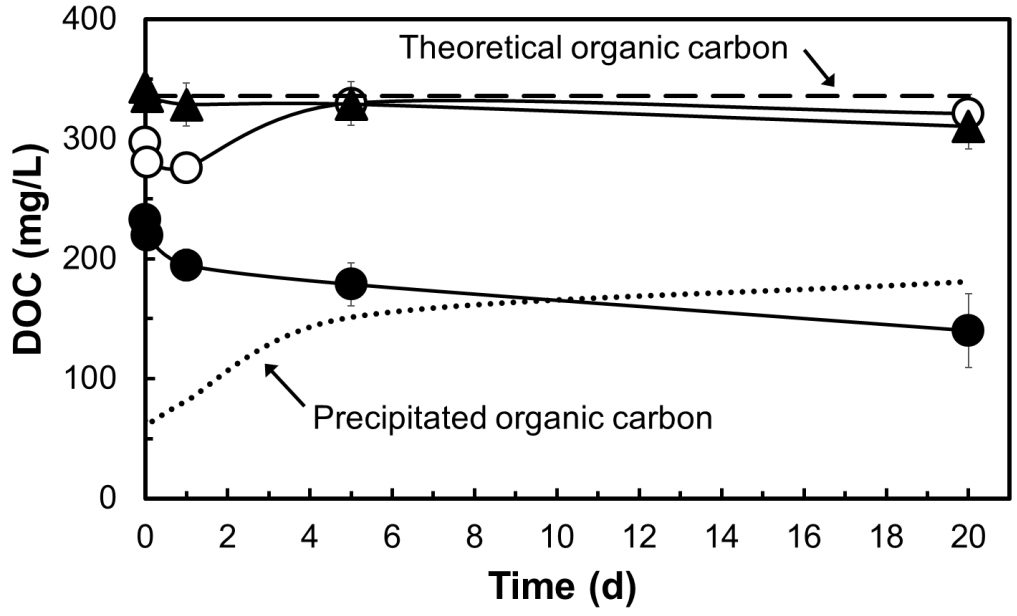

Our results suggest that DAAN incorporation into quinone moieties of NOM can be applied as a natural attenuation strategy coupled to DNAN anaerobic reduction by microorganisms or reactive minerals in the soil. The literature shows that DNAN biotransformation in many soils is followed by DAAN irreversible disappearance (HAWARI *et al.*, 2015; OLIVARES *et al.*, 2016a; OLIVARES *et al.*, 2017). MENA reduction to DAAN, and not the DAAN disappearance, was the frequent limiting step. Thus, the pool of quinones in most soils seems to be enough to lock DAAN inside NOM. If they are insufficient, phenoloxidase enzymes or other oxidants may be employed to oxidize the phenol moieties in NOM to quinone moieties that promptly initiate a polymerization/humification process in the presence of DAAN.

6.5 CONCLUSIONS

DAAN incorporation into model quinones moieties of NOM was driven by nucleophilic, and possibly radical, coupling reactions. The initial products participated in an oligomerization process involving Michael addition, imine formation, and azo bond formation that ultimately led to the precipitation of insoluble polymers. The self-coupling of DAAN resulting from the oxidation by quinones under anoxic conditions causes an azo dimer formation. Azo bonds were also found in the trimers and tetramers formed, indicating that this is a crucial mechanism for the entire oligomerization process. DAAN covalent binding with model humic moieties explains non-extractable bound residue formation after DNAN reduction in soil. The incorporation into NOM may represent a safe endpoint for DNAN remediation. Therefore, we hope that our findings provide valuable knowledge for developing remediation strategies in DNAN-contaminated sites.

7 CONCLUSIONS

Figure 30 summarizes the different strategies for insensitive munitions compounds remediation presented in this work.

Figure 30 – Summary of the biotic and abiotic strategies for insensitive munitions compounds remediation studied in this work.

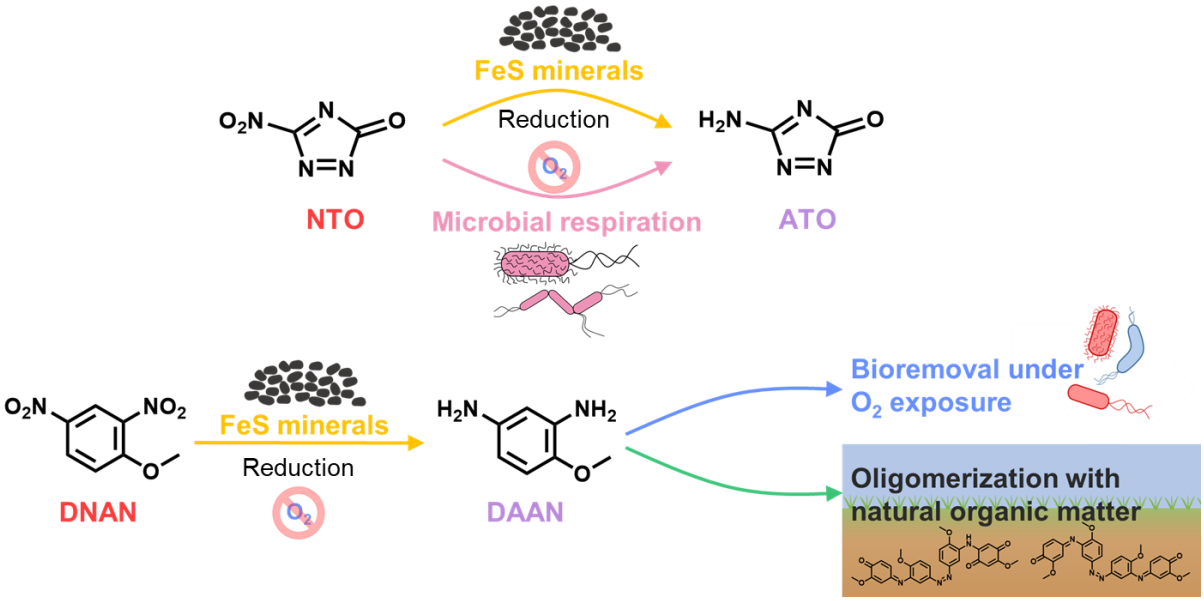

7.1 DNAN AND NTO REDUCTION BY FES MINERAL SURFACES

a) Mackinawite and commercial FeS (mostly containing pyrrhotite and troilite) can abiotically reduce DNAN and NTO to their amines daughter products.
b) Although mackinawite completely reduced DNAN, it only partially reduced MENA to DAAN, as opposed to commercial FeS that reduced DNAN all the way to DAAN.
c) The reactions are surface-mediated.
d) The layered structure of mackinawite is more suitable for the adsorption of MENA and DAAN than the three-dimensional structures of pyrrhotite and troilite.
e) DNAN and NTO can be rapidly transformed in soils subsurface and aquatic sediments with depleted oxygen and containing FeS minerals.
f) Further experiments should focus on the products of FeS minerals oxidation when reacting with IMCs.

7.2 NTO MICROBIAL RESPIRATION

a) A culture enriched from municipal anaerobic digester sludge can reduce NTO to ATO at the expense of oxidizing acetate to CO_2.
b) The enrichment culture is composed mainly of *Geobacter anodireducens* (89.3%) and *Thauera* sp. (5.5%).
c) The culture can perform the unusual process of NTO respiration based on multiple lines of evidence:
    - the enrichment culture can grow only when both NTO and acetate are present;
    - acetate consumption is dependent on the presence of NTO;
    - the enrichment culture exhibited high specificity to NTO;
    - CCCP, an uncoupler of oxidative phosphorylation, strongly inhibits the NTO reduction by the enrichment culture; and
    - the ATP content significantly increases only when the cells are simultaneously exposed to NTO and acetate.
d) Our findings can be useful for the anaerobic bioremediation of NTO-contaminated sites.
e) Future studies should focus on the enzymatic mechanism of the NTO respiration by *Geobacter anodireducens* and *Thauera* sp.

7.3 DAAN REMOVAL IN SLUDGE UNDER DIFFERENT ELECTRON ACCEPTOR CONDITIONS

a) DAAN removal in live sludge is faster under oxygen exposure compared to the other electron acceptor conditions tested (fermentative, with sulfate, and with nitrate).
b) DAAN autoxidation due to oxygen exposure, an abiotic process, contributes to DAAN removal under aerobic conditions;
c) DAAN reacted abiotically with heat-killed sludge up to a saturation limit.
d) Microorganisms could be enriched to remove DAAN under aerobic conditions.
e) The DAAN-removing aerobic culture mostly contains unclassified microorganisms.
f) An aerobic DAAN-removing step may be implemented after DNAN anaerobic biotransformation to improve DNAN-containing wastewater treatment.
g) Future work should focus on the metagenome and by-products of DAAN aerobic transformation.

7.4 DAAN INCORPORATION INTO MODEL HUMIC COMPOUNDS

a) Abiotic Reactions with quinone compounds representing quinones moieties of NOM drive the loss of DAAN under anoxic conditions, explaining non-extractable bound residue formation after DNAN reduction in soil.
b) DAAN loss occurs in less than 6 seconds when reacting with excess quinones.
c) The reactions are Michael addition, imine formation, and azo bond formation.
d) The oligomerization generates dimers, trimers, and tetramers and ultimately leads to the formation of insoluble polymers.
e) The incorporation into NOM may represent a safe endpoint for DNAN remediation.

REFERENCES

ADRIAN, P.; LAHANIATIS, E. S.; ANDREUX, F.; MANSOUR, M.; SCHEUNERT, I.; KORTE, F. Reaction of the Soil Pollutant 4-Chloroaniline with the Humic-Acid Monomer Catechol. **Chemosphere**, v. 18, n. 7-8, p. 1599-1609, 1989.

AGRAWAL, A.; TRATNYEK, P. G. Reduction of nitro aromatic compounds by zero-valent iron metal. **Environmental Science & Technology**, v. 30, n. 1, p. 153-160, 1996.

AHN, S. C.; CHA, D. K.; KIM, B. J.; OH, S. Y. Detoxification of PAX-21 ammunitions wastewater by zero-valent iron for microbial reduction of perchlorate. **Journal of Hazardous Materials**, v. 192, n. 2, p. 909-914, 2011.

AMARAL, H. I. F.; FERNANDES, J.; BERG, M.; SCHWARZENBACH, R. P.; KIPFER, R. Assessing TNT and DNT groundwater contamination by compound-specific isotope analysis and H-3-He-3 groundwater dating: A case study in Portugal. **Chemosphere**, v. 77, n. 6, p. 805-812, 2009.

AMES, B. N.; KAMMEN, H. O.; YAMASAKI, E. Hair Dyes Are Mutagenic - Identification of a Variety of Mutagenic Ingredients. **Proceedings of the National Academy of Sciences of the United States of America**, v. 72, n. 6, p. 2423-2427, 1975.

APHA. **Standard Methods for the Examination of Water &Wastewater**. 23 ed. American Public Health Association, American Water Works Association, and Water Environment Federation, 2017.

AUNE, T.; DYBING, E. Mutagenic Activation of 2,4-Diaminoanisole and 2-Aminofluorene Invitro by Liver and Kidney Fractions from Aromatic Hydrocarbon Responsive and Nonresponsive Mice. **Biochemical Pharmacology**, v. 28, n. 18, p. 2791-2797, 1979.

BARRETO-RODRIGUES, M.; SILVA, F. T. d.; PAIVA, T. C. B. d. Caracterização física, química e ecotoxicológica de efluente da indústria de fabricação de explosivos. **Química Nova**, v. 30, p. 1623-1627, 2007.

BARTEL, L. C.; DE MECCA, M. M.; CASTRO, J. A. Nitroreductive metabolic activation of some carcinogenic nitro heterocyclic food contaminants in rat mammary tissue cellular fractions. **Food and Chemical Toxicology**, v. 47, n. 1, p. 140-144, 2009.

BELZILE, N.; CHEN, Y. W.; CAI, M. F.; LI, Y. R. A review on pyrrhotite oxidation. **Journal of Geochemical Exploration**, v. 84, n. 2, p. 65-76, 2004.

BENITES, V.M., MADARI, B., MACHADO, P. L. O. A. **Extração e Fracionamento Quantitativo de Substâncias Húmicas do Solo: um Procedimento Simplificado de Baixo Custo**. Ministério da Agricultura, Pecuária e Abastecimento, 2003.

BERNER, R. A. Iron Sulfides Formed from Aqueous Solution at Low Temperatures and Atmospheric Pressure. **Journal of Geology**, v. 72, n. 3, p. 293-306, 1964.

BERNSTEIN, A.; RONEN, Z. Biodegradation of the Explosives TNT, RDX and HMX. **Microbial Degradation of Xenobiotics**, p. 135-176, 2012.

BIALK, H. M.; HEDMAN, C.; CASTILLO, A.; PEDERSEN, J. A. Laccase-mediated michael addition of N-15-sulfapyridine to a model humic constituent. **Environmental Science & Technology**, v. 41, n. 10, p. 3593-3600, 2007.

BODDU, V. M.; ABBURI, K.; FREDRICKSEN, A. J.; MALONEY, S. W.; DAMAVARAPU, R. Equilibrium and column adsorption studies of 2,4-dinitroanisole (DNAN) on surface modified granular activated carbons. **Environmental Technology**, v. 30, n. 2, p. 173-181, 2009.

BODDU, V. M.; ABBURI, K.; MALONEY, S. W.; DAMAVARAPU, R. Thermophysical properties of an insensitive munitions compound, 2,4-dinitroanisole. **Journal of Chemical and Engineering Data**, v. 53, n. 5, p. 1120-1125, 2008.

BOLLAG, J. M. Decontaminating Soil with Enzymes. **Environmental Science & Technology**, v. 26, n. 10, p. 1876-1881, 1992.

BOMMER, M.; KUNZE, C.; FESSELER, J.; SCHUBERT, T.; DIEKERT, G.; DOBBEK, H. Structural basis for organohalide respiration. **Science**, v. 346, n. 6208, p. 455-458, 24 2014.

BRANNON, J. M.; PENNINGTON, J. C. **Environmental fate and transport process descriptors for explosives**. Vicksburg: U.S. Army Engineer Research and Development Center, 2002.

BRASIL. Lei nº 12.305, de 2 de agosto de 2010. Institui a Política Nacional de Resíduos Sólidos; altera a Lei nº 9.605, de 12 de fevereiro de 1998; e dá outras providências. **Diário Oficial da União**, 2010.

BRINDLEY, G. W. X-Ray Identification and Crystal Structures of Clay Minerals. **American Mineralogist**, v. 36, n. 7-8, p. 632-632, 1951.

BUSWELL, J. A.; HAMP, S.; ERIKSSON, K. E. Intracellular Quinone Reduction in Sporotrichum-Pulverulentum by a Nad(P)H-Quinone Oxidoreductase - Possible Role in Vanillic Acid Catabolism. **Febs Letters**, v. 108, n. 1, p. 229-232, 1979.

BUTLER, E. C.; HAYES, K. F. Effects of solution composition and pH on the reductive dechlorination of hexachloroethane by iron sulfide. **Environmental Science & Technology**, v. 32, n. 9, p. 1276-1284, 1998.

CAMARERO, S.; CANAS, A. I.; NOUSIAINEN, P.; RECORD, E.; LOMASCOLO, A.; MARTINEZ, M. J.; MARTINEZ, A. T. p-hydroxycinnamic acids as natural mediators for laccase oxidation of recalcitrant compounds. **Environmental Science & Technology**, v. 42, n. 17, p. 6703-6709, 2008.

CAMARERO, S.; IBARRA, D.; MARTINEZ, M. J.; MARTINEZ, A. T. Lignin-derived compounds as efficient laccase mediators for decolorization of different types of recalcitrant dyes. **Applied and Environmental Microbiology**, v. 71, n. 4, p. 1775-1784, 2005.

CARUNCHIO, F.; CRESCENZI, C.; GIRELLI, A. M.; MESSINA, A.; TAROLA, A. M. Oxidation of ferulic acid by laccase: identification of the products and inhibitory effects of some dipeptides. **Talanta**, v. 55, n. 1, p. 189-200, 2001.

CHEN, H.; ZHANG, Z. L.; MINGBAO, F. B.; LIU, W.; WANG, W. J.; YANG, Q.; HU, Y. N. Degradation of 2,4-dichlorophenoxyacetic acid in water by persulfate activated with FeS (mackinawite). **Chemical Engineering Journal**, v. 313, p. 498-507, 2017.

COLES, C. A.; RAO, S. R.; YONG, R. N. Lead and cadmium interactions with mackinawite: Retention mechanisms and the role of pH. **Environmental Science & Technology**, v. 34, n. 6, p. 996-1000, 2000.

COLON, D.; WEBER, E. J.; BAUGHMAN, G. L. Sediment-associated reactions of aromatic amines. 2. QSAR development. **Environmental Science & Technology**, v. 36, n. 11, p. 2443-2450, 2002.

CROUSE, L. C.; LENT, E. M.; LEACH, G. J. Oral toxicity of 3-nitro-1, 2, 4-triazol-5-one in rats. **International journal of toxicology**, v. 34, n. 1, p. 55-66, 2015.

DAVIES, P. J.; PROVATAS, A. **Characterisation of 2, 4-dinitroanisole: an ingredient for use in low sensitivity melt cast formulations**. Edinburgh: Weapons Systems Division, DSTO Defence Science and Technology Organisation, 2006.

DEC, J.; BOLLAG, J. M. Phenoloxidase-mediated interactions of phenols and anilines with humic materials. **Journal of Environmental Quality**, v. 29, n. 3, p. 665-676, 2000.

DHARIWAL, A.; CHONG, J.; HABIB, S.; KING, I. L.; AGELLON, L. B.; XIA, J. MicrobiomeAnalyst: a web-based tool for comprehensive statistical, visual and meta-analysis of microbiome data. **Nucleic Acids Research**, v. 45, n. W1, p. W180-W188, 2017.

DODARD, S. G.; SARRAZIN, M.; HAWARI, J.; PAQUET, L.; AMPLEMAN, G.; THIBOUTOT, S.; SUNAHARA, G. I. Ecotoxicological assessment of a high energetic and insensitive munitions compound: 2,4-Dinitroanisole (DNAN). **Journal of Hazardous Materials**, v. 262, p. 143-150, 2013.

DOLFING, J.; TIEDJE, J. Growth yield increase linked to reductive dechlorination in a defined 3-chlorobenzoate degrading methanogenic coculture. **Archives of microbiology**, v. 149, n. 2, p. 102-105, 1987.

EDWARDS, E. A. Breathing the unbreathable. **Science**, v. 346, n. 6208, p. 424-425, 2014.

EMBREE, M.; QIU, Y.; SHIEU, W. D.; NAGARAJAN, H.; O'NEIL, R.; LOVLEY, D.; ZENGLER, K. The Iron Stimulon and Fur Regulon of Geobacter sulfurreducens and Their Role in Energy Metabolism. **Applied and Environmental Microbiology**, v. 80, n. 9, p. 2918-2927, 2014.

ESTEVE-NUÑEZ, A.; LUCCHESI, G.; PHILIPP, B.; SCHINK, B.; RAMOS, J. L. Respiration of 2, 4, 6-Trinitrotoluene by Pseudomonassp. Strain JLR11. **Journal of Bacteriology**, v. 182, n. 5, p. 1352-1355, 2000.

FIDA, T. T.; PALAMURU, S.; PANDEY, G.; SPAIN, J. C. Aerobic Biodegradation of 2,4-Dinitroanisole by Nocardioides sp Strain JS1661. **Applied and Environmental Microbiology**, v. 80, n. 24, p. 7725-7731, 2014.

FIELD, J. A.; STAMS, A. J.; KATO, M.; SCHRAA, G. Enhanced biodegradation of aromatic pollutants in cocultures of anaerobic and aerobic bacterial consortia. **Antonie Van Leeuwenhoek**, v. 67, n. 1, p. 47-77, 1995.

FIORELLA, P. D.; SPAIN, J. C. Transformation of 2,4,6-trinitrotoluene by Pseudomonas pseudoalcaligenes JS52. **Applied and Environmental Microbiology**, v. 63, n. 5, p. 2007-2015, 1997.

FUCHS, G. Anaerobic metabolism of aromatic compounds. **Annals of the New York Academy of Sciences**, v. 1125, p. 82-99, 2008.

FUCHS, G.; BOLL, M.; HEIDER, J. Microbial degradation of aromatic compounds - from one strategy to four. **Nature Reviews Microbiology**, v. 9, n. 11, p. 803-816, 2011.

GALLEGOS, T. J.; HYUN, S. P.; HAYES, K. F. Spectroscopic investigation of the uptake of arsenite from solution by synthetic mackinawite. **Environmental Science & Technology**, v. 41, n. 22, p. 7781-7786, 2007.

GOMES, M. A. F.; BARIZON, R. R. M. **Panorama da Contaminação Ambiental por Agrotóxicos e Nitrato de origem Agrícola no Brasil: cenário 1992/2011**. Jaguariúna: Embrapa Meio Ambiente, 2014.

GONG, Y. Y.; TANG, J. C.; ZHAO, D. Y. Application of iron sulfide particles for groundwater and soil remediation: A review. **Water Research**, . 89, p. 309-320, 2016.

GONZALEZ-ESTRELLA, J.; GALLAGHER, S.; SIERRA-ALVAREZ, R.; FIELD, J. A. Iron sulfide attenuates the methanogenic toxicity of elemental copper and zinc oxide nanoparticles and their soluble metal ion analogs. **Science of the Total Environment**, v. 548, p. 380-389, 2016.

GULKOWSKA, A.; KRAUSS, M.; RENTSCH, D.; HOLLENDER, J. Reactions of a Sulfonamide Antimicrobial with Model Humic Constituents: Assessing Pathways and Stability of Covalent Bonding. **Environmental Science & Technology**, v. 46, n. 4, p. 2102-2111, 2012a.

GULKOWSKA, A.; SANDER, M.; HOLLENDER, J.; KRAUSS, M. Covalent Binding of Sulfamethazine to Natural and Synthetic Humic Acids: Assessing Laccase Catalysis and Covalent Bond Stability. **Environmental Science & Technology**, v. 47, n. 13, p. 6916-6924, 2013.

HALASZ, A.; HAWARI, J.; PERREAULT, N. N. New Insights into the Photochemical Degradation of the Insensitive Munition Formulation IMX-101 in Water. **Environmental Science & Technology**, v. 52, n. 2, p. 589-596, 2018.

HAWARI, J.; MONTEIL-RIVERA, F.; PERREAULT, N. N.; HALASZ, A.; PAQUET, L.; RADOVIC-HRAPOVIC, Z.; DESCHAMPS, S.; THIBOUTOT, S.; AMPLEMAN, G.

Environmental fate of 2,4-dinitroanisole (DNAN) and its reduced products. **Chemosphere**, v. 119, p. 16-23, 2015.

HAYAISHI, O. **Molecular mechanisms of oxygen activation**. Elsevier, 2012.

HSU, T. S.; BARTHA, R. Hydrolyzable and Nonhydrolyzable 3,4-Dichloroaniline Humus Complexes and Their Respective Rates of Biodegradation. **Journal of Agricultural and Food Chemistry**, v. 24, n. 1, p. 118-122, 1976.

HUANG, J.; NING, G.; LI, F.; SHENG, G. D. Biotransformation of 2,4-dinitrotoluene by obligate marine Shewanella marisflavi EP1 under anaerobic conditions. **Bioresource Technology**, v. 180, p. 200-206, 2015.

HYUN, S. P.; DAVIS, J. A.; SUN, K.; HAYES, K. F. Uranium(VI) Reduction by Iron(II) Monosulfide Mackinawite. **Environmental Science & Technology**, v. 46, n. 6, p. 3369-3376, 2012.

JACKOVITZ, A. M.; KOISTINEN, K. A.; LENT, E. M.; BANNON, D. I.; QUINN JR, M. J.; JOHNSON, M. S. Neuromuscular anomalies following oral exposure to 3-nitro-1, 2, 4-triazol-5-one (NTO) in a one-generation study with Japanese quail (Coturnix japonic a). **Journal of Toxicology and Environmental Health, Part A**, v. 81, n. 15, p. 718-733, 2018.

JACOB, H. E. Chapter IV Redox Potential. *In*: NORRIS, J. R. e RIBBONS, D. W. (Ed.). **Methods in Microbiology**: Academic Press, 1970. v. 2, p. 91-123.

JEONG, H. Y.; KIM, H.; HAYES, K. F. Reductive dechlorination pathways of tetrachloroethylene and trichloroethylene and subsequent transformation of their dechlorination products by mackinawite (FeS) in the presence of metals. **Environmental Science & Technology**, v. 41, n. 22, p. 7736-7743, 2007.

JEONG, H. Y.; LEE, J. H.; HAYES, K. F. Characterization of synthetic nanocrystalline mackinawite: Crystal structure, particle size, and specific surface area. **Geochimica Et Cosmochimica Acta**, v. 72, n. 2, p. 493-505, 2008.

JU, K. S.; PARALES, R. E. Nitroaromatic Compounds, from Synthesis to Biodegradation. **Microbiology and Molecular Biology Reviews**, v. 74, n. 2, p. 250-+, 2010.

KADOYA, W. M.; SIERRA-ALVAREZ, R.; JAGADISH, B.; WONG, S.; ABRELL, L.; MASH, E. A.; FIELD, J. A. Coupling reactions between reduced intermediates of insensitive munitions compound analog 4-nitroanisole. **Chemosphere**, v. 222, p. 789-796, 2019.

KADOYA, W. M.; SIERRA-ALVAREZ, R.; JAGADISH, B.; WONG, S.; ABRELL, L.; MASH, E. A.; FIELD, J. A. Covalent bonding of aromatic amine daughter products of 2,4-dinitroanisole (DNAN) with model quinone compounds representing humus via nucleophilic addition. **Environmental Pollution**, v. 268, p. 115862, 2021.

KADOYA, W. M.; SIERRA-ALVAREZ, R.; WONG, S.; ABRELL, L.; MASH, E. A.; FIELD, J. A. Evidence of anaerobic coupling reactions between reduced intermediates of 4-nitroanisole. **Chemosphere**, v. 195, p. 372-380, 2018.

KAHNG, H. Y.; KUKOR, J. J.; OH, K. H. Characterization of strain HY99, a novel microorganism capable of aerobic and anaerobic degradation of aniline. **FEMS Microbiology Letters**, v. 190, n. 2, p. 215-221, 2000.

KATO, S.; CHINO, K.; KAMIMURA, N.; MASAI, E.; YUMOTO, I.; KAMAGATA, Y. Methanogenic degradation of lignin-derived monoaromatic compounds by microbial enrichments from rice paddy field soil. **Scientific Reports**, v. 5, p. 14295, 2015.

KEEGAN, K. P.; GLASS, E. M.; MEYER, F. MG-RAST, a Metagenomics Service for Analysis of Microbial Community Structure and Function. **Microbial Environmental Genomics (Meg)**, v. 1399, p. 207-233, 2016.

KHATIWADA, R.; ABRELL, L.; LI, G. B.; ROOT, R. A.; SIERRA-ALVAREZ, R.; FIELD, J. A.; CHOROVER, J. Adsorption and oxidation of 3-nitro-1,2,4-triazole-5-one (NTO) and its transformation product (3-amino-1,2,4-triazole-5-one, ATO) at ferrihydrite and birnessite surfaces. **Environmental Pollution**, v. 240, p. 200-208, 2018a.

KHATIWADA, R.; OLIVARES, C.; ABRELL, L.; ROOT, R. A.; SIERRA-ALVAREZ, R.; FIELD, J. A.; CHOROVER, J. Oxidation of reduced daughter products from 2,4-dinitroanisole (DNAN) by Mn(IV) and Fe(III) oxides. **Chemosphere**, v. 201, p. 790-798, 2018b.

KHATIWADA, R.; ROOT, R. A.; ABRELL, L.; SIERRA-ALVAREZ, R.; FIELD, J. A.; CHOROVER, J. Abiotic reduction of insensitive munition compounds by sulfate green rust. **Environmental Chemistry**, v. 15, n. 5, p. 259-266, 2018c.

KIM, D.; KIM, Y. S.; KIM, S. K.; KIM, S. W.; ZYLSTRA, G. J.; KIM, Y. M.; KIM, E. Monocyclic aromatic hydrocarbon degradation by Rhodococcus sp. strain DK17. **Applied and Environmental Microbiology**, v. 68, n. 7, p. 3270-3278, 2002.

KIM, J. E.; FERNANDES, E.; BOLLAG, J. M. Enzymatic coupling of the herbicide bentazon with humus monomers and characterization of reaction products. **Environmental Science & Technology**, v. 31, n. 8, p. 2392-2398, 1997.

KIRK, T. K.; LORENZ, L. F. Methoxyhydroquinone, an Intermediate of Vanillate Catabolism by Polyporus-Dichrous. **Applied Microbiology**, v. 26, n. 2, p. 173-175, 1973.

KITCHER, E.; BRAIDA, W.; KOUTSOSPYROS, A.; PAVLOV, J.; SU, T. L. Characteristics and products of the reductive degradation of 3-nitro-1,2,4-triazol-5-one (NTO) and 2,4-dinitroanisole (DNAN) in a Fe-Cu bimetal system. **Environmental Science and Pollution Research**, v. 24, n. 3, p. 2744-2753, 2017.

KONAKA, R.; KURUMA, K.; TERABE, S. Mechanisms of Oxidation of Aniline and Related Compounds in Basic Solution. **Journal of the American Chemical Society**, v. 90, n. 7, p. 1801-&, 1968.

KOUTSOSPYROS, A.; PAVLOV, J.; FAWCETT, J.; STRICKLAND, D.; SMOLINSKI, B.; BRAIDA, W. Degradation of high energetic and insensitive munitions compounds by Fe/Cu bimetal reduction. **Journal of Hazardous Materials**, v. 219, p. 75-81, 2012.

KOVACIC, P.; SOMANATHAN, R. Nitroaromatic compounds: Environmental toxicity, carcinogenicity, mutagenicity, therapy and mechanism. **Journal of Applied Toxicology**, v. 34, n. 8, p. 810-824, 2014.

KRAUS, S. P. Q. **Aerobic and Anaerobic Biotransformation of Chloroanilines, Chlorobenzenes, and Dichlonitrobenzenes at a Complex Industrial Site in Brazil and Analysis of Associated Microbial Communities**. 2018. 161 f. Thesis (Masters) -Chemical Engineering and Applied Chemistry, University of Toronto, Toronto, 2020.

KRZMARZICK, M. J.; KHATIWADA, R.; OLIVARES, C. I.; ABRELL, L.; SIERRA-ALVAREZ, R.; CHOROVER, J.; FIELD, J. A. Biotransformation and Degradation of the Insensitive Munitions Compound, 3-Nitro-1,2,4-triazol-5-one, by Soil Bacterial Communities. **Environmental Science & Technology**, v. 49, n. 9, p. 5681-5688, 2015.

KUTYREV, A. A. Nucleophilic Reactions of Quinones. **Tetrahedron**, 47, n. 38, p. 8043-8065, 1991.

KWON, M. J.; FINNERAN, K. T. Microbially Mediated Biodegradation of Hexahydro-1,3,5-Trinitro-1,3,5- Triazine by Extracellular Electron Shuttling Compounds. **Applied and Environmental Microbiology**, v. 72, n. 9, p. 5933-5941, 2006.

LAHA, S.; LUTHY, R. G. Oxidation of Aniline and Other Primary Aromatic-Amines by Manganese-Dioxide. **Environmental Science & Technology**, v. 24, n. 3, p. 363-373, 1990.

LE CAMPION, L.; OUAZZANI, J. Synthesis of 5-amino-1,2,4-triazole-3-one through the nitroreduction of 5-nitro-1,2,4-triazole-3-one. Comparison between chemical and microbiological catalysis. **Biocatalysis and Biotransformation**, v. 17, n. 1, p. 37-44, 1999a.

LE CAMPION, L.; VANDAIS, A.; OUAZZANI, J. Microbial remediation of NTO in aqueous industrial wastes. **FEMS microbiology letters**, v. 176, n. 1, p. 197-203, 1999b.

LENT, E. M.; NARIZZANO, A. M.; KOISTINEN, K. A.; JOHNSON, M. S. Chronic oral toxicity of 3-nitro-1,2,4-triazol-5-one (NTO) in rats. **Regulatory Toxicology and Pharmacology**, v. 112, 2020.

LEWIS, K.; NARODITSKAYA, V.; FERRANTE, A.; FOKINA, I. Bacterial resistance to uncouplers. **Journal of bioenergetics and biomembranes**, v. 26, n. 6, p. 639-646, 1994.

LIANG, J.; OLIVARES, C.; FIELD, J. A.; SIERRA-ALVAREZ, R. Microbial toxicity of the insensitive munitions compound, 2,4-dinitroanisole (DNAN), and its aromatic amine metabolites. **Journal of Hazardous Materials**, v. 262, p. 281-287, 2013.

LIE, T. J.; PITTA, T.; LEADBETTER, E. R.; GODCHAUX III, W.; LEADBETTER, J. R. Sulfonates: novel electron acceptors in anaerobic respiration. **Archives of microbiology**, v. 166, n. 3, p. 204-210, 1996.

LIN, W. C., COPPI, M. V., LOVLEY, D. R. Geobacter sulfurreducens can grow with oxygen as a terminal electron acceptor. **Applied and Environmental Microbiology**, v. 70, p. 2525-2528, 2004.

LIN'KOVA, Y. V.; DYAKONOVA, A. T.; GLADCHENKO, M. A.; KALYUZHNYI, S. V.; KOTOVA, I. B.; STAMS, A.; NETRUSOV, A. I. Methanogenic degradation of (amino)aromatic compounds by anaerobic microbial communities. **Applied Biochemistry and Microbiology**, v. 47, n. 5, p. 507-514, 2011.

LINKER, B. R.; KHATIWADA, R.; PERDRIAL, N.; ABRELL, L.; SIERRA-ALVAREZ, R.; FIELD, J. A.; CHOROVER, J. Adsorption of novel insensitive munitions compounds at clay mineral and metal oxide surfaces. **Environmental Chemistry**, v. 12, n. 1, p. 74-84, 2015.

LIU, D. F.; MIN, D.; CHENG, L.; ZHANG, F.; LI, D. B.; XIAO, X.; SHENG, G. P.; YU, H. Q. Anaerobic reduction of 2,6-dinitrotoluene by Shewanella oneidensis MR-1: Roles of Mtr respiratory pathway and NfnB. **Biotechnology and Bioengineering**, v. 114, n. 4, p. 761-768, 2017.

LUDWICHK, R.; HELFERICH, O. K.; KIST, C. P.; LOPES, A. C.; CAVASOTTO, T.; SILVA, D. C.; BARRETO-RODRIGUES, M. Characterization and photocatalytic treatability of red water from Brazilian TNT industry. **Journal of Hazardous Materials**, v. 293, p. 81-86, 2015.

MADEIRA, C. L.; FIELD, J. A.; SIMONICH, M. T.; TANGUAY, R. L.; CHOROVER, J.; SIERRA-ALVAREZ, R. Ecotoxicity of the insensitive munitions compound 3-nitro-1,2,4-triazol-5-one (NTO) and its reduced metabolite 3-amino-1,2,4-triazol-5-one (ATO). **Journal of Hazardous Materials**, v. 343, p. 340-346, 2018.

MADEIRA, C. L.; JOG, K. V.; VANOVER, E. T.; BROOKS, M. D.; TAYLOR, D. K.; SIERRA-ALVAREZ, R.; WAIDNER, L. A.; SPAIN, J. C.; KRZMARZICK, M. J.; FIELD, J. A. Microbial Enrichment Culture Responsible for the Complete Oxidative Biodegradation of 3-Amino-1,2,4-triazol-5-one (ATO), the Reduced Daughter Product of the Insensitive Munitions Compound 3-Nitro-1,2,4-triazol-5-one (NTO). **Environmental Science & Technology**, v. 53, n. 21, p. 12648-12656, 2019a.

MADEIRA, C. L.; KADOYA, W. M.; LI, G. B.; WONG, S.; SIERRA-ALVAREZ, R.; FIELD, J. A. Reductive biotransformation as a pretreatment to enhance in situ chemical oxidation of nitroaromatic and nitroheterocyclic explosives. **Chemosphere**, v. 222, p. 1025-1032, 2019b.

MADEIRA, C. L.; SPEET, S. A.; NIETO, C. A.; ABRELL, L.; CHOROVER, J.; SIERRA-ALVAREZ, R.; FIELD, J. A. Sequential anaerobic-aerobic biodegradation of emerging insensitive munitions compound 3-nitro-1,2,4-triazol-5-one (NTO). **Chemosphere**, v. 167, p. 478-484, 2017.

MAYMOGATELL, X.; CHIEN, Y. T.; GOSSETT, J. M.; ZINDER, S. H. Isolation of a bacterium that reductively dechlorinates tetrachloroethene to ethene. **Science**, v. 276, n. 5318, p. 1568-1571, 1997.

MECHICHI, T.; PATEL, B. K. C.; SAYADI, S. Anaerobic degradation of methoxylated aromatic compounds by Clostridium methoxybenzovorans and a nitrate-reducing bacterium Thauera sp. strain Cin3,4. **International Biodeterioration & Biodegradation**, v. 56, n. 4, p. 224-230, 2005.

MENEZES, O.; BRITO, R.; HALLWASS, F.; FLORENCIO, L.; KATO, M. T.; GAVAZZA, S. Coupling intermittent micro-aeration to anaerobic digestion improves tetra-azo dye Direct Black 22 treatment in sequencing batch reactors. **Chemical Engineering Research & Design**, v. 146, p. 369-378, 2019.

MENEZES, O.; MELO, N.; PARAISO, M.; FREITAS, D.; FLORÊNCIO, L.; KATO, M. T.; GAVAZZA, S. The key role of oxygen in the bioremoval of 2,4-diaminoanisole (DAAN), the biotransformation product of the insensitive munitions compound 2,4-dinitroanisole (DNAN), over other electron acceptors. **Chemosphere**, p. 128862, 2020.

MESLE, M.; DROMART, G.; HAESELER, F.; OGER, P. M. Classes of organic molecules targeted by a methanogenic microbial consortium grown on sedimentary rocks of various maturities. **Frontiers in Microbiology**, v. 6, p. 589, 2015.

MITCHELL, P. Chemiosmotic Coupling in Oxidative and Photosynthetic Phosphorylation. **Biological Reviews of the Cambridge Philosophical Society**, v. 41, n. 3, p. 445-&, 1966.

MORSE, J. W.; MILLERO, F. J.; CORNWELL, J. C.; RICKARD, D. The Chemistry of the Hydrogen-Sulfide and Iron Sulfide Systems in Natural-Waters. **Earth-Science Reviews**, v. 24, n. 1, p. 1-42, 1987.

MUYZER, G.; STAMS, A. J. M. The ecology and biotechnology of sulphate-reducing bacteria. **Nature Reviews Microbiology**, v. 6, n. 6, p. 441-454, 2008.

NGUYEN, C. H.; ZENG, C.; BOITANO, S.; FIELD, J. A.; SIERRA-ALVAREZ, R. Cytotoxicity Assessment of Gallium- and Indium-Based Nanoparticles Toward Human Bronchial Epithelial Cells Using an Impedance-Based Real-Time Cell Analyzer. **International Journal of Toxicology**, v. 39, n. 3, p. 218-231, 2020.

NIEDZWIECKA, J. B.; DREW, S. R.; SCHLAUTMAN, M. A.; MILLERICK, K. A.; GRUBBS, E.; THARAYIL, N.; FINNERAN, K. T. Iron and Electron Shuttle Mediated (Bio)degradation of 2,4-Dinitroanisole (DNAN). **Environmental Science & Technology**, v. 51, n. 18, p. 10729-10735, 2017.

NURMI, J. T.; TRATNYEK, P. G. Electrochemical properties of natural organic matter (NOM), fractions of NOM, and model biogeochemical electron shuttles. **Environmental Science & Technology**, v. 36, n. 4, p. 617-624, 2002.

OH, S. Y.; KANG, S. G.; KIM, D. W.; CHIU, P. C. Degradation of 2,4-dinitrotoluene by persulfate activated with iron sulfides. **Chemical Engineering Journal**, v. 172, n. 2-3, p. 641-646, 2011.

OLIVARES, C.; LIANG, J. D.; ABRELL, L.; SIERRA-ALVAREZ, R.; FIELD, J. A. Pathways of reductive 2,4-dinitroanisole (DNAN) biotransformation in sludge. **Biotechnology and Bioengineering**, v. 110, n. 6, p. 1595-1604, 2013.

OLIVARES, C. I.; ABRELL, L.; KHATIWADA, R.; CHOROVER, J.; SIERRA-ALVAREZ, R.; FIELD, J. A. (Bio)transformation of 2,4-dinitroanisole (DNAN) in soils. **Journal of Hazardous Materials**, v. 304, p. 214-221, 2016a.

OLIVARES, C. I.; MADEIRA, C. L.; SIERRA-ALVAREZ, R.; KADOYA, W.; ABRELL, L.; CHOROVER, J.; FIELD, J. A. Environmental Fate of 14C Radiolabeled 2,4-Dinitroanisole in Soil Microcosms. **Environmental Science & Technology**, v. 51, n. 22, p. 13327-13334, 2017.

OLIVARES, C. I.; SIERRA-ALVAREZ, R.; ABRELL, L.; CHOROVER, J.; SIMONICH, M.; TANGUAY, R. L.; FIELD, J. A. Zebrafish Embryo Toxicity of Anaerobic Biotransformation Products from the Insensitive Munitions Compound 2,4-Dinitroanisole. **Environmental Toxicology and Chemistry**, v. 35, n. 11, p. 2774-2781, 2016b.

OLIVARES, C. I.; SIERRA-ALVAREZ, R.; ALVAREZ-NIETO, C.; ABRELL, L.; CHOROVER, J.; FIELD, J. A. Microbial toxicity and characterization of DNAN (bio)transformation product mixtures. **Chemosphere**, v. 154, p. 499-506, 2016c.

ONONYE, A. I.; GRAVEEL, J. G. Modeling the Reactions of 1-Naphthylamine and 4-Methylaniline with Humic Acids - Spectroscopic Investigations of the Covalent Linkages. **Environmental Toxicology and Chemistry**, v. 13, n. 4, p. 537-541, 1994.

ONONYE, A. I.; GRAVEEL, J. G.; WOLT, J. D. Kinetic and spectroscopic investigations of the covalent binding of benzidine to quinones. **Environmental Toxicology and Chemistry**, v. 8, n. 4, p. 303-308, 1989.

OTTEN, M. F.; REIJNDERS, W. N. M.; BEDAUX, J. J. M.; WESTERHOFF, H. V.; KRAB, K.; VAN SPANNING, R. J. M. The reduction state of the Q-pool regulates the electron flux through the branched respiratory network of Paracoccus denitrificans. **European Journal of Biochemistry**, v. 261, n. 3, p. 767-774, 1999.

OU, C. J.; ZHANG, S.; LIU, J. G.; SHEN, J. Y.; HAN, W. Q.; SUN, X. Y.; LIA, J. S.; WANG, L. J. Enhanced reductive transformation of 2,4-dinitroanisole in a anaerobic system: the key role of zero valent iron. **Rsc Advances**, v. 5, n. 92, p. 75195-75203, 2015.

PARK, D. **Metagenome analysis of an enrichment culture that degrades the 3-nitro-1,2,4-triazol-5-one (NTO) explosive**. 2020. 50 f. Thesis (Masters) - Environmental Engineering, Georgia Institute of Technology, Atlanta, 2020.

PARK, J.; COMFORT, S. D.; SHEA, P. J.; MACHACEK, T. A. Remediating munitions-contaminated soil with zerovalent iron and cationic surfactants. **Journal of Environmental Quality**, v. 33, n. 4, p. 1305-1313, 2004.

PARK, J. W.; DEC, J.; KIM, J. E.; BOLLAG, J. M. Effect of humic constituents on the transformation of chlorinated phenols and anilines in the presence of oxidoreductive enzymes or birnessite. **Environmental Science & Technology**, v. 33, n. 12, p. 2028-2034, 1999.

PARKS, D. H.; TYSON, G. W.; HUGENHOLTZ, P.; BEIKO, R. G. STAMP: statistical analysis of taxonomic and functional profiles. **Bioinformatics**, v. 30, n. 21, p. 3123-3124, 2014.

PARRIS, G. E. Covalent Binding of Aromatic-Amines to Humates .1. Reactions with Carbonyls and Quinones. **Environmental Science & Technology**, v. 14, n. 9, p. 1099-1106, 1980.

PARRY, R.; NISHINO, S.; SPAIN, J. Naturally-occurring nitro compounds. **Natural Product Reports**, v. 28, n. 1, p. 152-167, 2011.

PEREIRA, R.; PEREIRA, L.; VAN DER ZEE, F. P.; MADALENA ALVES, M. Fate of aniline and sulfanilic acid in UASB bioreactors under denitrifying conditions. **Water Research**, v. 45, n. 1, p. 191-200, 2011.

PLATTEN, W. E.; BAILEY, D.; SUIDAN, M. T.; MALONEY, S. W. Biological transformation pathways of 2,4-dinitro anisole and N-methyl paranitro aniline in anaerobic fluidized-bed bioreactors. **Chemosphere**, v. 81, n. 9, p. 1131-1136, 2010.

PLATTEN, W. E.; BAILEY, D.; SUIDAN, M. T.; MALONEY, S. W. Treatment of Energetic Wastewater Containing 2,4-Dinitroanisole and N-Methyl Paranitro Aniline. **Journal of Environmental Engineering-Asce**, v. 139, n. 1, p. 104-109, 2013.

POWELL, I. J. Insensitive Munitions - Design Principles and Technology Developments. **Propellants Explosives Pyrotechnics**, v. 41, n. 3, p. 409-413, 2016.

PRAJAPATI, V. S.; PUROHIT, H. J.; RAJE, D. V.; PARMAR, N.; PATEL, A. B.; JONES, O. A. H.; JOSHI, C. G. The effect of a high-roughage diet on the metabolism of aromatic compounds by rumen microbes: a metagenomic study using Mehsani buffalo (Bubalus bubalis). **Applied Microbiology and Biotechnology**, v. 100, n. 3, p. 1319-1331, 2016.

PUROHIT, V.; BASU, A. K. Mutagenicity of nitroaromatic compounds. **Chemical Research in Toxicology**, v. 13, n. 8, p. 673-692, 2000.

RATASUK, N.; NANNY, M. A. Characterization and quantification of reversible redox sites in humic substances. **Environmental Science & Technology**, v. 41, n. 22, p. 7844-7850, 2007.

RAVEL, B.; NEWVILLE, M. ATHENA, ARTEMIS, HEPHAESTUS: data analysis for X-ray absorption spectroscopy using IFEFFIT. **Journal of Synchrotron Radiation**, v. 12, p. 537-541, 2005.

RAZO-FLORES, E.; LETTINGA, G.; FIELD, J. A. Biotransformation and biodegradation of selected nitroaromatics under anaerobic conditions. **Biotechnology Progress**, v. 15, n. 3, p. 358-365, 1999.

RAZO-FLORES, E.; SMULDERS, P.; PRENAFETA-BOLDÚ, F.; LETTINGA, G.; FIELD, J. A. Treatment of anthranilic acid in an anaerobic expanded granular sludge bed reactor at low concentrations. **Water Science and Technology**, v. 40, n. 8, p. 187-194, 1999.

RICHARD, T.; WEIDHAAS, J. Biodegradation of IMX-101 explosive formulation constituents: 2,4-Dinitroanisole (DNAN), 3-nitro-1,2,4-triazol-5-one (NTO), and nitroguanidine. **Journal of Hazardous Materials**, v. 280, p. 372-379, 2014a.

RICHARD, T.; WEIDHAAS, J. Dissolution, sorption, and phytoremediation of IMX-101 explosive formulation constituents: 2,4-dinitroanisole (DNAN), 3-nitro-1,2,4-triazol-5-one (NTO), and nitroguanidine. **Journal of Hazardous Materials**, v. 280, p. 561-569, 2014b.

RICKARD, D. Kinetics of Fes Precipitation .1. Competing Reaction-Mechanisms. **Geochimica Et Cosmochimica Acta**, v. 59, n. 21, p. 4367-4379, 1995.

RICKARD, D.; LUTHER, G. W. Chemistry of iron sulfides. **Chemical Reviews**, v. 107, n. 2, p. 514-562, 2007.

RICKARD, D.; MORSE, J. W. Acid volatile sulfide (AVS). **Marine Chemistry**, v. 97, n. 3-4, p. 141-197, 2005.

ROLDÁN, M. D.; PÉREZ-REINADO, E.; CASTILLO, F.; MORENO-VIVIÁN, C. Reduction of polynitroaromatic compounds: the bacterial nitroreductases. **FEMS microbiology reviews**, v. 32, n. 3, p. 474-500, 2008.

SAXENA, A.; BARTHA, R. Binding of 3,4-Dichloroaniline by Humic-Acid and Soil - Mechanism and Exchangeability. **Soil Science**, v. 136, n. 2, p. 111-116, 1983.

SCOTT, D. T.; MCKNIGHT, D. M.; BLUNT-HARRIS, E. L.; KOLESAR, S. E.; LOVLEY, D. R. Quinone moieties act as electron acceptors in the reduction of humic substances by humics-reducing microorganisms. **Environmental Science & Technology**, v. 32, n. 19, p. 2984-2989, 1998.

SERDP-ESTCP. **Contaminant 101**. Available at: https://www.serdp-estcp.org/energetic_compound/Contaminant-101. Accessed on: 07 nov. 2020.

SHCHERBAKOVA, V. A.; LAURINAVICHYUS, K. S.; CHUVIL'SKAYA, N. A.; RYZHMANOVA, Y. V.; AKIMENKO, V. K. Anaerobic bacteria involved in the degradation of aromatic sulfonates to methane. **Applied Biochemistry and Microbiology**, v. 51, n. 2, p. 209-214, 2015.

SHEN, J. Y.; OU, C. J.; ZHOU, Z. Y.; CHEN, J.; FANG, K. X.; SUN, X. Y.; LI, J. S.; ZHOU, L.; WANG, L. J. Pretreatment of 2,4-dinitroanisole (DNAN) producing wastewater using a combined zero-valent iron (ZVI) reduction and Fenton oxidation process. **Journal of Hazardous Materials**, v. 260, p. 993-1000, 2013.

SIKDER, A. K.; SIKDER, N. A review of advanced high performance, insensitive and thermally stable energetic materials emerging for military and space applications. **Journal of Hazardous Materials**, v. 112, n. 1-2, p. 1-15, 2004.

SIMMONS, K. E.; MINARD, R. D.; BOLLAG, J. M. Oxidative Co-Oligomerization of Guaiacol and 4-Chloroaniline. **Environmental Science & Technology**, v. 23, n. 1, p. 115-121, 1989.

SOMERVILLE, C. C.; NISHINO, S. F.; SPAIN, J. C. Purification and Characterization of Nitrobenzene Nitroreductase from Pseudomonas Pseudoalcaligenes Js45. **Journal of Bacteriology**, v. 177, n. 13, p. 3837-3842, 1995.

SPAIN, J. C. Biodegradation of Nitroaromatic Compounds. **Annual Review of Microbiology**, v. 49, p. 523-555, 1995.

STAMS, A. J.; DE BOK, F. A.; PLUGGE, C. M.; VAN EEKERT, M. H.; DOLFING, J.; SCHRAA, G. Exocellular electron transfer in anaerobic microbial communities. **Environmental Microbiology**, v. 8, n. 3, p. 371-382, 2006.

STOOKEY, L. L. Ferrozine - a New Spectrophotometric Reagent for Iron. **Analytical Chemistry**, v. 42, n. 7, p. 779-&, 1970.

SUFLITA, J. M.; HOROWITZ, A.; SHELTON, D. R.; TIEDJE, J. M. Dehalogenation: a novel pathway for the anaerobic biodegradation of haloaromatic compounds. **Science**, v. 218, n. 4577, p. 1115-1117, 1982.

SUNAHARA, G. I.; LOTUFO, G.; KUPERMAN, R. G.; HAWARI, J. **Ecotoxicology of explosives**. CRC Press, 2009.

TAYLOR, L.; FINGER, L. Structural refinement and composition of mackinawite. **Carnegie Instution of Washington, Geophysical Laboratory Annual Report**, v. 69, p. 318-322, 1970.

TAYLOR, S.; DONTSOVA, K.; WALSH, M. E.; WALSH, M. R. Outdoor dissolution of detonation residues of three insensitive munitions (IM) formulations. **Chemosphere**, v. 134, p. 250-256, 2015a.

TAYLOR, S.; PARK, E.; BULLION, K.; DONTSOVA, K. Dissolution of three insensitive munitions formulations. **Chemosphere**, v. 119, p. 342-348, 2015b.

TAYLOR, S.; WALSH, M. E.; BECHER, J. B.; RINGELBERG, D. B.; MANNES, P. Z.; GRIBBLE, G. W. Photo-degradation of 2,4-dinitroanisole (DNAN): An emerging munitions compound. **Chemosphere**, v. 167, p. 193-203, 2017.

THORN, K. A.; ARTERBURN, J. B.; MIKITA, M. A. N-15 and C-13 Nmr Investigation of Hydroxylamine-Derivatized Humic Substances. **Environmental Science & Technology**, v. 26, n. 1, p. 107-116, 1992.

THORN, K. A.; GOLDENBERG, W. S.; YOUNGER, S. J.; WEBER, E. J. Covalent binding of aniline to humic substances - Comparison of nucleophilic addition, enzyme-, and metal-catalyzed reactions by N-15 NMR. **Humic and Fulvic Acids**, v. 651, p. 299-326, 1996a.

THORN, K. A.; KENNEDY, K. R. (15)N NMR investination of the covalent binding of reduced TNT amines to soil humic acid, model compounds, and lignocellulose. **Environmental Science & Technology**, v. 36, n. 17, p. 3787-3796, 2002.

THORN, K. A.; PETTIGREW, P. J.; GOLDENBERG, W. S. Covalent binding of aniline to humic substances .2. N-15 NMR studies of nucleophilic addition reactions. **Environmental Science & Technology**, v. 30, n. 9, p. 2764-2775, 1996b.

TSEZOS, M.; BELL, J. P. Comparison of the Biosorption and Desorption of Hazardous Organic Pollutants by Live and Dead Biomass. **Water Research**, v. 23, n. 5, p. 561-568, 1989.

UCHIMIYA, M.; STONE, A. T. Aqueous oxidation of substituted dihydroxybenzenes by substituted benzoquinones. **Environmental Science & Technology**, v. 40, n. 11, p. 3515-3521, 2006.

UCHIMIYA, M.; STONE, A. T. Reversible redox chemistry of quinones: impact on biogeochemical cycles. **Chemosphere**, v. 77, n. 4, p. 451-458, 2009.

VAN DER MEULEN, R.; CAMU, N.; VAN VOOREN, T.; HEYMANS, C.; DE VUYST, L. In vitro kinetic analysis of carbohydrate and aromatic amino acid metabolism of different members of the human colon. **International Journal of Food Microbiology**, v. 124, n. 1, p. 27-33, 2008.

VAN DER ZEE, F. P.; LETTINGA, G.; FIELD, J. A. Azo dye decolourisation by anaerobic granular sludge. **Chemosphere**, v. 44, n. 5, p. 1169-1176, 2001.

VAZQUEZ-RODRIGUEZ, G. A.; BELTRAN-HERNANDEZ, R. I.; LUCHO-CONSTANTINO, C. A.; BLASCO, J. L. A method for measuring the anoxic biodegradability under denitrifying conditions. **Chemosphere**, v. 71, n. 7, p. 1363-1368, 2008.

WALTON, M. I.; WORKMAN, P. Nitroimidazole Bioreductive Metabolism - Quantitation and Characterization of Mouse-Tissue Benznidazole Nitroreductases Invivo and Invitro. **Biochemical Pharmacology**, v. 36, n. 6, p. 887-896, 1987.

WANARATNA, P.; CHRISTODOULATOS, C.; SIDHOUM, M. Kinetics of RDX degradation by zero-valent iron (ZVI). **Journal of Hazardous Materials**, v. 136, n. 1, p. 68-74, 2006.

WANG, C. J.; THIELE, S.; BOLLAG, J. M. Interaction of 2,4,6-trinitrotoluene (TNT) and 4-amino-2,6-dinitrotoluene with humic monomers in the presence of oxidative enzymes. **Archives of Environmental Contamination and Toxicology**, v. 42, n. 1, p. 1-8, 2002.

WEBER, E. J.; SPIDLE, D. L.; THORN, K. A. Covalent binding of aniline to humic substances .1. Kinetic studies. **Environmental Science & Technology**, v. 30, n. 9, p. 2755-2763, 1996.

WIDLER, A. M.; SEWARD, T. M. The adsorption of gold(I) hydrosulphide complexes by iron sulphide surfaces. **Geochimica Et Cosmochimica Acta**, v. 66, n. 3, p. 383-402, 2002.

WISCHGOLL, S.; HEINTZ, D.; PETERS, F.; ERXLEBEN, A.; SARNIGHAUSEN, E.; RESKI, R.; VAN DORSSELAER, A.; BOLL, M. Gene clusters involved in anaerobic benzoate degradation of Geobacter metallireducens. **Molecular Microbiology**, v. 58, n. 5, p. 1238-1252, 2005.

WU, Y.-G.; HUI, L.; LI, X.; ZHANG, Y.-Z.; ZHANG, W.-C. Degradation of aniline in weihe riverbed sediments under denitrification conditions. **Journal of Environmental Science and Health, Part A**, v. 42, n. 4, p. 413-419, 2007.

YOU, I. S.; JONES, R. A.; BARTHA, R. Evaluation of a Chemically Defined Model for the Attachment of 3,4-Dichloroaniline to Humus. **Bulletin of Environmental Contamination and Toxicology**, v. 29, n. 4, p. 476-482, 1982.

YUAN, X.; DAVIS, J. A.; NICO, P. S. Iron-Mediated Oxidation of Methoxyhydroquinone under Dark Conditions: Kinetic and Mechanistic Insights. **Environmental Science & Technology**, v. 50, n. 4, p. 1731-1740, 2016.

ZHANG, C.-L.; YU, Y.-Y.; FANG, Z.; NARAGINTI, S.; ZHANG, Y.; YONG, Y.-C. Recent advances in nitroaromatic pollutants bioreduction by electroactive bacteria. **Process biochemistry**, v. 70, p. 129-135, 2018.

ZHOU, X.; KANG, F.; QU, X.; FU, H.; LIU, J.; ALVAREZ, P. J.; ZHU, D. Probing extracellular reduction mechanisms of Bacillus subtilis and Escherichia coli with nitroaromatic compounds. **Science of The Total Environment**, v. 724, p. 138291, 2020.

APPENDIX A – SUPPLEMENTARY INFORMATION FOR SECTION 3

Figure 31 – XRD spectrum for the synthetic mackinawite. The vertical black lines represent the expected peaks exhibited by mackinawite in XRD.

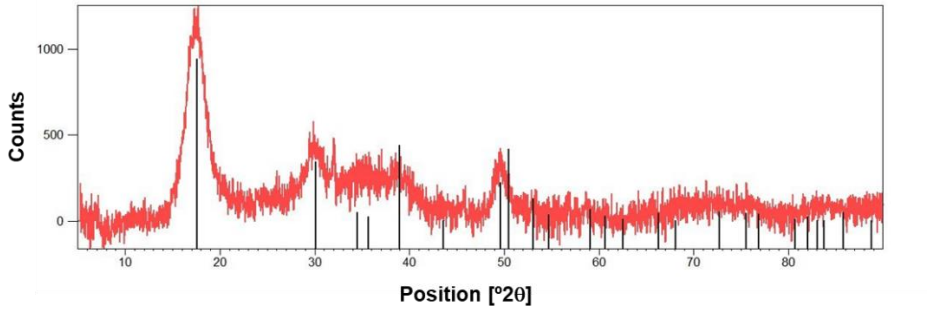

Figure 32 – Controls with DNAN and Fe^{2+} at different pH values.

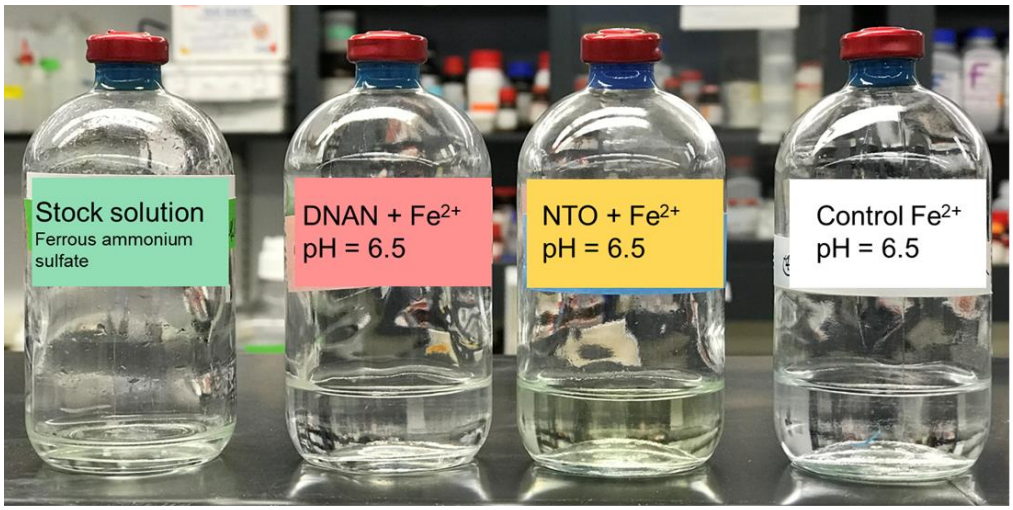

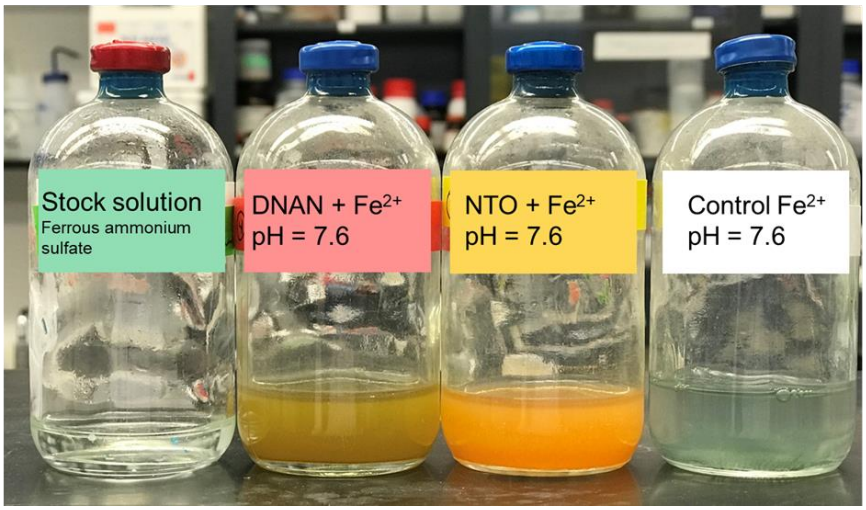

Figure 33 – DNAN in controls with Fe^{2+} at different pH values. Panel A: DNAN + Fe^{2+} at pH 6.5. Panel B: DNAN + Fe^{2+} at pH 7.6. Legend: DNAN (●), MENA (▲), iMENA (△), DAAN (○), and DNAN + MENA + iMENA + DAAN (dashed line). Symbols represent the average of three replicates, and error bars represent the standard deviation.

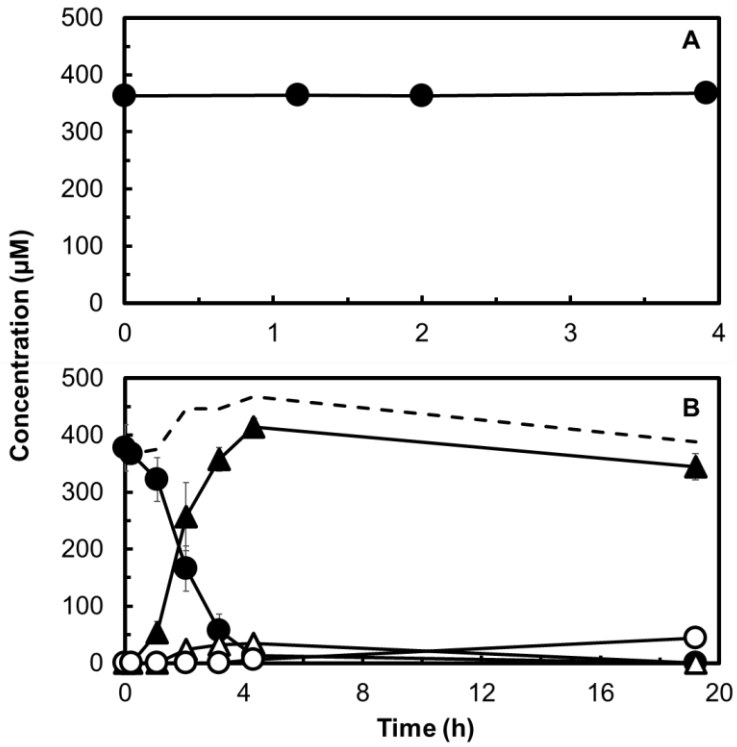

Figure 34 – DNAN in controls with S^{2-} at different pH values. Panel A: DNAN + S^{2-} at pH 6.5. Panel B: DNAN + S^{2-} at pH 7.6. Legend: DNAN (●). Symbols represent the average of three replicates, and error bars represent the standard deviation.

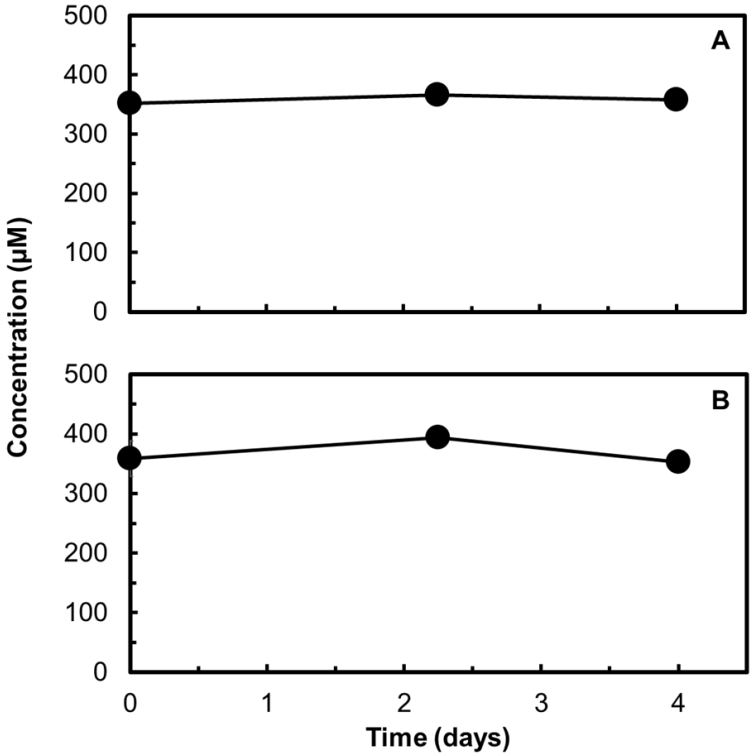

Figure 35 – NTO in controls with Fe^{2+} at different pH values. Panel A: NTO + Fe^{2+} at pH 6.5. Panel B: NTO + Fe^{2+} at pH 7.6. Legend: Legend: NTO (⧫), ATO (◊), and NTO + ATO (dashed line). Symbols represent the average of three replicates, and error bars represent the standard deviation.

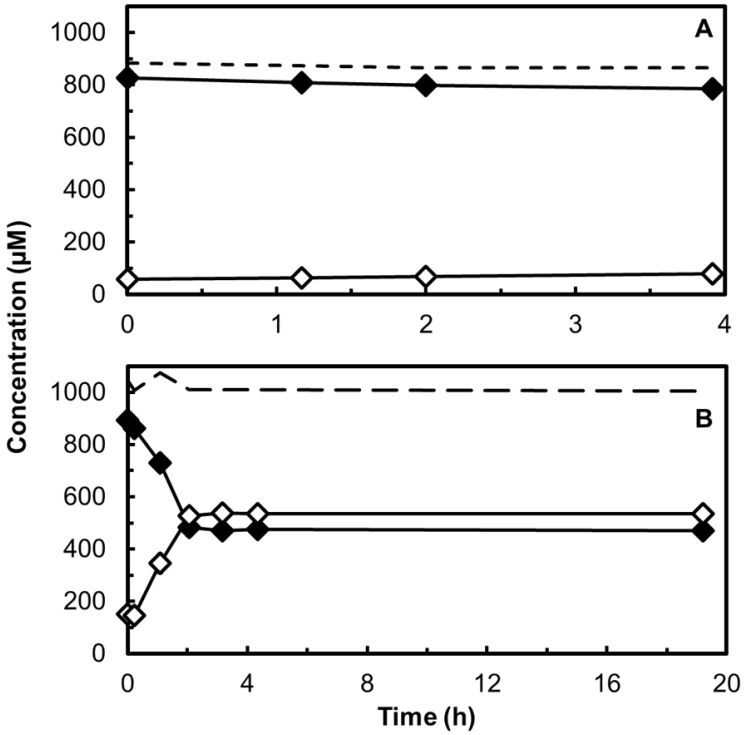

Figure 36 – NTO in controls with S^{2-} at different pH values. Panel A: NTO + S^{2-} at pH 6.5. Panel B: NTO + S^{2-} at pH 7.6. Legend: Legend: NTO (⧫), ATO (◊), and NTO + ATO (dashed line). Symbols represent the average of three replicates, and error bars represent the standard deviation.

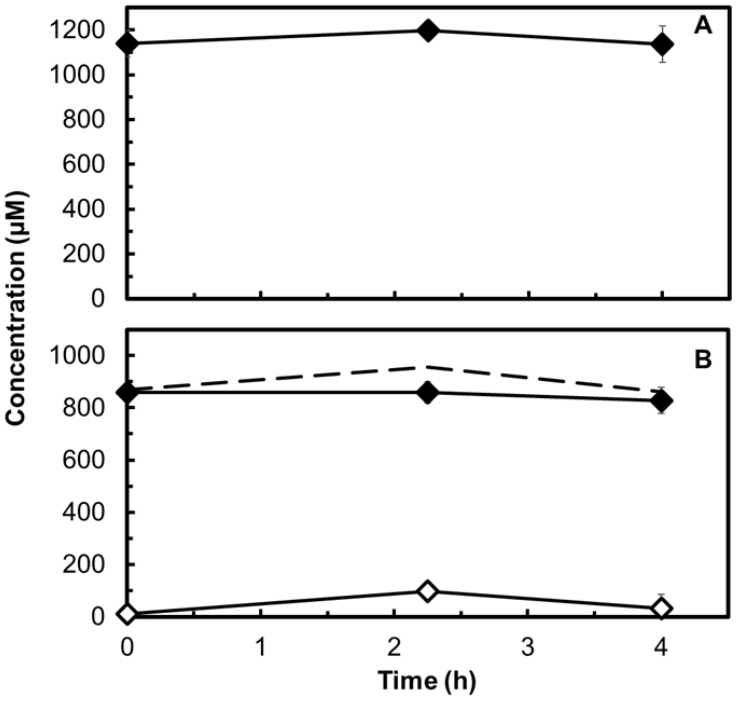

APPENDIX B – SUPPLEMENTARY INFORMATION FOR SECTION 4

BIOMASS X OD600

Bottles containing different concentrations of substrates and the enrichment culture were incubated, and after the complete reduction of NTO was observed, samples of the suspension were taken for OD600 analysis. The remaining suspension of each bottle was filtered using a 0.22 µm membrane. The filters were dried at 105ºC for 3 hours, and the weight of the dry mass was recorded. The same procedure was performed for abiotic controls. The dry mass obtained for the abiotic controls was subtracted from the dry mass of the biotic treatment to account for inorganic solids. A correlation was established for the OD600 and biomass (R^2 = 0.9639), as shown in Figure 37.

Figure 37 – Correlation between optical density at 600 nm (OD600) and biomass production by the NTO-acetate enrichment culture (mg VSS L^{-1}) after complete reduction of different concentrations of NTO.

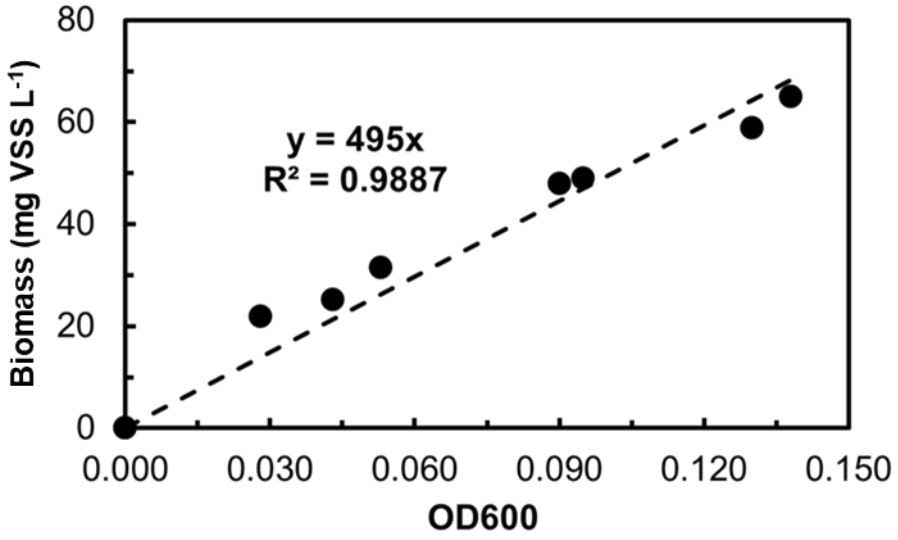

ATP RAW DATA

Figure 38 – ATP production of the enrichment culture incubated with NTO and acetate. Panel A: ATP production in different incubation conditions. Panel B: NTO consumption and ATO formation by the enrichment culture incubated with both NTO and acetate. Legend: EC + NTO + acetate (■), EC + acetate (△), EC + NTO (⧫), EC (✕), NTO concentration (●), and ATO concentration (○). Symbols represent the average of three replicates, and error bars represent the standard deviation.

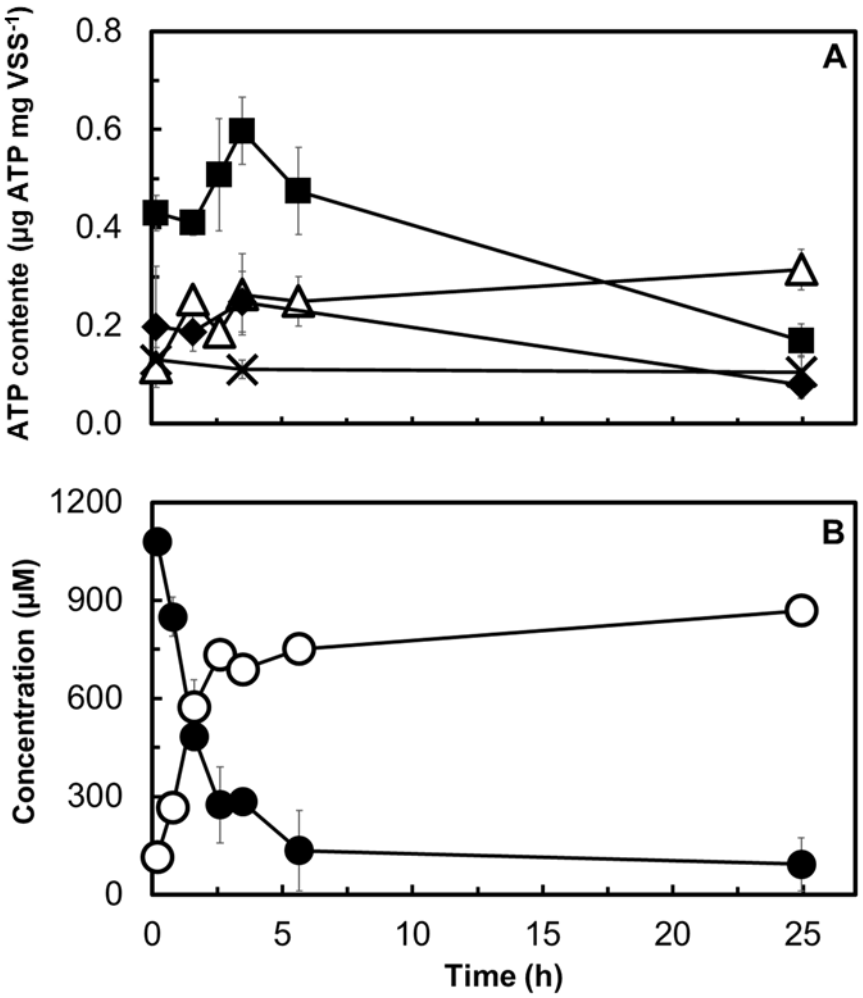

APPENDIX C – SUPPLEMENTARY INFORMATION FOR SECTION 5

ABIOTIC CONTROLS

Figure 39 – DAAN concentration over time at different abiotic conditions (without sludge). Panel A: without e- acceptors. Panel B: without e- acceptor and with pyruvate as a co-substrate. Panel C: with sulfate. Panel D: with nitrate. Legend: DAAN (●), pyruvate (◇), sulfate (□), and nitrate (△). Symbols represent the average of three replicates, and error bars represent the standard deviation.

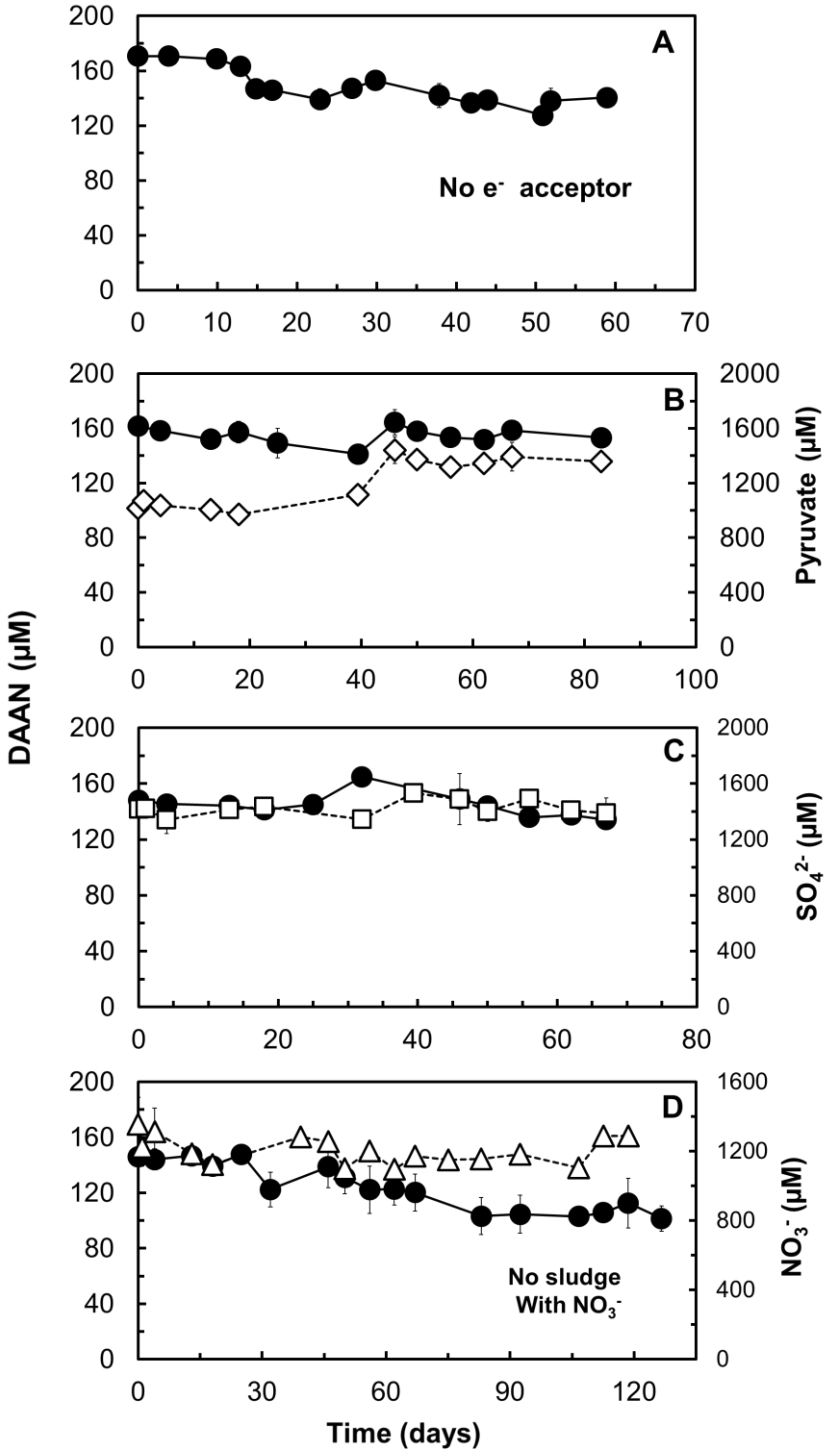

CONSUMPTION RATE IN BIOTIC AND ABIOTIC MICROCOSMS

Table 6 – Consumption rate (k_1, first-order) for the different biotic and abiotic conditions tested. R^2 of all consumption rates were within 0.86 to 0.99.

Treatment	k_1 (d^{-1})			
	With sludge			Without sludge
	1st spike	2nd spike	3rd spike	
No e^- acceptor	0.14 [a]	0.35	n/a [c]	0.00
No e^- acceptor + pyruvate	0.28 [a]	1.17	n/a [c]	0.00
With SO_4^{2-}	n/a [c]	n/a [c]	0.34	0.00
With NO_3^-	0.17	0.05	0.04	0.01
With O_2	0.53	0.88	0.47	0.14
Heat-killed sludge	0.39	0.06 [b]	n/a [c]	n/a [c]

[a] Rates calculated for phase 3 (Figure 19).
[b] Rate calculated from 7 to 53 d.
[c] n/a means not available or not applicable.

DAAN INCUBATED WITH HUMIC AND FULVIC ACIDS EXTRACTED FROM SLUDGE

Humic and fulvic acids were extracted from sludge following Benites *et al*. (2003). For that, we added 20 mL of a NaOH solution (0.1 M) to the sludge samples and let them rest for 24 h. Then, we centrifuged the samples for 40 min at 4000 rpm and transferred the supernatant to a glass flask. Subsequently, we repeated the process using the precipitated material, but with a 1-h resting interval. Afterward, we acidified the supernatant with H_2SO_4 to pH 1, let it rest for 18 h, and filtered it with a 0.45-µm membrane. The filtered liquid corresponded to the fulvic acids solution. Then, the membrane was washed with NaOH 0.1 M, forming the humic acids solution. We finally adjusted the pH of both fulvic and humic acids solutions to 7. We incubated DAAN anaerobically with humic and fulvic acids solution separately in the same conditions described for the anaerobic microcosms. The experiment was performed in triplicates. Humic or fulvic acids content per bottle corresponded to the amounted extracted from the sludge content of one microcosm.

Figure 40 – DAAN concentration over time when incubated with humic or fulvic acids extracted from sludge. Legend: DAAN incubated with humic acids (●), and DAAN incubated with fulvic acids (○). Symbols represent the average of three replicates, and error bars represent the standard deviation.

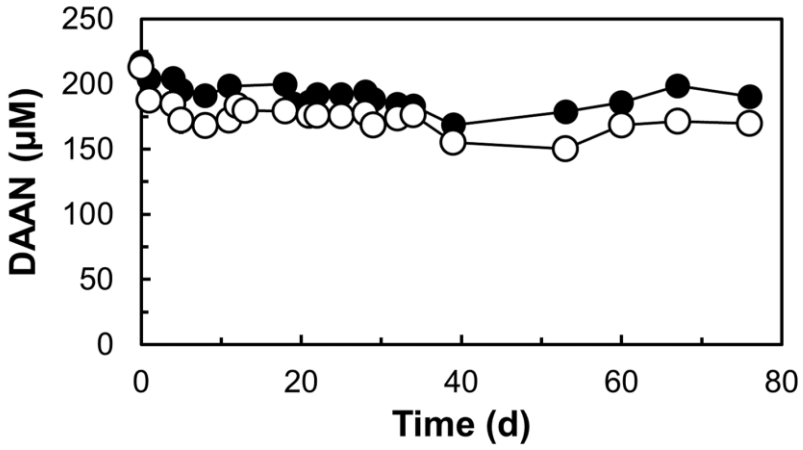

CHARACTERIZATION OF MICROBIAL COMMUNITIES SEQUENCING

Figure 41 – Rarefaction curves of the 16S rRNA sequencing.

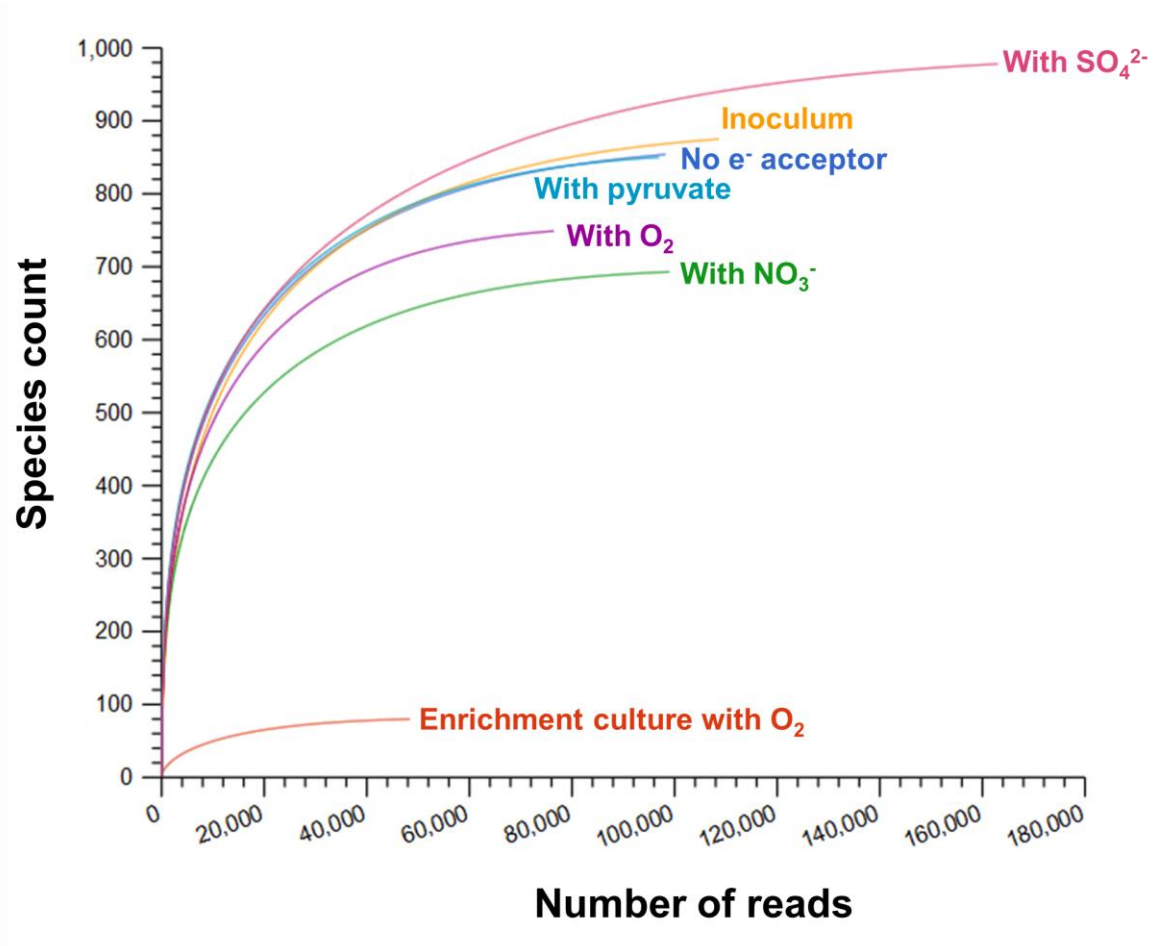

Table 7 – Estimated diversity and evenness indexes of the microbial communities analyzed.

	Inoculum	**No e^- acceptor**	**No e^- acceptor + pyruvate**	**With SO_4^{2-}**	**With NO_3^-**	**With O_2**	**Enrichment culture with O_2**
Number of reads	98,056	83,127	89,602	142,636	88,296	68,759	34516
Number of genera	354	342	348	373	290	302	22
Chao1 (coverage)	379 (93.4%)	369 (92.8%)	378 (92.0%)	399 (93.6%)	310 (93.7%)	325 (93.1%)	22 (98.3%)
Simpson	0.804	0.904	0.903	0.902	0.908	0.912	0.271
Shannon (H)	2.729	3.192	3.186	3.238	3.290	3.303	0.501
Evenness	0.043	0.071	0.070	0.068	0.093	0.090	0.081
Berger-parker	0.420	0.232	0.239	0.262	0.256	0.228	0.848

APPENDIX D – SUPPLEMENTARY INFORMATION FOR SECTION 6

METHOD TO STOP THE REACTIONS BETWEEN DAAN AND QUINONES

We paired DAAN (1 mM) and methoxybenzoquinone (MBQ, 3 mM) in the same conditions described in section 2.2.1 of the text. The reaction was stopped at 20 s by injecting 15 mL of acetonitrile and vortexing immediately. We took samples after 40 s, 4 min, and 15 min from the reaction start. Samples were analyzed in the HPLC for MBQ, MHQ, and DAAN. Figure 42 shows the results, proving that the injection of acetonitrile was enough to stop the reaction. We performed this assay in duplicates.

Figure 42 – Concentrations of DAAN (●), MBQ (▲), and MHQ (■) in a control assay testing the ability of acetonitrile to stop the reactions between DAAN and MBQ.

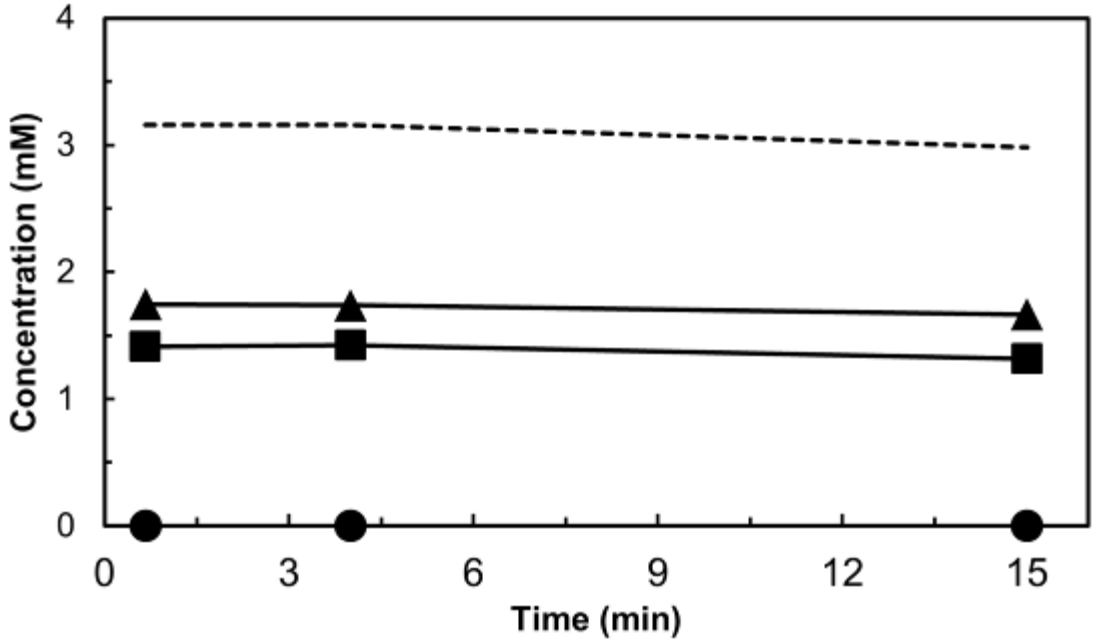

CONTROLS – PAIRING DAAN AND QUINONES

Figure 43 – Concentrations of DAAN (●), BQ (▲), and HQ (■) in the following controls: BQ (3 mM) incubated individually (panel A), HQ (3 mM) incubated individually (panel B), DAAN (1 mM) incubated individually (panel C), and DAAN (1 mM) and HQ (3 mM) incubated together (panel D). The dashed line represents the sum BQ + HQ. The controls did not present significative change in the concentration of the analyzed compounds.

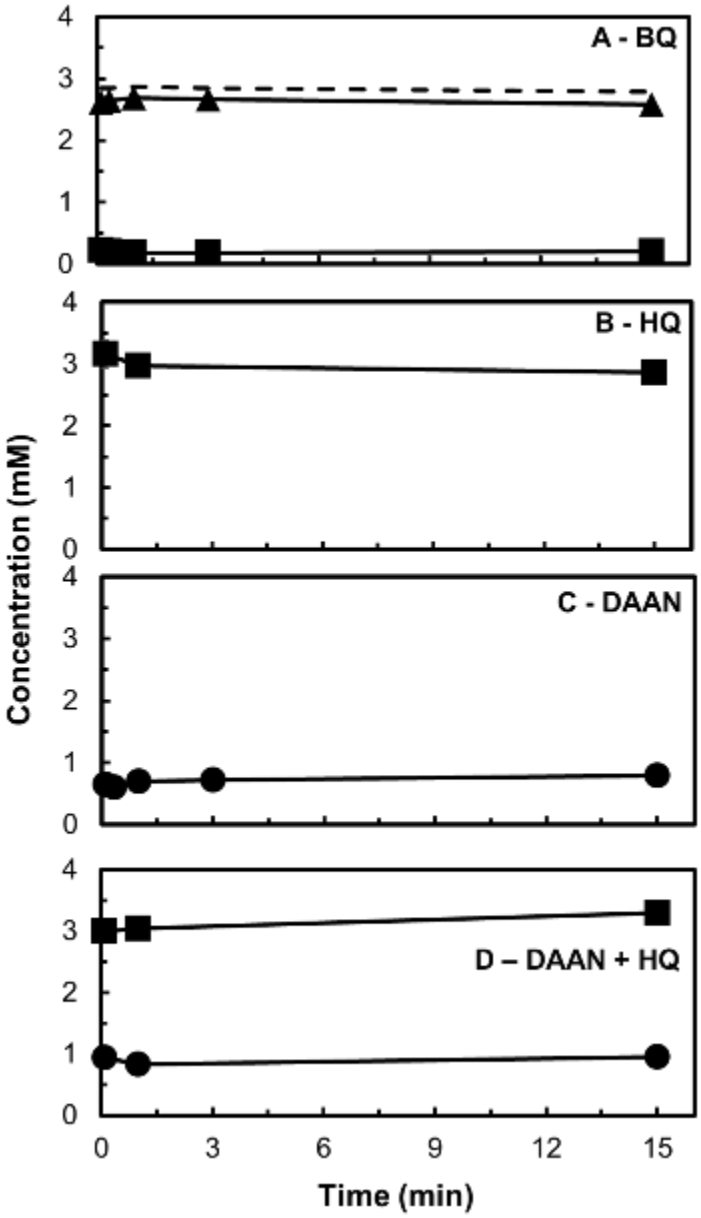

Figure 44 – Concentrations of DAAN (●), MBQ (▲), and MHQ (■) in the following controls: MBQ (3 mM) incubated individually (panel A), MHQ (3 mM) incubated individually (panel B), and DAAN (1 mM) and MHQ (3 mM) incubated together (panel C). The dashed line represents the sum MBQ + MHQ. The controls did not present significative change in the concentration of the analyzed compounds.

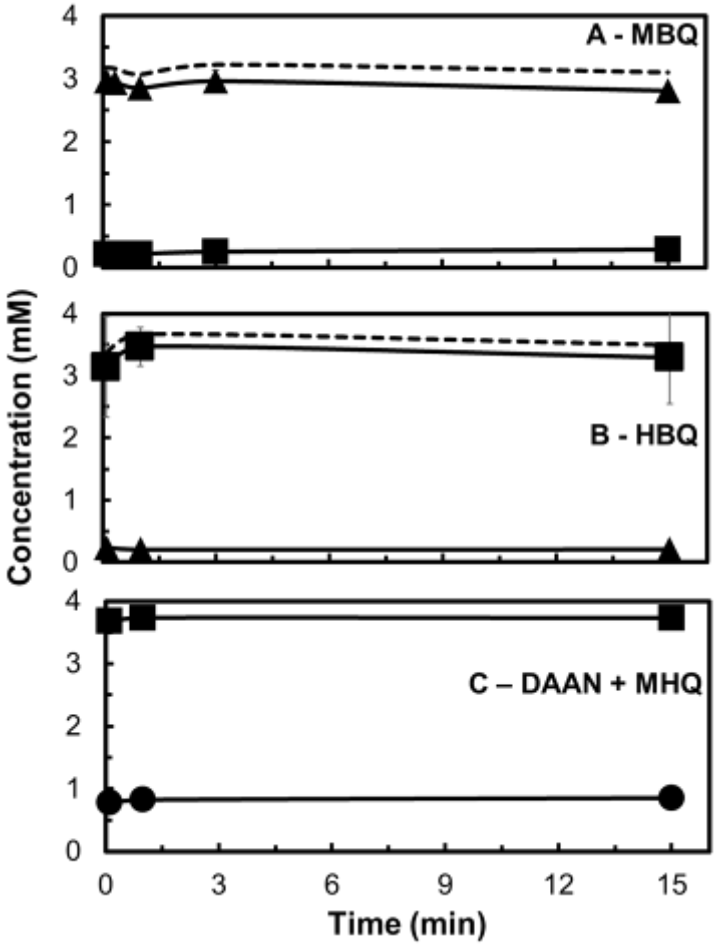

Figure 45 – Concentrations of DAAN (●) and MHQ (■) incubated together in the following controls: DAAN (10 mM) and MHQ (1 mM) in panel A and DAAN (1 mM) and MHQ (10 mM) in panel B.

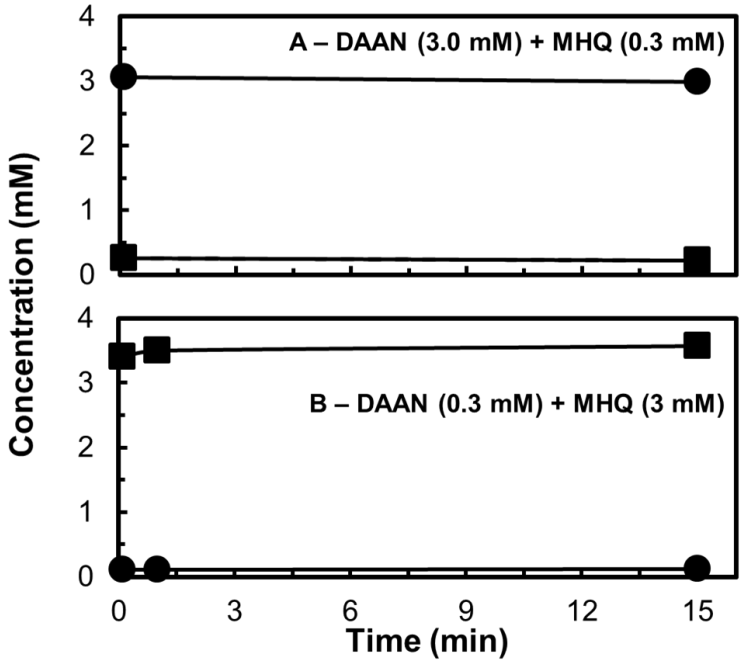

FORMATION OF COLORED PRODUCTS AND INSOLUBLE POLYMERS

Figure 46 – Gradual formation of colored products from the reactions between DAAN (1 mM) and MBQ (3 mM).

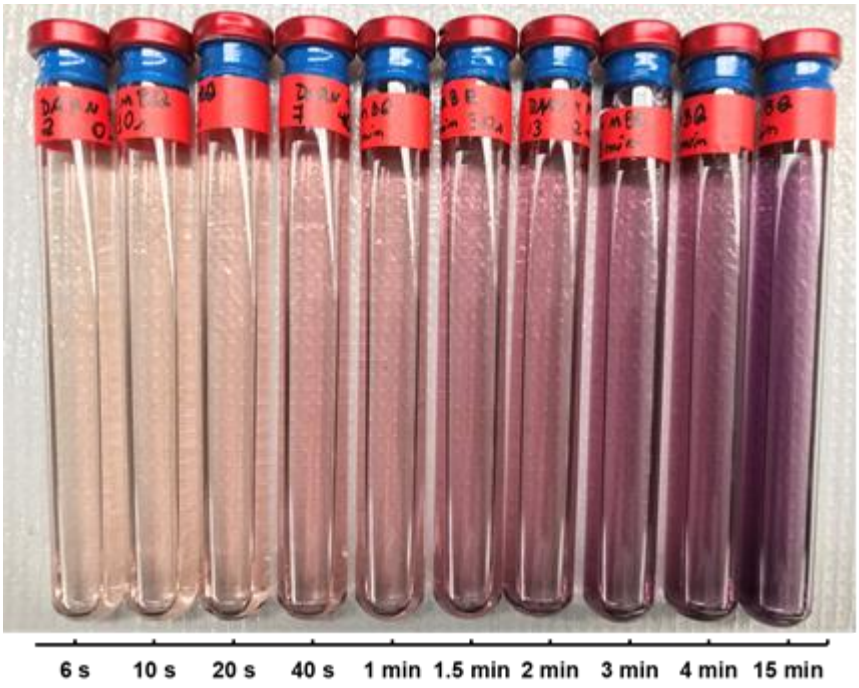

Figure 47 – Formation of precipitated polymers from the reactions between DAAN (1 mM) and MBQ (3 mM) after 20 days of incubation. Controls (DAAN + MHQ incubated together, DAAN incubated individually, and MBQ incubated individually) did not present precipitated material.

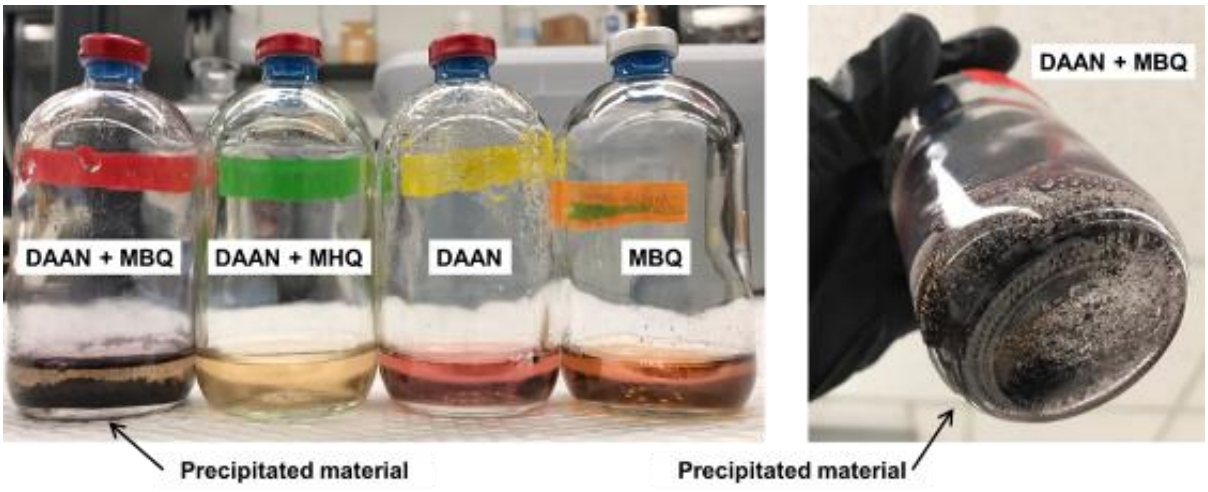

COMPOUNDS **F** AND **P** ALTERNATIVE STRUCTURES

Figure 48 – Alternative structures for compounds F and P. In section 6.4.2, we justified why the structures on the left, with azo bonds, are more probable than those on the right, with azoxy bonds.

Compound F – ($C_{20}H_{18}N_4O_4$)

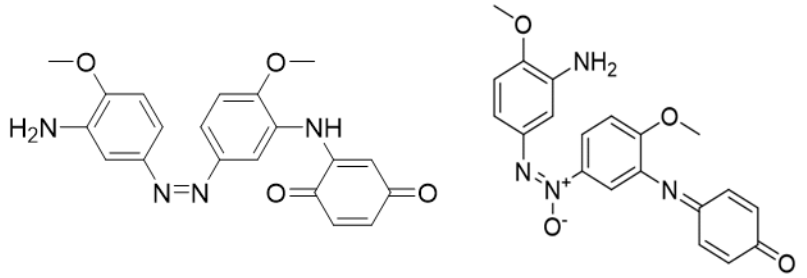

Compound P – ($C_{28}H_{24}N_4O_7$)

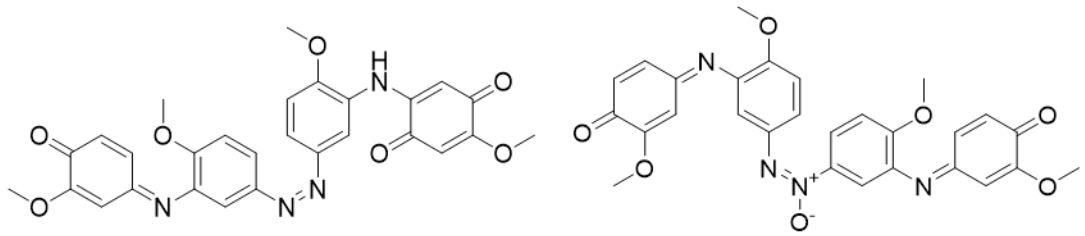

CHROMATOGRAPHIC PEAK AREAS OF THE IDENTIFIED PRODUCTS

Figure 49 – Peak areas (●) from mass chromatograms in the UHPLC-HRAM-MS/MS analysis corresponding to the different compounds detected from the reactions between DAAN (1 mM) and BQ (3 mM).

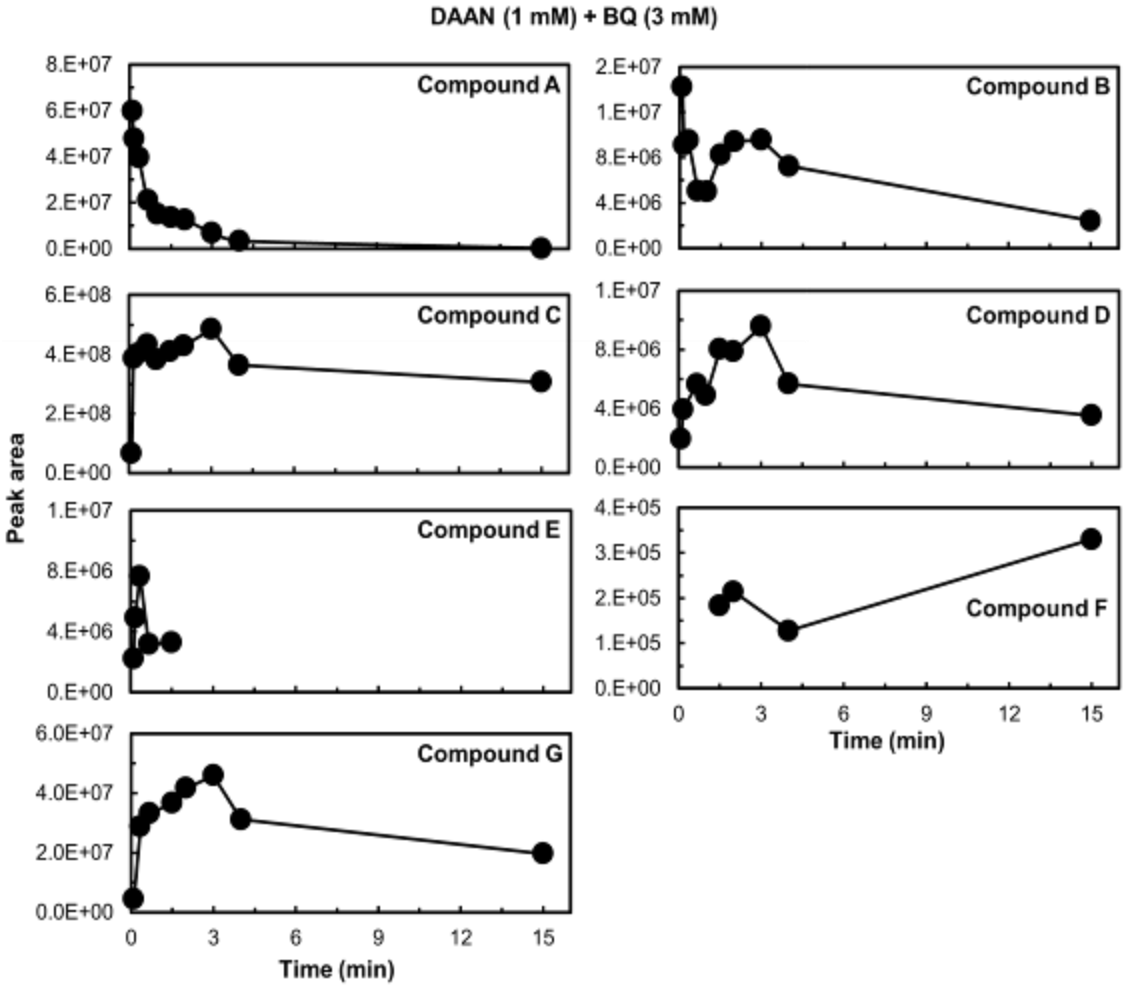

Figure 50 – Peak areas (●) from mass chromatograms in the UHPLC-HRAM-MS/MS analysis corresponding to the different compounds detected from the reactions between DAAN (1 mM) and MBQ (3 mM).

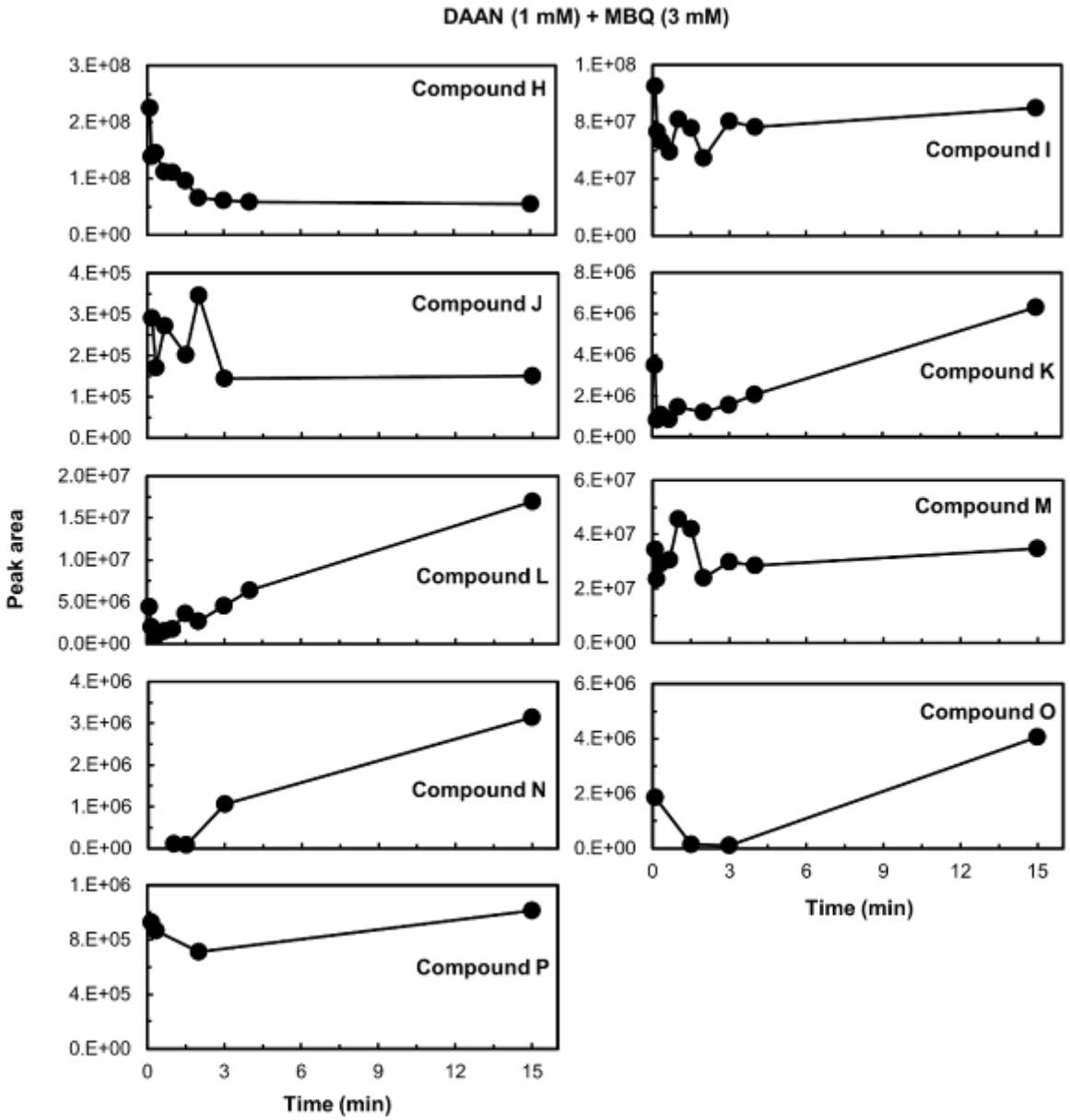

Figure 51 – Peak areas (●) from mass chromatograms in the UHPLC-HRAM-MS/MS analysis corresponding to the different compounds detected from the reactions between DAAN and MBQ in two different DAAN:MBQ molar ratios (1:10 in the panels on the left and 10:1 in the panels on the right).

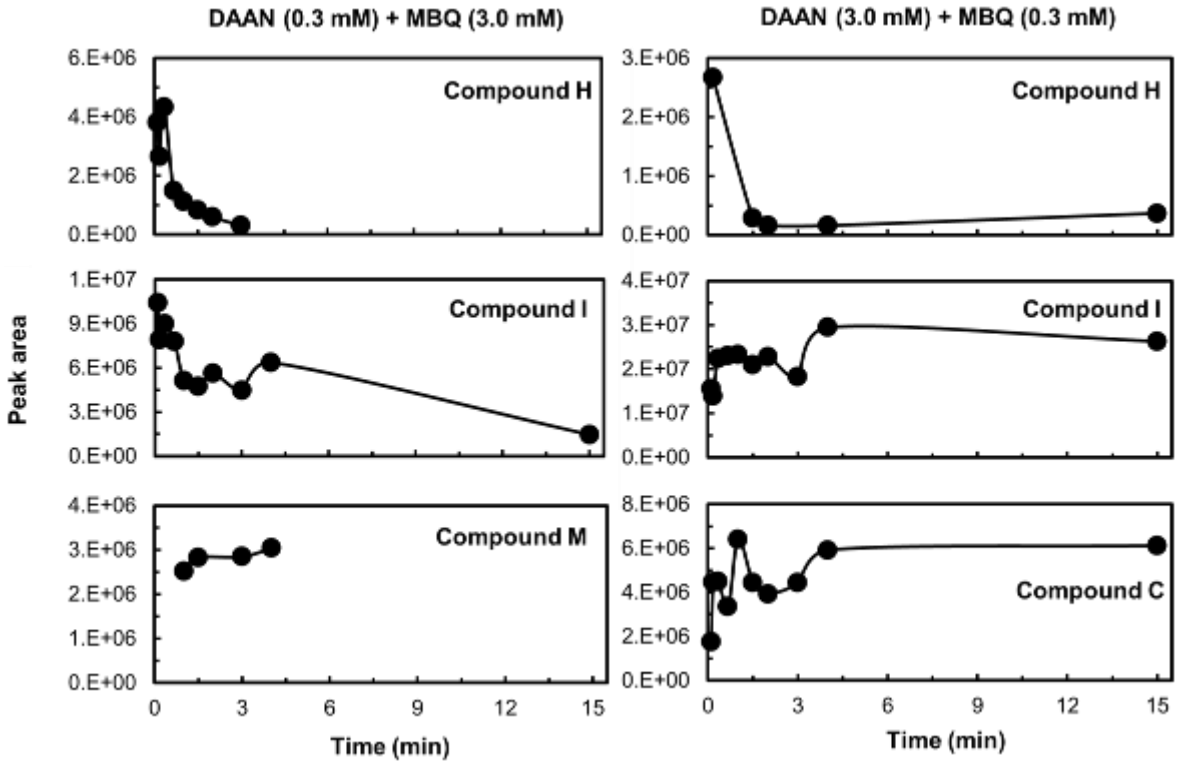

APPENDIX E – RESUMO EXPANDIDO EM PORTUGUÊS

ESTRATÉGIAS BIÓTICAS E ABITÓTICAS PARA REMEDIAÇÃO DE COMPOSTOS DE MUNIÇÕES INSENSÍVEIS

Introdução

Compostos insensíveis de munição, como 2,4-dinitroanisole (DNAN) e 3-Nitro-1,2,4-triazol-5-ona (NTO), estão substituindo compostos tradicionais nas formulações de explosivos. Suas vantagens estão relacionadas a uma maior resistência a explosões acidentais, facilitando manuseio, transporte e armazenamento. O DNAN é tóxico para organismos metanogênicos, bactérias nitrificantes, bactérias bioluminescentes, algas, azevém, minhocas e peixe-zebra. Já o NTO foi relatado de causar toxicidade testicular em ratos, anomalias neuromusculares em codornas japonesas e comportamento anormal de natação em embriões de peixe-zebra.

A redução do grupo nitro na posição orto do DNAN produz 2-metoxi-5-nitroanilina (MENA), enquanto a redução do grupo nitro na posição para produz 4-metoxi-5-nitroanilina (iMENA). A redução adicional do grupo nitro restante de MENA ou iMENA forma 2,4-diaminoanisol (DAAN), uma amina aromática tóxica para muitos microrganismos e carcinogênica para mamíferos. Em ambientes anaeróbios, NTO é reduzido para 3-amino-1,2,4-triazol-5-ona (ATO), um composto que teve toxicidade demonstrada em *Daphnia magna* e embriões de peixes-zebra.

Objetivos

Objetivo geral

Desenvolver novas estratégias para a transformação redutiva dos compostos de munições insensíveis DNAN e NTO e para a remoção do DAAN, produto reduzido do DNAN.

Objetivos específicos

a) Avaliar a capacidade de minerais de FeS, como a mackinawita, em reduzir abioticamente o DNAN e o NTO;
b) investigar o processo biótico da respiração NTO por uma cultura de enriquecimento anaeróbia;

c) avaliar a remoção de DAAN em lodo biológico sob diferentes condições de aceptores de elétrons; e

d) descrever a natureza das reações abióticas DAAN com a matéria orgânica natural do solo em ambientes anóxicos usando quinonas como modelos para compostos húmicos.

Figura 52 - Esquema de liberação de compostos de munições em uma área de treinamento militar. Legenda: NG (nitroglicerina), DNT (2,4- e 2,6-dinitrotolueno), NQ (nitroguanidina), TNT (2,4,6-trinitrotolueno), RDX (1,3,5-hexahidro-1,3 , 5-trinitro-1,3,5-triazina), HMX (octa-hidro-1,3,5,7-tetranitro-1,3,5,7-tetrazocina), DNAN (2,4-dinitroanisol), NTO (3-nitro-1,2,4-triazol-5-ona) e AP (perclorato de amônio).

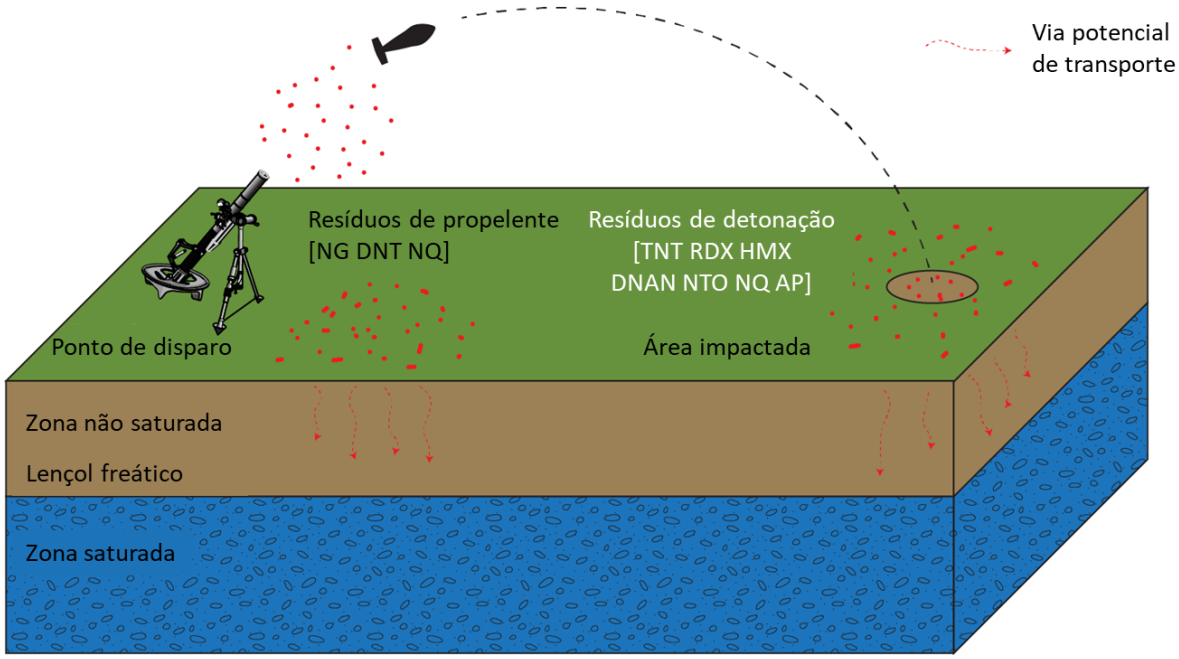

Fonte: adaptado de SERDP-ESTCP (2020)

Redução abiótica de NTO e DNAN por minerais de FeS

À medida que as aplicações militares dos compostos insensíveis de munições (IMCs) 2,4-dinitroanisol (DNAN) e 2-nitro-1,2,3-triazol-5-ona (NTO) aumentam, surge uma necessidade de compreensão do destino desses contaminantes no meio ambiente e do desenvolvimento de novas estratégias de remediação. Os minerais de FeS são muito abundantes em sedimentos aquáticos, depósitos hidrotérmicos e como camada de revestimento de minerais do solo. Neste trabalho, mostramos que as superfícies de FeS podem transformar abioticamente DNAN e NTO em suas correspondentes aminas sob condições anóxicas e em condições ambientais de pH e temperatura. Observamos que a mackinawita, um FeS tetragonal com estrutura em camadas, reduziu o DNAN principalmente a 2-metoxi-5-nitroanilina (MENA),

que foi parcialmente reduzido a 2-4-diaminoanisol (DAAN). As camadas na estrutura mackinawita foram provavelmente responsáveis pela adsorção parcial de MENA e DAAN. Um FeS comercial (composto principalmente de pirrotita e troilita) reduziu o DNAN até DAAN. O NTO foi totalmente reduzido para 3-amino-1,2,4-triazol-5-ona (ATO) tanto pela mackinawita, quanto pelo FeS comercial. Mostramos que as reações são mediadas pela superfície mineral, uma vez que não ocorreram quando apenas Fe^{2+} e S^{2-} dissolvidos estavam presentes no meio. Este é o primeiro estudo a relatar a redução de IMCs, incluindo um composto nitro-heterocíclico (NTO), por superfícies minerais de FeS. Nossos resultados indicam que DNAN e NTO podem ser rapidamente transformados em suas aminas correspondentes em solos e sedimentos aquáticos ricos em minerais de FeS.

Principais pontos

a) O FeS comercial era composto principalmente por pirrotita e troilita.
b) A mackinawita e o FeS comercial reduziram o DNAN para MENA, iMENA e DAAN e o NTO para ATO.
c) A mackinawita adsorveu parcialmente o MENA e o DAAN provavelmente devido à sua estrutura em camadas.
d) As reações são mediadas pela superfície dos minerais de FeS, uma vez que DNAN e NTO não foram reduzidos pelas formas solúveis Fe^{2+} e S^{2-}.
e) Experimentos futuros devem determinar qual o produto da oxidação da mackinawita e do FeS comercial pela reação com os IMCs.
f) A redução de IMCs por minerais de FeS contribui para o entendimento das transformações geoquímicas de IMCs no solo e em sedimentos aquáticos.
g) Nossos resultados também sugerem que mackinawita e FeS comercial podem ser aplicados em técnicas de engenharia voltadas à remediação de DNAN e NTO.

Figura 53 – Resumo gráfico da redução abiótica de NTO e DNAN por minerais de FeS.

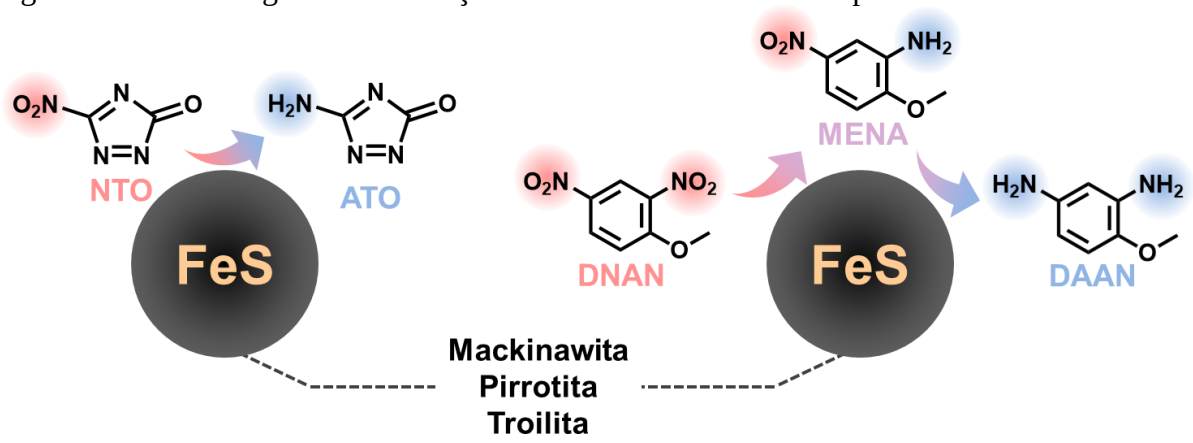

Respiração microbiana do NTO

3-Nitro-1,2,4-triazol-5-ona (NTO) é um componente essencial das formulações de munições insensíveis. Seu destino ambiental está ganhando relevância devido ao seu crescente uso pelos militares. Aqui, apresentamos a respiração de NTO, um novo processo de respiração microbiana. Uma cultura anaeróbia altamente enriquecida a partir de lodo de águas residuárias reduziu estequiometricamente o NTO para 3-amino-1,2,4-triazol-5-ona (ATO), enquanto oxidava acetato a CO_2. Observamos crescimento celular simultaneamente à redução de NTO. A cultura foi incapaz de crescer na presença de acetato apenas, descartando uma redução cometabólica de NTO. Um desacoplador de fosforilação oxidativa inibiu a redução de NTO, indicando que o processo estava ligado à formação de ATP. A evidência final da respiração de NTO foi a produção de ATP pela cultura de enriquecimento quando exposta a NTO e acetato simultaneamente. Nenhuma produção significativa de ATP foi observada quando NTO ou acetato estavam ausentes. Um estudo metagenômico revelou que os dois principais microrganismos presentes na cultura foram *Geobacter anodireducens* (abundância relativa de 89,3%) e *Thauera* sp. (abundância relativa de 5,5%). Este estudo representa a primeira vez que foi observado um composto nitro-heterocíclico sendo usado como um aceptor de elétrons na respiração anaeróbia, lançando nova luz sobre os processos microbianos que conduzem a biotransformação do NTO.

Principais pontos

a) O crescimento da cultura de enriquecimento foi dependente da presença simultânea de NTO e acetato.

b) Acetato não foi consumido quando NTO estava ausente no meio.
c) A cultura de enriquecimento exibiu alta especificidade ao NTO, o que foi evidenciado pela falta de habilidade em reduzir outros compostos com grupo nitro.
d) CCCP, um inibidor de fosforilação oxidativa, inibiu fortemente a redução de NTO pela cultura de enriquecimento.
e) O conteúdo de ATP das células aumentou quando expostas simultaneamente a NTO e acetato, evidenciando a respiração do NTO.
f) Estudos futuros de biologia molecular devem focar nos mecanismos enzimáticos da redução do NTO.
g) Nossos achados podem ser aplicados no desenvolvimento de estratégias de biorremediação para limpar locais contaminadas com NTO.
h) Também podem ser aplicados na avaliação da atenuação natural de contaminação por NTO em ambientes anaeróbicos.

Figura 54 – Resumo gráfico da respiração microbiana do NTO.

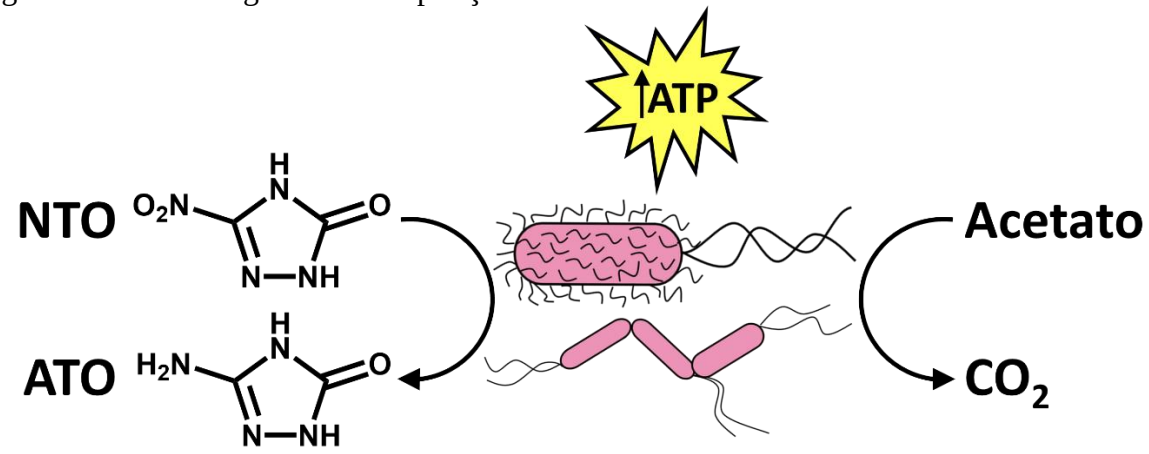

Remoção do DAAN em lodo biológico sob diferentes condições de aceptores de elétrons

Compostos de munições insensíveis, como o 2,4-dinitroanisol (DNAN), estão substituindo os explosivos convencionais. DNAN é anaerobiamente reduzido a 2,4-diaminoanisol (DAAN), uma amina aromática tóxica. No entanto, a remoção de DAAN em diferentes condições redox ainda não foi elucidada. Aqui, analisamos o consumo de DAAN em microcosmos bióticos e abióticos quando expostos a diferentes condições redox (sem adição de aceptor de elétrons; sem adição aceptor de elétrons, mas com piruvato como cossubstrato; com sulfato; com nitrato; e com oxigênio), usando um lodo anaeróbia como inóculo. Observamos que a autoxidação do DAAN, uma reação abiótica, foi relevante em ambientes aeróbios. DAAN

também reagiu abioticamente com lodo autoclavado até um limite de saturação de 67,4 μmol DAAN (g VSS lodo autoclavado)$^{-1}$. Entre as condições testadas, o oxigênio causou a remoção mais rápida do DAAN em lodo vivo. Os tratamentos sem adição de aceptores de elétrons (com ou sem piruvato) apresentaram desempenhos de remoção de DAAN semelhantes, embora mais lentos que o tratamento aeróbio. O sulfato não exibiu nenhum efeito na remoção de DAAN em comparação com o tratamento sem aceptores de elétrons. O nitrato, porém, inibiu o processo. Cultivamos uma cultura de enriquecimento a partir da condição com oxigênio usando DAAN como o único substrato em condições aeróbicas. O enriquecimento mudou profundamente a comunidade microbiana. Microrganismos não classificados foram responsáveis por 85% da abundância relativa na cultura de enriquecimento, sugerindo que a remoção aeróbia do DAAN envolveu organismos que ainda não foram descritos. Nossos resultados sugerem que o tratamento aeróbio DAAN pode ser acoplado à redução anaeróbia DNAN no lodo, melhorando o tratamento de águas residuais contendo DNAN.

Principais pontos

a) A remoção do DAAN em lodo vivo foi mais rápida em condições aeróbias.
b) O DAAN reagiu abioticamente com lodo autoclavado até um limite de saturação.
c) A autoxidação de DAAN foi significante sob exposição ao oxigênio.
d) Microrganismos foram enriquecidos para remover DAAN em condições aeróbias.
e) A cultura aeróbia capaz de remover DAAN contém principalmente microorganismos não classificados.
f) Uma etapa de remoção de DAAN pode ser implementada após a biotransformação anaeróbica de DNAN para melhorar o tratamento de águas residuais contendo DNAN.
g) Trabalhos futuros devem focar no metagenoma da cultura de enriquecimento aeróbia e nos subprodutos da transformação aeróbica DAAN.

Figura 55 – Resumo gráfico da remoção do DAAN em lodo sob diferentes condições de aceptores de elétrons

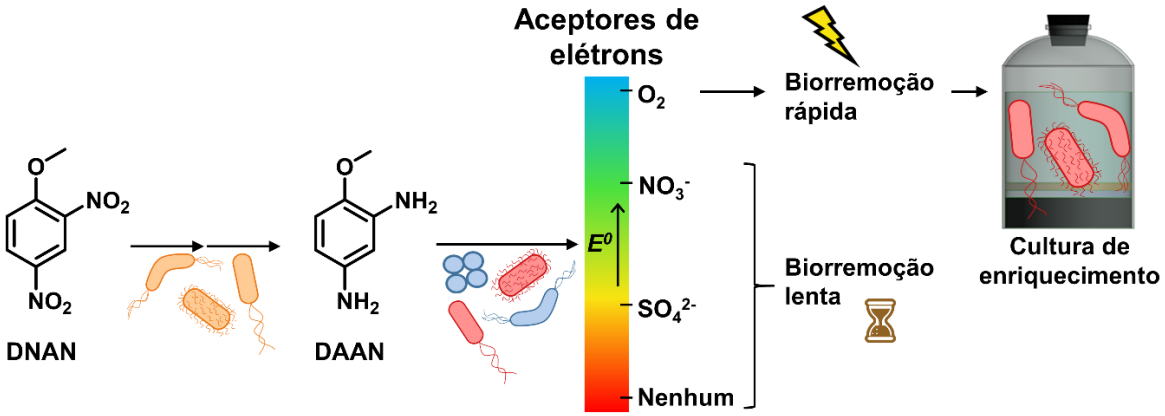

Incorporação do DAAN em grupos quinônicos da matéria orgânica natural

2,4-Dinitroanisol (DNAN) é um composto de munições insensíveis que substitui o 2,4,6-trinitrotolueno (TNT). O produto da redução do DNAN no meio ambiente é o 2,4-diaminoanisol (DAAN), uma amina aromática tóxica. O DAAN é conhecido por desaparecer no solo logo após a redução de DNAN. Foi observado que resíduos não-extraíveis de DNAN marcado radioativamente com C^{14} estavam ligados à matéria orgânica natural do solo. Neste trabalho, investigamos as reações entre DAAN e matéria orgânica natural sob condições anóxicas, usando 1,4-benzoquinona (BQ) e metoxibenzoquinona (MBQ) como modelos de substâncias húmicas na matéria orgânica natural. Desenvolvemos um método para interromper as rápidas reações entre o DAAN e as quinonas, permitindo uma avaliação dos produtos formados e uma investigação dos mecanismos envolvidos. DAAN reagiu completamente com quinonas em excesso em menos de 6 segundos. Nossos resultados mostram que a incorporação de DAAN na matéria orgânica natural (representado por modelos BQ e MBQ) foi conduzida por reações dependentes da presença de quinonas, tais como: adições de Michael, formação de iminas (bases de Schiff) e formação de ligações azo. Depois que dímeros foram formados, diferentes reações de incorporação continuaram, o que levou a uma oligomerização resultando em trímeros e tetrâmeros. Após 20 dias, observamos precipitação de 56,4% do carbono orgânico dissolvido de uma mistura de DAAN (1 mM) e MBQ (3 mM). A perda de carbono orgânico dissolvido indica uma polimerização extensa, com DAAN sendo incorporado a compostos húmicos de alto peso molecular. Nossos resultados lançam uma nova luz sobre os mecanismos abióticos de incorporação do DAAN na matéria orgânica natural, mostrando que este processo

não requer condições aeróbicas nem um catalisador específico. A incorporação irreversível do DAAN na matéria orgânica natural pode ser potencialmente aplicada como uma estratégia de remediação acoplada à biotransformação anaeróbica do DNAN.

Principais pontos

a) Reações com quinonas conduzem à perda do DAAN em condições anóxicas.
b) A perda de DAAN ocorre em menos de 6 segundos ao reagir com quinonas em excesso.
c) As reações que governam esse processo são adições de Michael, formação de iminas e formação de ligações azo.
d) A oligomerização gera dímeros, trímeros e tetrâmeros.
e) Polímeros insolúveis são formados após vários dias.
f) A incorporação do DAAN na matéria orgânica natural do solo pode representar uma destinação final seguro para a remediação do DNAN.

Figura 56 – Resumo gráfico da incorporação do DAAN em grupos quinônicos da matéria orgânica natural